UNIVERSITA' DEGLI STUDI DI PADOVA

DOCTORATE SCHOOL OF CROP SCIENCE

CURRICULUM AGROBIOTECHNOLOGY - CICLO XXI

Department of Environmental Agronomy and Crop Science

SEXUALITY DEVIATION IN PLANTS, A MULTILEVEL APPROACH TO STUDY APOMIXIS

Director of the School : Ch.mo Prof. Andrea Battisti

Supervisor : Ch.mo Prof. Gianni Barcaccia

PhD Student : Giulio Galla

02 febbraio 2009

Declaration

I hereby declare that this submission is my own work and that, to the best of my knowledge and belief, it contains no material previously published or written by another person nor material which to a substantial extent has been accepted for the award of any other degree or diploma of the university or other institute of higher learning, except where due acknowledgment has been made in the text.

Giulio Galla / 02 febbraio 2009

A copy of the thesis will be available at *http://paduaresearch.cab.unipd.it/*

Dichiarazione

Con la presente affermo che questa tesi è frutto del mio lavoro e che, per quanto io ne sia a conoscenza, non contiene materiale precedentemente pubblicato o scritto da un'altra persona né materiale che è stato utilizzato per l'ottenimento di qualunque altro titolo o diploma dell'università o altro istituto di apprendimento, a eccezione del caso in cui ciò venga riconosciuto nel testo.

Giulio Galla / 02 febbraio 2009

Una copia della tesi sarà disponibile presso *http://paduaresearch.cab.unipd.it/*

Contents

Riassunto

Il ciclo vitale nelle piante è determinato dall'alternanza della generazione sporofitica e gametofitica, quest'ultima costituita dal granulo pollinico e dal sacco embrionale. La sessualità nelle piante, riassumibile con la generazione dei gameti e la loro fusione, dà la possibilità di originare nuovi genotipi nelle progenie, derivanti dalla ricombinazione dei geni durante la meiosi nei genotipi parentali e dalla loro combinazione attraverso la fecondazione. Al contrario, tra le angiosperme, diverse specie sia monocotiledoni che dicotiledoni sono caratterizzate da riproduzione apomittica, ovvero da formazione di seme geneticamente materno prodotto in maniera agamica, in assenza di meiosi e di fecondazione. Tra le specie utilizzate come modello per lo studio dell'apomissia, *Hypericum* spp. e *Boechera* spp. sono sicuramente due tra quelle più importanti. Inoltre, mutanti caratterizzati dalla produzione di megaspore apomeiotiche sono stati scoperti e descritti in popolazioni naturali di numerose specie sessuali. All'interno della definizione generale di apomissia, due principali modelli sono stati definiti per spiegare l'origine materna delle progenie in conformità alle caratteristiche genetiche e funzionali del prodotto finale del processo agamico. Più in dettaglio, le due tipologie di apomissia gametofitica e sporofitica definiscono due strategie riproduttive alternative che portano rispettivamente alla formazione di un gametofito apomeiotico, come nel caso di *Boechera* spp. e *Hypericum* spp., o alla generazione di un sporofito avventizio, come in *Citrus* spp. Concentrandosi sulla prima categoria, i due possibili modelli aposporico e diplosporico sono attivi, rispettivamente, nei due generi *Hypericum* e *Boechera*.

Recentemente è stato ipotizzato il coinvolgimento del gene *Mob1*-simile nella progressione alterata della meiosi in un mutante apomeiotico di erba medica produttore di ovocellule non ridotte. Una dettagliata analisi bioinformatica, realizzata studiando 192 sequenze dedotte dai 43 genomi attualmente sequenziati, ha consentito di delucidare la struttura della famiglia multigenica di cui fa parte questo gene e di indagare l'evoluzione della famiglia passando da organismi unicellulari ad organismi pluricellulari. Lo studio delle possibili funzioni del gene in relazione al processo riproduttivo è stato realizzato nella pianta modello *Arabidopsis thaliana*, attraverso il silenziamento post-trascrizionale del gene mediante RNAi. Le analisi morfologiche e cito-istologiche condotte nelle linee transgeniche hanno evidenziato alterazioni nell'architettura della pianta e soprattutto una

parziale sterilità, come dimostrato dalla forte riduzione della produzione di seme. Osservazioni citologiche condotte negli ovuli hanno messo in evidenza alterazioni multiple a carico dei processi di sporogenesi e gametogenesi femminile responsabili, rispettivamente, della formazione di megaspore binucleate e della degenerazione di megagametofiti. L'identificazione di piante poliploidi nelle progenie delle piante silenziate per il gene *Mob1*-simile suggerisce l'esistenza di meccanismi apomeiotici responsabili della produzione di ovocellule non ridotte funzionali.

Informazioni recentemente acquisite hanno dimostrato che *H. perforatum* può essere considerato un sistema adatto allo studio del modello aposporico dell'apomissia. Un approccio multidisciplinare è stato perseguito nel tentativo di chiarire le basi genetico-molecolari e citologiche dell'apomissia in *Hypericum* spp. La formazione del sacco embrionale e la costituzione genetica del seme sono stati analizzati, rispettivamente, per mezzo di indagini citologiche di ovuli ed ovari in combinazioni con analisi DIC e attraverso analisi di citometria di flusso di semi (FCSS). Una indagine dettagliata della sporogenesi e della gametogenesi femminile ha permesso di definire le principali caratteristiche morfologiche delle strutture che svolgono un ruolo chiave nella formazione del sacco embrionale. Al contempo le analisi FCSS, attraverso la stima del contenuto di DNA nucleare di embrione ed endosperma, hanno fornito un potente strumento per lo studio del complesso scenario di riproduzione che si origina in *Hypericum* attraverso la concomitante produzione di gameti maschili e femminili sia ridotti che non ridotti. Inoltre, l'organizzazione del genoma di *H. perforatum*, con *H. maculatum* e *H. attenuatum* è stata studiata per mezzo di diversi approcci genetico-molecolari. L'ipotesi che *H. perforatum* possa essersi originato da un antico evento di ibridazione interspecifica tra la specie diploidi *H. attenuatum* e *H. maculatum* è stato valutato attraverso l'isolamento di marcatori molecolari co-dominanti di tipo SNP e la loro applicazione in *H. perforatum* e nei putativi progenitori. Inoltre, una nuova tecnologia di marcatori molecolari è stata messa a punto per l'amplificazione selettiva di membri di famiglie multigeniche ed in seguito applicata per la costruzione di mappe genetico-molecolari funzionali di *H. perforatum*. Infine, l'espressione temporale di due geni della famiglia genica APOSTART, ritenuti potenzialmente coinvolti nella regolazione dell'apomissia, è stata

studiata mediante Real-Time PCR al fine di chiarire il loro ruolo sul controllo genetico dell'apomissia in *H. perforatum*.

Summary

Plant life cycle is determined through the alternation of a sphorophytic (2n) and gametophytic (n) generations, the latter being constituted by the pollen grain and the embryo sac. Sexuality in plants, exemplified by the generation and fusion of gametes, represents the challenge of potentially new genotype formation by combining previous genome sets. By contrast to sexualtiy, apomixis defines a number of strategies leading to the production of seed without fertilization. Within angiosperms, both monocotyledons and dicotyledons plants are known to reproduce asexually by seeds, *i.e*. apomixis. Among the species used as a model for reproduction studies, *Hypericum* spp. and *Boechera* spp. are undoubtedly two of the most important ones. Moreover, the occurrence of mutants producing apomeiotic megaspores in wild populations have been reported in different sexual species. Besides the general definition of apomixis, two main models have been defined to explain the asexual behaviour on the basis on the functional characteristics of the final product of the illegitimate process. More in detail, gametophytic and sporophytic apomixis define reproductive strategies leading to the formation of a functional megagametophyte, as in *Boechera* spp. and *Hypericum* spp., or to a newly generated sporophyte, as in *Citrus* spp. and *Malus* spp. Focusing on the former category, the two aposporic and diplosporic models have been reported as actively present within the genera *Hypericum* and *Boechera*, respectively. A candidate gene for apomeiosis, named *Mob1*-like, was recently identified in a *Medicago* spp. mutant where non-conventional production of 2*n* egg cells takes place. A computational approach was attempted to clarify the Mob1 multigene family structure and its member composition. Results suggested that an expansion of this family occurred concomitant to the evolution from unicellular to multicellular organisms. Moreover, in order to study the reproductive implications of the *Mob1*-like gene, its functional characterization was carried out by post-transcriptional gene silencing using the model species *Arabidopsis* as biological system. Morphological and cyto-histological analyses mainly were focused on the reproductive process and, besides an alteration of the plant architecture, partial plant sterility was documented in the transgenic lines. Moreover, detailed inspections of ovule development led to the identification of multiple alterations of the mega-sporogenesis and gametogenesis

pathways responsible for the formation of unreduced megaspores and altered megagametophytes.

Concerning the aposporous type of apomixis, recently gained information has shown that *H. perforatum* is an attractive model system for the study of the asexual process. A multidisciplinary approach was attempted to shed light on the molecular and cytological bases of apomixis in *Hypericum* spp. The embryo sac formation and the seed genetic constitution were studied by means of stain-clearing supported by DIC microscopy of ovules/ovaries and FCSS analyses of embryos/endosperm, respectively. Our detailed analyses of female sporogenesis and gametogenesis enabled to define the major morphological features of all elements playing a role in the formation of aposporic initials and embryo sacs. FCSS analysis provided a powerful tool to study the complex reproductive scenarios involving reduced and unreduced male and female gametes. Furthermore, the genome organization of *H. perforatum* along with *H. maculatum* and *H. attenuatum* was investigated by means of different genetic approaches. The hypothesis that *H. perforatum* arose from an ancient interspecific hybridization event between the diploids *H. attenuatum* and *H. maculatum* was tested by the isolation of codominant SNP markers and their investigation in *H. perforatum* and its putative ancestors. Moreover, a new technology of DNA fingerprint has been tested and applied for the construction of the first linkage maps in *Hypericum perforatum*. Finally, the temporal expression of two Apostart genes, potentially involved in the apomictic reproductive machinery, were investigated by Real-Time PCR, providing new insights on the genetic control of apomixis in *H. perforatum*.

Capitolo I

Characterization and evolution of the cell cycle-associated Mob domain-containing proteins in Eukaryotes

Abstract

The MOB family includes a group of cell cycle-associated proteins highly conserved throughout eukaryotes, whose founding members are implicated in mitotic exit and co-ordination of cell cycle progression with cell polarity and morphogenesis. Here we report the characterization and evolution of the MOB domain-containing proteins as inferred from the 43 eukaryotic genomes so far sequenced. We show that genes for Mob-like proteins are present in at least 41 of these genomes, confirming the universal distribution of this protein family and suggesting its prominent biological function. The phylogenetic analysis reveals five distinct MOB domain classes, showing a progressive expansion of this family from unicellular to multicellular organisms, reaching the highest number in mammals. Plant Mob genes appear to have evolved from a single ancestor, most likely after the loss of one or more genes during the early stage of Viridiplantae evolutionary history. Three of the Mob classes are widespread among most of the analyzed organisms. The possible biological and molecular function of Mob proteins and their role in conserved signaling pathways related to cell proliferation, cell death and cell polarity are also presented and critically discussed.

Introduction

Normal development of multicellular organisms requires appropriate cell numbers and organ sizes, and it is determined by coordinated cell proliferation, cell growth and programmed cell death (reviewed by Danial and Korsmeyer, 2004; Murray 2004; Sherr, 2004). Disruption or malfunction of these processes can cause diseases, such as cancer. Recent studies in yeasts and higher eukaryotes have led to the identification of a number of proteins and their interactors as key components of specific metabolic pathways that control the coordination between cell proliferation, morphogenesis and programmed cell death (Lai *et al*., 2005).

Members of the NDR (nuclear Dbf2-related) family, a subclass of AGC-type protein kinases, are essential components of pathways that control important cellular processes, such as mitotic exit, cytokinesis, cell proliferation and morphogenesis, and apoptosis (reviewed by Hergovich *et al*., 2006). Some recent progress in this field has shed light on the mechanisms that underlie the regulation and function of the NDR proteins by means of the co-activator Mob (Mps1-one binder) proteins. Combined data from yeast, worms, flies, mice and human cells have highlighted the conserved and important roles of MOB-domain containing proteins in the activation of NDR kinases (Manning *et al*., 2002; Hergovich *et al*., 2006). In particular, Mob proteins play a critical role in cell-cycle regulation chiefly by interacting with and activating the Dbf2-related protein kinases (Komarnitsky *et al*., 1998; Lee *et al*., 2001; Mah *et al*., 2001). This subfamily of serine/threonine kinases includes Dbf2, Dbf20 and Cbk1 in *Saccharomyces cerevisiae*, Ndr1, Ndr2, Lats1 and Lats2 in human, Warts (aka dLats) and Trc (aka dNdr) in *Drosophila melanogaster* and Sax1 (aka ceNdr) and a hypothetical Lats homolog in *Caenorhabditis elegans*. Like their Mob protein partners, this subfamily of protein kinases regulates cell growth, cell division and cell morphology (Justice *et al*., 1995; Xu *et al*., 1995; Zallen *et al*., 2000). In metazoans, members of the NDR family act as tumour suppressors (for example, LATS1) or potential proto-oncogenes (for example, NDR1). In the molecular regulation of the NDR family kinases, an important role is also played by protein kinases belonging to the sterile 20 (STE20)-like kinase group (for review see

Hergovich *et al*., 2006). A summary of available informations on Mob-domain containing proteins and its interacting NDR-type kinases is given on Table 1.

Mob proteins interact with NDR kinases by binding a conserved stretch of primary sequence at their N terminus, also known as NTR (N-terminal regulatory) domain. The interaction of Mob proteins with the NTR activation site is a conserved feature of all members of the NDR-kinase family that have been tested so far in yeasts, flies and human cells (Mrkobrada *et al*., 2006). Interestingly, Mob proteins do not function solely as co-activators of NDR kinases, but are also required for the localization of yeast NDR kinases. Recent evidence further indicates that the targeting of Mob proteins to the plasma membrane is sufficient to fully activate mammalian NDR1/2 (Hergovich *et al*., 2005; Stegert *et al*., 2005) and LATS1 (Hergovich *et al*., 2006). Taken together, these findings indicate that Mob binding to the N terminus of NDR family members allows efficient auto-phosphorylation on the activation segment and at the same time recruits NDRs to activation sites, thereby bringing this protein into close proximity with its upstream activating kinase.

The MOB family includes a group of cell cycle-associated, non-catalytic proteins highly conserved in eukaryotes, whose founding members are implicated in mitotic exit and co-ordination of cell polarity with cell cycle progression (Luca *et al*., 2001; Stegmeier *et al*., 2002). Two distinct Mob proteins, Mob1 and Mob2, are known in fungi, while an expansion in metazoans gives rise to six in human, four in *D. melanogaster*, and four in *C. elegans* (Mrkobrada *et al*., 2006). Mob1 proteins have been demonstrated to be important for both mitosis completion and cell plate formation in yeast (Luca and Winey, 1998; Salimova *et al*., 2000). Moreover, the Mob1-related proteins Mob2 physically associates with specific kinases throughout the cell cycle, being required and periodically activated in yeast to promote polarized growth (Weiss *et al*., 2002; Nelson *et al*., 2003). Mob1-like proteins have been also found in animals (Stavridi *et al*., 2003; Ponchon *et al*., 2004; Devroe *et al*., 2004). Plant genomes such as alfalfa, rice and *Arabidopsis* contain uncharacterized Mob1-related genes (Van Damme *et al*., 2004; Citterio *et al*., 2005; 2006). Although there are data to suggest that Mob proteins act as kinase activating subunits in higher eukaryotes, their function remains to be proved.

Table 1. Summary of available data on Mob-domain containing proteins and its interacting NDR-type kinases.

Organism	Protein name	Accession	Description	Group	Subcellular localization	Interacting kinases
Saccharomyces cerevisiae	Mob1p	NP_012160	Component of the MEN	-	Spindle pole body and bud neck	Dbf2-Dbf20
	Mob2p	NP_116618	Component of the RAM signalling network	-	Nucleus, cytoplasm and cortex	Cbk1
Schizosaccharomyces pombe	Mob1p	NP_595191	Component of the SIN	-	Spindle pole body and mitotic septum	Sid2p
	Mob2p	NP_587851	Involved in cell polarity maintenance	-	Mitotic septum	Orb6p
Caenorhabditis elegans	-	NP_510184	F09A5.4c	-		
	-	NP_502248	F38H4.10	-		
	-	NP_498798	C30A5.3	3		
	-	NP_501179	T12B3.4	4		
Drosophila melanogaster	dMob1	NP_729716	CG11711-PB. Mob1, isoform B	2		Trc (dNDR)/Warts (Lats)
	Mats	NP_651041	CG13852-PA. Mob as tumor suppressor	1		Trc (dNDR)/Warts (Lats)
	dMob3	NP_609364	CG4946-PA	4		-
	dMob4	NP_610229	CG3403-PA	3		-
Homo sapiens	hMOB1	NP_775739	MOB-KL1A, MOB kinase activator-like 1A (MOB1A)	1	Nucleus, cytoplasm and membrane	LATS1/2 (low affinity for NDR1/2)
	MATS1	NP_060691	MOB-KL1B, MOB kinase activator-like 1B (MOB1B)	1	Centrosome, poles of mitotic spindle and midbody	LATS1

Table 1. Continue from the previous page.

Organism	Protein name	Accession	Description	Group	Subcellular localization	Interacting kinases
	hMOB2	NP_443731	HCCA2 protein	2	Nucleus, perinuclear region and cytoplasm	NDR1/2
	hMOB3A	NP_955776	PREI3, preimplantation protein (Phocein)	3	Perinuclear region, membrane	PP2A
mo sapiens	hMOB3B	NP_079037	MOB-KL2B, MOB kinase activator-like 2B	4b		
	hMOB3C	NP_958805	MOB-KL2C, MOB kinase activator-like 2C	4a		
	MOB-LAK	NP_570719	MOB-LAK, metal ion binding	4b	Intracellular	
	Mob1A	NP_199368	Similar to yeast Mob1p	p	Nucleus	
	Mob1B	NP_193640	Mob1-like domain containing protein	p		
Arabidopsis thaliana	Mob2A	NP_197544	Similar to yeast Mob2p	p	Nucleus	
	Mob2B	NP_197543	Similar to yeast Mob2p	p	Fragmoplast	
	Mob1A	CAC41010	Similar to yeast Mob1p	p	Cytoplasm and cell plate	
Medicago sativa	Mob1B	CAG25780	Similar to yeast Mob1p	p		
	Mob1A	AAL10512	Mob1-1 essential for cytokinesis but not for mitotic exit	-	Cytoplasm	tbPK50 (functional homologof Orb6)
Trypanosoma brucei	Mob1B	AAL10513	Cell cycle associated protein Mob1-2	-		

This chapter deals with the characterization and evolution of the cell cycle-associated and morphogenesis-related MOB domain-containing proteins belonging to 43 eukaryotic genomes. Results on the structural characteristics and phylogenesis of Mob proteins are reported, and adopted for the classification of family members using a novel nomenclature. The biological and molecular function of Mob proteins and their role in conserved signaling pathways related to cell proliferation, cell death and cell polarity are also presented and critically discussed.

Methods for bioinformatic analyses

To perform a complete and exhaustive analysis on the Mob domain distribution and phylogenetic relationship among eukaria, the proteomes of 43 complete and ongoing eukaryotic genomes were downloaded from NCBI (ftp://ftp.ncbi.nih.gov/genomes/), ENSEMBL (ftp://ftp.ensembl.org/pub) and DOE Joint Genome Institute (http://genome.jgi-psf.org/euk_home.html) sites.

The hidden Markov model profile for the Mob domain (Pfam code: PF03637) was downloaded from the Pfam site (http://www.sanger.ac.uk/Software/Pfam/) (Sonnhammer *et al*., 1998) and was used to search for similarity against the proteome databases using HMMER software (Durbin *et al*., 1998).

Using a cut-off expectation value equal or lower than e^{-20}, a total of 202 MOB domain containing proteins were identified. Among these, ten sequences were not considered in the subsequent analysis because of low quality problems. As many as 192 Mob domains were extracted from the original sequences and aligned using the progressive alignment algorithm implemented in CLUSTALW (Higgins *et al*., 1992), and the result was edited to remove any ambiguous region.

The ProtTest software (http://darwin.uvigo.es/) (Abascal *et al*., 2005) was used to select the most appropriate amino acid substitution models for tree construction. Phylogenetic tree was generated from Mob domain amino acid sequences using the linux version of PhyML (Guindon *et al.*, 2003) with JTT+I+G as protein model evolution and with a bootstrap analysis of 200 re-sampling runs.

The phylogenetic analysis allowed the identification of different Mob groups. The proteins belonging to different branches of the phylogenetic tree were aligned using CLUSTALW software and a consensus sequence was extracted for each group. The consensus sequences reflect the most common sequences in the alignment. For a more detailed analysis and visualization of each aligned group, a web logo was created using the web version of WebLogo software (http://weblogo.berkeley.edu).

Results: structural analysis of Mob proteins

Primary structure characteristics and classification of family members

Mob proteins are a small family of highly conserved proteins, found in all eukaryotes, approximately 210 to 240 amino acid residues in length. The evolution of MOB family genes is poorly understood and a classification and nomenclature of Mob genes is not fully established. Here we propose some insight into the evolutionary dynamics of this family and a system of classification based on a phylogenetic analysis of Mob genes in all complete and ongoing eukaryotic genome sequences.

Mrkobrada *et al.* (2006) proposed a classification based on the alignment of the core domain of Mob proteins from yeast to human, identifying three distinct groups defined by similarity between the conserved N-terminal regions. On the basis of the distribution of ScMob1 and ScMob2 members within the clusters, they referred to the groups as Mob1-like, Mob2-like and Mob3-like. The Mob1-like group contains two subgroups (A and B): Mob1A contains the ortholog of ScMob1 in fungal species and single proteins from *H. sapiens* and *D. melanogaster*, whereas the Mob1B group contains one or more Mob proteins from *H. sapiens*, *D. melanogaster*, *D. rerio, C. elegans* and *X. laevis.* The Mob2-like cluster contains two groups, Mob2A, consisting of the fungal ortholog ScMob2 and a second group, Mob2B, containing metazoan genes. Finally, the Mob3-like group is the most divergent one and contains a single protein from each metazoan organism analyzed. Moreover, two mammalian homologs to yeast MOB genes have been described, the mammalian Mob homolog (MMh), that has high similarity with *S. cerevisiae* Mob2 genes, and phocein or mammalian Mob1 distantly related to MOB1 and MOB2 (Hennebold *et al.*, 2000; Baillat *et al.*, 2001; 2002; Moreno *et al.*, 2001). Stavridi *et al.* (2003) proposed

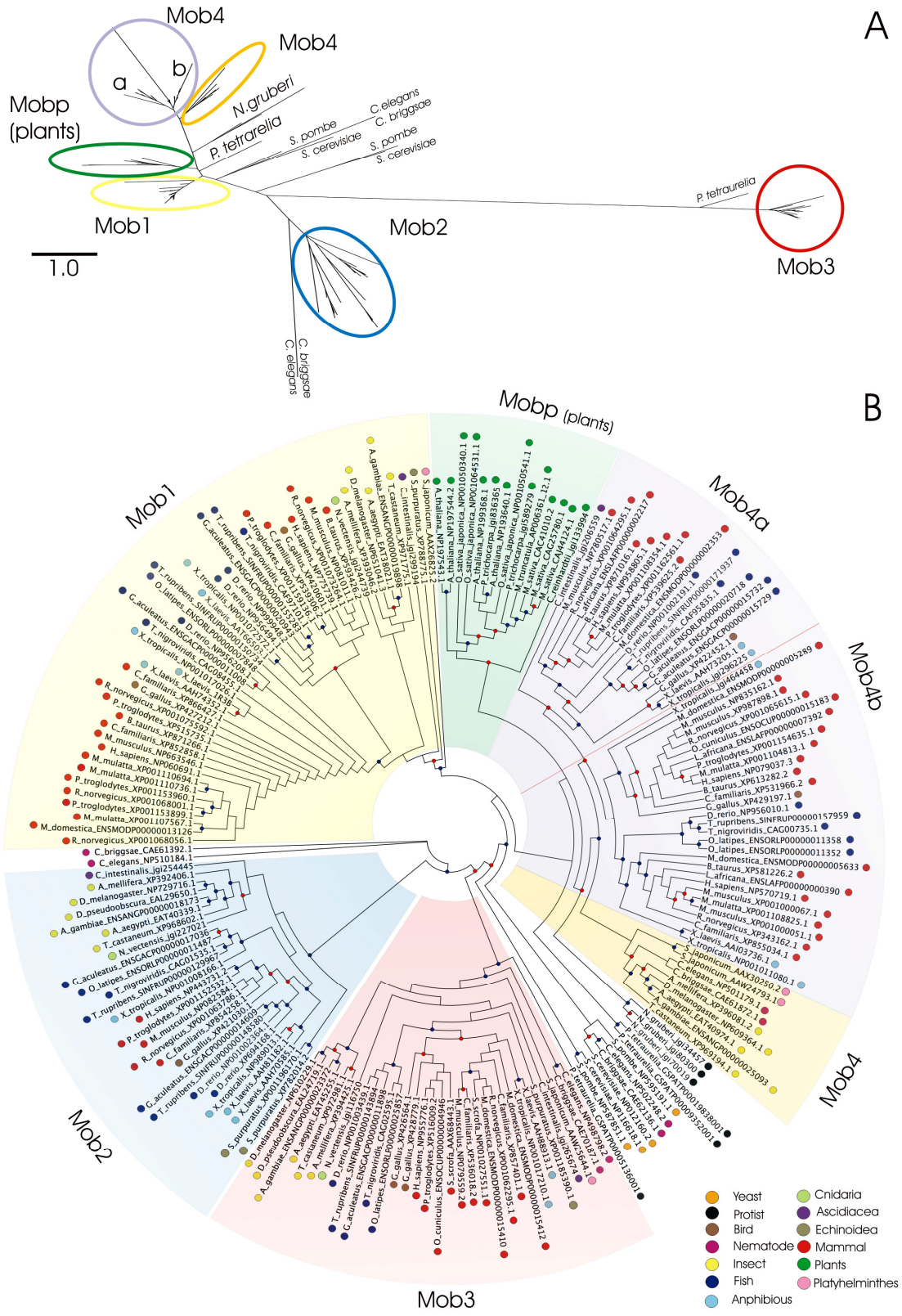

Figure 1. Phylogenetic tree of the 192 Mob domain proteins. Mob groups identified with the phylogenetic analysis are shown and highlighted in different colors.

Continue - Figure 1 The Panel A shows a maximum likelihood Mob protein phylogenetic tree (the scale represents the number of amino acid substitution per site). The Panel B shows a maximum likelihood cladogram without branch length for an easier visualization of the Mob groups (the colored dot on each organism name refers to the taxonomy classifi cation). The red dot on each node of the tree represents a bootstrap value equal or higher than 50%, while the blue dot a bootstrap value equal or higher than 70%.

that 2MMh be referred to as Mob2 and that phocein/mMob1 be referred to only as phocein.

To classify the Mob domain into related groups of sequences, a phylogenetic analysis was performed, by searching Mob domain hidden Markov model profile on all complete or ongoing available eukaryotic genomes. Figure 1 shows the phylogenetic tree for 192 Mob genes. The results highlight that Mob domain is clearly separated into five classes: Mob1, Mob2, Mob3, Mob4 and Mobp with high bootstrap support. Among the different classes, Mob3 is the most divergent clade.

The numbers of genes in class Mob1, Mob2, Mob3, Mob4 and Mobp are 47, 28, 31, 57 and 14 respectively. Some of the *C. elegans* and *C. briggsae*, and *S. cerevisiae*, *S. pombe* and Protist Mob related proteins clustered outside these groups and they will be treated separately. Mob4 class can be subdivided into two phylogenetic clades, corresponding to invertebrate (9 genes) and vertebrate Mob-like genes (48).Moreover, vertebrate Mob-like genes can be further subdivided into other two subgroups, Mob4a, containing 19 genes, and Mob4b with 29 Mob like proteins. The average amino acid identity within Mob classes is 92% (Mob1), 54% (Mob2), 86% (Mob3), 70% (Mob4), 86% (Mob4a), 84% (Mob4b) and 78% (Mobp).

The results partially support the previous classification by Mrkobrada *et al.* (2006). The main differences are probably due to the higher number of genes analyzed in this study and concern the Mob1 class which was previously subdivided into two groups, Mob1A and Mob1B. Our analysis allowed us to recognize a Mob1 class that corresponds to Mob1A group and a Mob4 class that contains the previously established Mob1B group (see Mrkobrada *et al*., 2006). Moreover, both Mob4a and Mob4b groups proved to contain Mob-like genes previously annotated as part of the Mob1B group (Mrkobrada *et al*., 2006).

Phylogenesis: distribution and evolution of Mob genes in eukaryotic genomes

The phylogenetic tree shown in Figure 1 has been generated from the available proteomes of 43 complete and draft genomes. Only in two plant genomes, *Ostreococcus tauri* and *Zea mays*, it was not possible to identify Mob-like proteins. This could be due to the consensus sequence quality and to the genome assembly; both of them being quite important issues for producing a high quality alignment and a reliable counting of Mob genes. Figure 2 shows the distribution of Mob-like proteins among the organisms used for the analysis. Vertebrates (mammals, birds, amphibian and fish) have the highest number of Mob genes, distributed in all the Mob classes. Interestingly, all the vertebrate genes of the Mob4 class are included in a single branch that is supported by a bootstrap value of 77%. This suggests that all Mob4-like vertebrate genes derived from a single ancestral gene at the basis of Mob4 chordata/hemichordate gene evolution.

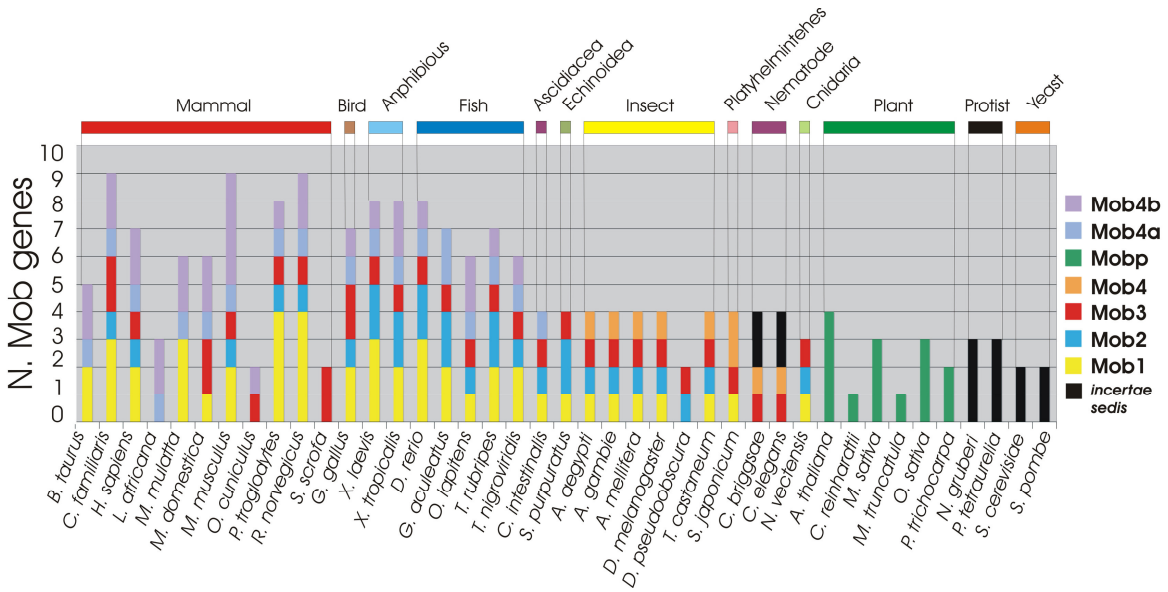

Figure 2. Mob protein distribution among organisms used in the analysis. Different Mob groups are represented with different color and the species grouped on the base of the taxonomy classifi cation. The label "*incertae sedis*" refers to Mob proteins that have an undefined position on the phylogenetic tree.

The two subclasses Mob4a and Mob4b found in vertebrates must have arisen from an early duplication, which further subdivided this class into two subgroups. Among vertebrates, mammals reveal the highest number of Mob genes. *M. musculus* have the highest number of Mob4b genes (4), while *P. troglodytes* and *R. norvegicus* have the highest number of Mob1 genes (4). *L. africana*, *O. cuniculus* and *S. scrofa*, compared to the other mammals, present a smaller number of Mob genes, probably reflecting a still limited coverage of the entire gene space of these organisms.

Mrkobrada *et al.* (2006) reports that the genome of *Homo sapiens* contains six Mob-like proteins whereas in our analysis we found seven Mob-like proteins. Nomenclature of Mob genes not only is poorly established but often can be quite misleading. Proteins identified by codes NP_060691 and NP_775739 are annotated as "Mob4B" and "MOB1, Mps One Binder kinase activator-like 1A" respectively, while in our phylogenetic tree they both fall in Mob1 group. NP_443731 is a member of the Mob2 group but it is annotated as "HCCA2 protein". Moreover protein NP_955776 in public databases is defined as "preimplantation protein 3 isoform 2" and in our analysis belongs to the Mob3 group. Finally, NP_958805 , NP_079037, NP_570719 proteins, annotated respectively as "MOB1, Mps One Binder kinase activator-like 2C isoform 2", "MOB1, Mps One Binder kinase activator-like 2B" and "MOB-LAK", are all members of the Mob4 group, with the first one belonging to Mob4a and the last two to Mob4b group.

All insects show four Mob genes belonging respectively to Mob1, Mob2, Mob3 and Mob4 classes, except *D. pseudoobscura*, in which only two Mob genes can be found, probably due to genome assembly quality. Finally, plants represent a monophyletic group defined as Mobp class.

The phylogenetic tree shows that *S. cereviseae* (NP_012160, NP_116618), *S. pombe* (NP_595191, NP_587851), *C. elegans* (NP_502248, NP_510184), *C. briggsae* (CAE62136, CAE61392) and Protist proteins are listed as *incertae sedis*. Because of historical reasons, in the previous literature Mob yeast genes have been generally described as the founding members of the Mob family (Stavridi *et al.*, 2003, Mrkobrada *et al.*, 2006). However, the protein sequences analyzed in this work, mostly of multicellular organisms, do not allow a clear definition of the phylogenetic relationships existing among the yeast and the other Mob genes. In this regard it is interesting to point out that

NP_116618 and NP_587851 yeast proteins, described as Mob2A in Mrkobrada *et al.* (2006), did not cluster with any other protein, possibly due to an early divergence of these orthologs in the lineage that generated modern Fungi.

Even if it is quite difficult to reconstruct the evolution of the Mob family as a whole, some possible scenarios can be drawn by looking at the distribution of genes in the so far sequenced organisms. If plants are not considered, Figure 2 indicates a minimum of two genes in all the eukaryotic genomes analyzed. This in turn seems to suggest a duplication of the ancestral Mob gene at an early stage of the eukaryotic evolution.

Going from unicellular to multicellular organisms there is a progressive expansion of the Mob family, reaching the highest number in mammals. Moreover, plant Mob-like genes appear to have evolved from a single ancestor, most likely due to the loss of one or more genes during the early evolution of Viridiplantae. Compared to vertebrates, plants show a significant decrease in Mob-like gene possibly due to the adaptation to a much more simple life style. The relationship observed among genes of the same organism and/or different organisms suggests that the Mob gene family evolved under a birth-and-death type of evolution. In this model new genes are created by duplication, and some duplicated genes are maintained in the genome for a long time whereas other are deleted or become nonfunctional through deleterious mutations (Nei and Rooney, 2005).

Mob like protein structure and architecture of Mob-domain containing proteins

Three Mob1 protein structures have been described in literature. Human and *Xenopus laevis* structures correspond to the most conserved C-terminal core but lack the variable N-terminal region, whereas *Saccharomyces* Mob1 structure contains both the conserved C-terminal core and the variable N-terminal region (Stavridi *et al.*, 2003; Ponchon *et al.*, 2004; Mrkobrada *et al.*, 2006). In our phylogenetic tree, Human and *Xenopus* proteins used in structure analyses belong to the Mob1 group, while *Saccharomyces* Mob-like proteins have been assigned as *incertae sedis*. To compare the different Mob classes, a consensus sequence for each identified group was constructed. Figure 3 shows the amino acid sequence conservation over all positions for each of the seven Mob groups: Mob1, Mob2, Mob3, Mob4, Mob4a, Mob4b and Mobp.


Mob1
Mob2
Mob3
Mob4
Mob4a
Mob4b
Mobp

Figure 3. Sequence logos for each of the multiple alignment Mob groups: Mob1, Mob2, Mob3, Mob4, Mob4a, Mob4b and Mobp. Each logo consists of stacks of symbols, one stack for each position in the sequence: the overall height of the stack indicates the sequence conservation at that position, while the height of symbols within the stack indicates the relative frequency of each amino acid at that position. The yellow arrows represent the starting position adopted for the multiple alignment of Mob group consensus sequences.

These consensus sequences were then adopted to generate a new multiple protein alignment, using three additional Mob proteins, such as the *S. cerevisiae* Mob1 and Mob2 proteins (NP_116618 and NP_012160) and one *H. sapiens* Mob1 protein (NP_775739). The latter two proteins were added in the alignment since they have been structurally characterized (Stavridi *et al.*, 2003; Mrkobrada *et al.*, 2006). The final multiple alignment of Mob group consensus sequences in shown in Figure 4.

Mob proteins are approximately 210 to 240 amino acid residues in length, with the exception of *S. cerevisiae* Mob1, which has a further 78 residue N-terminal extension not conserved or even present in the closely related fungal proteins.

Mob1 adopts a globular structure consisting of seven α helices, two 3_{10}-helices and a β hairpin. The core of the structure consists of a helical bundle formed by four long α helices (H2, H4, H5, and H7). This left-handed four-helix bundle, comprising the H2 and H5 helices running anti-parallel to H4 and H7 helices, is capped at one end by two short helices (H3 and H6) and the β hairpin, which are stabilized to the helical bundle via a tetrahedrally coordinated zinc (Zn) atom. The sequences N-terminal to the core contribute one α helix (H1), whereas the sequences C-terminal to the core contribute helices H8 and H9 (Stavridi *et al.*, 2003). On one side, the structure has a flat surface consisting of H1 and H2 and parts of H3, H4, H6, and H7. Stavridi *et al.* (2003) reports that most of the conserved residues of Mob family members map to parts of the flat surface formed by H2 and two loops, L1 and L2, adjacent to the N-terminus of H2. Loop L1 in human Mob protein goes from residues 46 to 51 and Leu47 and Pro48 are highly conserved since are needed to stabilize the structure of the loop. These results are confirmed in our analysis, with the exception of position 47 in Mob3 consensus sequence where a Pro is present.

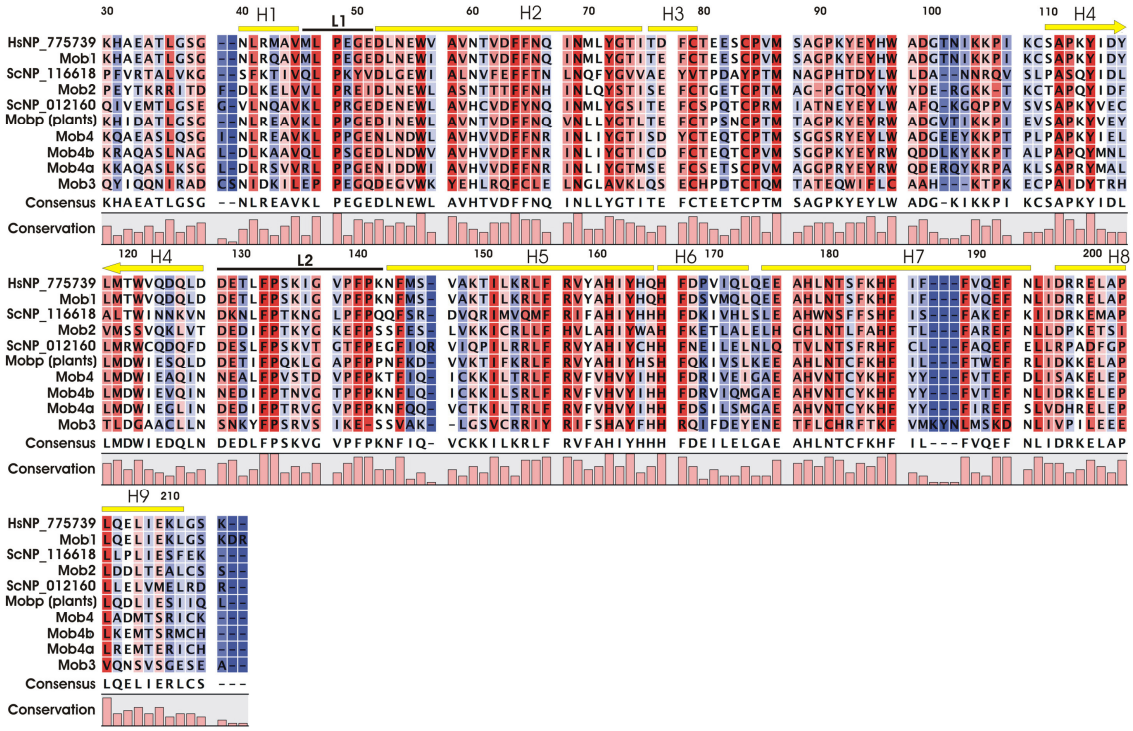

Figure 4. Multiple alignment of Mob group consensus sequences. The alignment was performed taking into consideration two structural defined Mob proteins, Hs NP_775739 and Sc NP_012160 plus Sc NP_116618. The helix (yellow lines) and loops (black lines) nomenclature and position on the alignment refer to Hs Mob protein as described by Stavridi *et al*. (2005). On each of the alignment columns, a colour scale going from red to blue represents high and low amino acid conservation respectively.

Moreover, Stavridi *et al.* (2003) reports the Glu51 is conserved only in Mob1 family. Figure 4 shows that Glu51 is conserved in Mob1 and Mob4 consensus sequences, while in Mob2 sequence is replaced by an isoleucine and in Mob3 by a glutamine. The L2 loop, consisting of residue 128-142, presents several highly conserved amino acids involved in structural interaction, such as Pro133 and Pro141 and Phe132 and Phe140 that, together with Phe144 from H5, form hydrophobic interactions with each other and with Ala58 and Ile151 from H2 and H5 respectively. Figure 4 shows that all these positions are conserved, except for Mob3 where various non-conservative amino acids changes can be seen in the consensus sequence (Phe140→Glu140, Phe144→Val144, Ala58→Tyr58). Moreover the Mob3 consensus sequence is missing the amino acid in position 141. Helix H2 has a large number of conserved residues, several of which have solvent exposed negatively charged side chains.While Stavridi *et al*. (2003) report that Asp52 is the only charged conserved residue in all Mob families, in our analysis we found that in Mob4 and Mob4a there is an

amino acid conservative substitution Asp→Asn. Moreover, we observed that Glu55, that makes a hydrogen bond with Glu51, is conserved in Mob1, Mob2 and Mobp groups while Mob4 contains aspartate and the consensus sequence of Mob3 contains a valine.

Asp63 interacts with His185, that is conserved in all Mob consensus sequences except for Mob3 that contains a lysine. Interestingly, Asp63 is conserved in all Mob4, Mobp and Mob1 classes, but it is replaced by a threonine in Mob2 and by a glutamine in Mob3.

Towards the C-terminal of helix H2 there is Asn69, the only polar residue other than tyrosines, that is conserved in all members of the Mob family. H2 also has several hydrophobic residues that are conserved to varying degrees in members of the Mob protein family: notably, Trp56 and Phe64, which should have buried side chains and participate in hydrophobic interactions that stabilize the protein fold, are conserved in all Mob consensus sequences.

A Zn binding site appears to be conserved in all Mob classes, with a peculiar exception in fungi. Considering human Mob1 protein as a reference, the Zn binding site is composed by Cys79 and Cys84 from loop connecting H3 to the first strand of the β hairpin and His161 and His166 from H5 (Stavridi *et al.*, 2003). The presence of the Zn atom contribute to the stability of the structure by anchoring H3 to the C terminus of H5. As reported in Mrkobrada *et al.* (2006) most of the yeast genes previously described as Mob2A apparently lack the Zn binding site, since the two cysteines are substituted with a valine and a tyrosine respectively, suggesting an alternative structural element for stability compensations. The consensus sequences alignment confirms these observations with the *S. cerevisiae* NP_116618 as the only Mob protein lacking the Zn binding site (Figure 4). To make sure that this observation was not due to a consensus artefact, we analyzed the complete 192 Mob-like protein multiple alignment and we found that essentially all the proteins analyzed contained a well conserved Zn binding site. The only exceptions, found in *M. musculus* XP_001000051, *S. purpuratus* XP_001185390 and *M. mulatta* XP_001108825, are probably due to bad quality sequences producing an unreliable alignment in the region that contains His161 and His166.

Biological roles of Mob proteins and conserved signaling pathways

Cell cycle progression and cytokinesis

The involvement of Mob proteins in cell proliferation was first suggested by Luca and Winey in 1998. They demonstrated that Mob1 is an essential yeast gene required for the completion of mitosis and maintenance of ploidy, as yeast Mob1 mutations resulted in a late nuclear division arrest at restrictive temperature. Following studies better elucidated the biological role of this protein in budding and fission yeasts. In *Saccharomyces cerevisiae* Mob1p is an essential regulator of the localization and activity of Dbf2 protein kinase, a component of the mitotic exit network (MEN). MEN is a GTPase driven signaling network that co-ordinates exit from mitosis with cytokinesis (Figure 5). It promotes the inactivation of the mitotic Cdk1-cyclin B complex and drives mitotic exit by leading to the release from the nucleolus and subsequent activation of the Cdc14p phosphatase during anaphase (Luca *et al.*, 2001; Stegmeier and Amon, 2004). Although inactivation of Cdk1-cyclin B complex is required for cytokinesis, the MEN was shown to be essential for cytokinesis, and in particular for actomyosin ring contraction and septum deposition, also independently of its role in mitotic exit. In fact, when MEN function is abrogated in conditions where mitotic exit is allowed by artificial suppression of mitotic CDK activity cytokinesis does not take place (Shou *et al.*, 1999; Lippincott *et al.*, 2001; Park *et al.*, 2003).

In *S. pombe* cytokinesis is regulated by a signaling cascade termed the septation initiation network (SIN). It is organized similarly to the MEN but is not involved in mitotic exit (reviewed by Simanis, 2003; Krapp *et al.*, 2004; Wolfe and Gould, 2005). In *S. pombe* Mob1 is part of the SIN and interacts with Sid2, the ortholog of *S. cereviasae* Dbf2, regulating its localization and kinase activity. Nevertheless, how Mob proteins can regulate kinase activity is still under investigation. By analyzing the NMR or X-ray crystal structures of *S. cerevisiae*, *X. laevis* and human Mob1p, it has been proposed that Mob proteins may regulate their target kinases through electrostatic interaction mediated by conserved charged surfaces. It seems that the negatively charged surface on MOB proteins

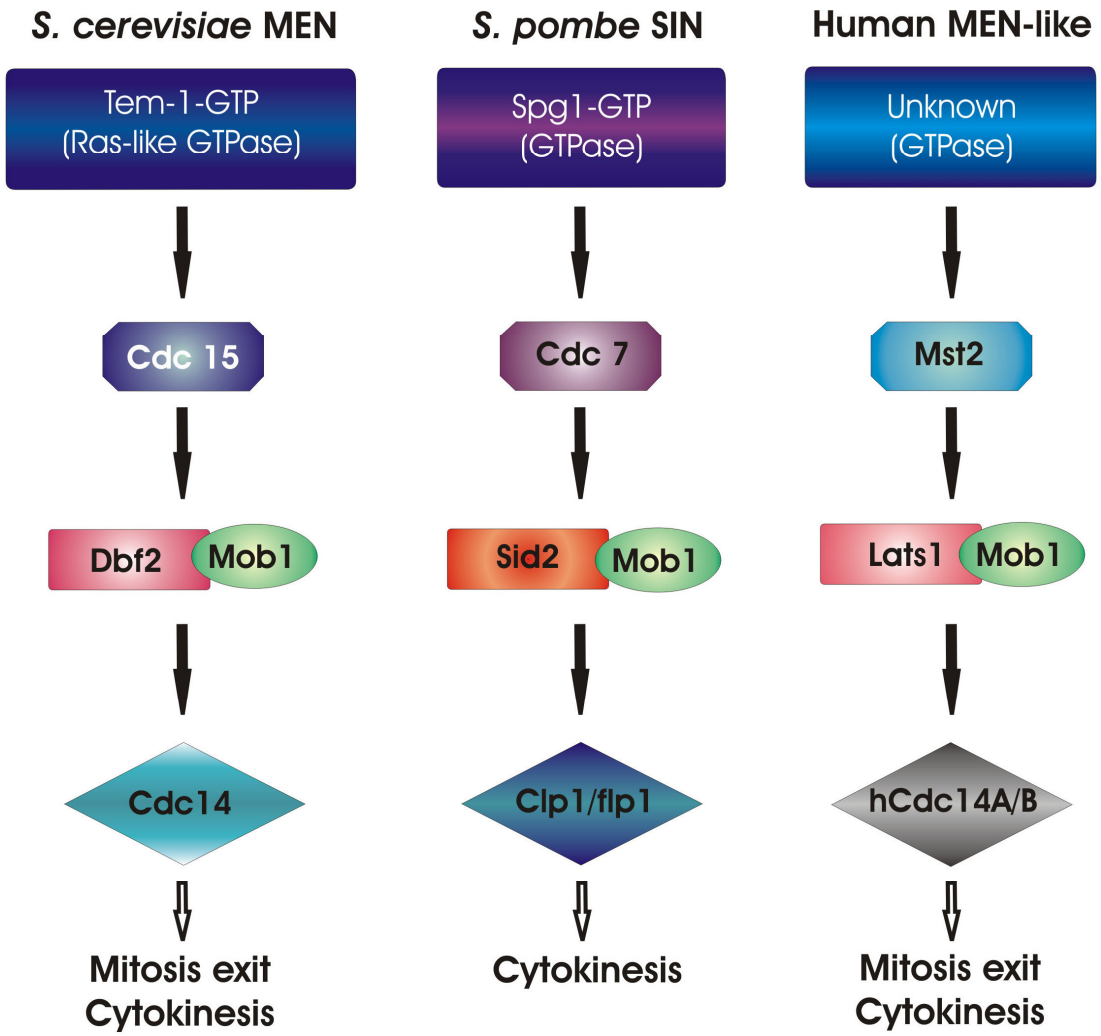

Figure 5. Components of the mitotic exit network (MEN) and septation initiation network (SIN) in yeasts *(Saccharomyces cerevisiae* and *Schizosaccharomyces pombe*), and of the MEN-like network in human cells. Exit from mitosis and co-ordination with cytokinesis is driven through a GTPase signaling network, where Mob1p is an essential regulator of the localization and activity of Dbf2 and Dbf2-like (Sid2 and Lats1) protein kinase. The network promotes the inactivation of the mitotic Cdk1-cyclin B complex and drives mitotic exit by leading to the release of the Cdc14p phosphatase from the nucleolus and its subsequent activation during anaphase.

interacts directly with the positively charged basic–hydrophobic N terminus of their target kinases Dbf2/Sid2, inducing a conformational change which enable the upstream kinase Cdc15/Cdc7 to phosphorilate and thereby stimulate DBf2/Sid2 activity. In this regard, MOB proteins may functionally resemble cyclins (Stavridi *et al.*, 2003; Ponchon *et al.*,

2004; Mrkobrada *et al.*, 2006). However, yeast Mob1 proteins do not function solely as activators of DBf2/Sid2, but are also required for Dbf2/Sid2 localization to activation sites (Frenz *et al.*, 2000; Lee *et al.*, 2001). It has been extensively reported that, in agreement with their functions in mitosis exit and cytokinesis, Dbf2/Sid2-Mob1 complexes localize to the spindle pole body (SPB) in anaphase and move to the division site in late mitosis (Stegmeier and Amon, 2004). Nevertheless, it must be underlined that the function of Dbf2/Sid2 in cytokinesis and how this complex ultimately leads to release of Cdc14 from the nucleolus during mitotic exit remain unclear. One reason is that, while the components of MEN that act upstream of Dbf2-Mob1 have been characterized, the molecular substrates for Dbf2-Mob1 have yet to be identified. At this regards Mah *et al.* (2005) determined that Dbf2-Mob1 preferentially phosphorylates serine over threonine and required an arginine three residues upstream of the phosphorilated serine in its substrate (RXXS motif).

Recent findings suggest also an involvement of MEN-Mob1p in coordinating chromosome segregation and/or spindle integrity with mitotic exit and cytokinesis via regulation of chromosome passenger proteins. Mob1p has been demonstrated to be essential for maintaining the localization of Aurora, INCENP, and Survivin chromosomal passenger proteins on anaphase spindles and for dissociating Aurora from the kinetochore region (Stoepel *et al.*, 2005). Consistent with these functions, the MEN protein kinase complex Mob1p-Dbf2p localizes to mitotic nuclei and partially co-localizes with Cdc14p and kinetochore proteins.

Overall the available data in yeast indicates an essential role of Mob1p in cell cycle progression, through the interaction with Dbf2/Sid2 protein kinases and reveals an essential temporal and spatial regulation of Mob1 activity.

MEN components are conserved through evolution and in particular Mob1 and Dbf2-related proteins have been found in both animal (Stavridi *et al.*, 2003; Ponchon *et al.*, 2004; Devroe *et al.*, 2004) and plant cells (Van Damme *et al.*, 2004; Citterio *et al.*, 2005, 2006), suggesting that their role in controlling cell cycle progression might be conserved in higher eukaryotes. The demonstration that animal Dbf2 homologous proteins NDR (nuclear Dbf2 related) genetically and physically interact with Mob1-related proteins (Bothos *et al.*, 2005; Hammarton *et al.*, 2005; He *et al.*, 2005; Lay *et al.*, 2005) and the

determination of the yeast, human and *X. laevis* Mob protein structures, suggest that Mob proteins act as kinase activating subunits also in higher eukaryotes.

Nevertheless the biological roles of MOB proteins are still to be understood. In higher eukaryotes multiple MOB members are involved in multiple pathways. To date two probably distinct signaling networks, namely MEN and HIPPO (Bothos *et al.*, 2005; Edgar, 2006), controlling cell proliferation and involving Mob1-like proteins have been recently proposed in *Drosophyla* and mammalian cells (see Hergovich *et al*., 2006). HIPPO pathway has been described in flies where participates to the control of tissue growth. This network includes cell cycle and cell death regulators, such as Hippo (Hpo), Salvador (Sav), Lats/Warts (dNDRs), Mats (Mob as tumor suppressor, dMob1) and Yorkie (Yki) factors (reviewed by Edgar, 2006). All components of the HIPPO pathway are well conserved in mammals and researchers have hypothesized that they share a similar function in humans. The complex Lats-Mob1A was also indicated as a component of the uncharacterized MEN network in higher eukaryotes. Bothos *et al.* (2005) have demonstrated that, similarly to ScMob1, hMob1A interacts and co-localizes with Lats1 at the centrosomes and midbody and that the suppression of Lats1 or hMob1A extends telophase but not other phases of mitosis. On the basis of the identification of evolutionary conserved MEN components the authors suggested the presence of a MEN conserved pathway in higher eukaryotes (Figure 5). Given the complexity of the interactions it is possible that different isoforms of hMob1A and Lats belong to specific network and/or that the activation of different pathways is organism, tissue and/or cellular context dependent. Also the subcellular localization of the hMob1A-Lats1 complex is likely determinant for Lats1 activation and function. Hergovich *et al.* (2006) demonstrated that the membrane-targeting of hMob1A results in a significant increase of Lats1 activity in mammalian cells, while the simple co-expression of Lats1 with hMob1A does not elevate Lats1 kinase activity. On the other hand, the presence of a MEN pathway in higher eukaryotes is also suggested by the study of Mob1 proteins in plants (Citterio *et al.*, 2006). *Medicago sativa* Mob1 proteins are mostly expressed in actively proliferating tissues and their localization pattern share many features with that of yeast, despite the differences in mitotic entry and progression between the two organisms. The subcellular localization of MsMob1-like proteins is cell cycle-regulated. In alfalfa cells, Mob1 proteins forms grains

in the cytoplasm from which fibrillar structures radiates in all directions, preferentially toward the cell mid-plane. These grains could likely correspond to sites in which microtubules are reorganized during cell cycle progression, the yeast SPBs, and barely detectable in G_1 and S cells, whereas become evident in G_2, forming cluster around the nucleus. In mitosis, they preferentially localize at the two opposite cellular poles. Differently from yeast, in alfalfa cells undefined Mob1 fibrillar structures are formed. In addition, during pre-prophase Mob1-like proteins mark the inner border of the cell wall in correspondence with the outer parts of the pre-prophase band, and in cytokinesis besides the progressive labeling of the septum, forms fibrillar structures, that partially co-localize with phragmoplast microtubules and partially form an aster, radiating from the growing septum poles. Overall the results collected so far in plants indicate that Mob1-like proteins are involved in cell proliferation, are expressed in a cell cycle-dependent manner and are localized to the cell division midplane during cytokinesis, marking the progressive formation of the phragmoplast, as shown in Figure 6. An interesting possibility is that Mob1-like proteins participate to the orientation of cell plate during cytokinesis, interacting with cytoskeletal structures and conjugating the determination of division site, marked by pre-prophase band before the onset of mitosis, with the septum formation (Citterio *et al*., 2006). Nevertheless the expression of MsMob1 could not rescue the lethality of the yeast mob1 mutant. This inability can be attributed to several reasons and does not rule out that the two genes do encode functional homologs. It is possible that MsMob1 does not bind efficiently to budding yeast Dbf2, thus explaining the lack of cross-complementation. Importantly, amino acid residues of ScMob1, such as T105, L196 and C221, that are changed in mob1 mutant alleles and presumably crucial for Mob1 function (Luca and Winey, 1998; Stavridi *et al.*, 2003), are replaced in a non-conservative way in the MsMob1 primary sequence, suggesting that in spite of their high degree of similarity the two proteins might have substantially diverged and that the interaction of Mob1 proteins with their effectors may be species-specific. On the whole, the available data strongly suggest that in higher eukaryotes as in yeast Mob1 members of MOB family play a role in the control of cell proliferation, through the regulation of NDR activity and localization. However further experiments are needed to better understand the roles of the single Mob1-like genes in each type of organism and tissue.

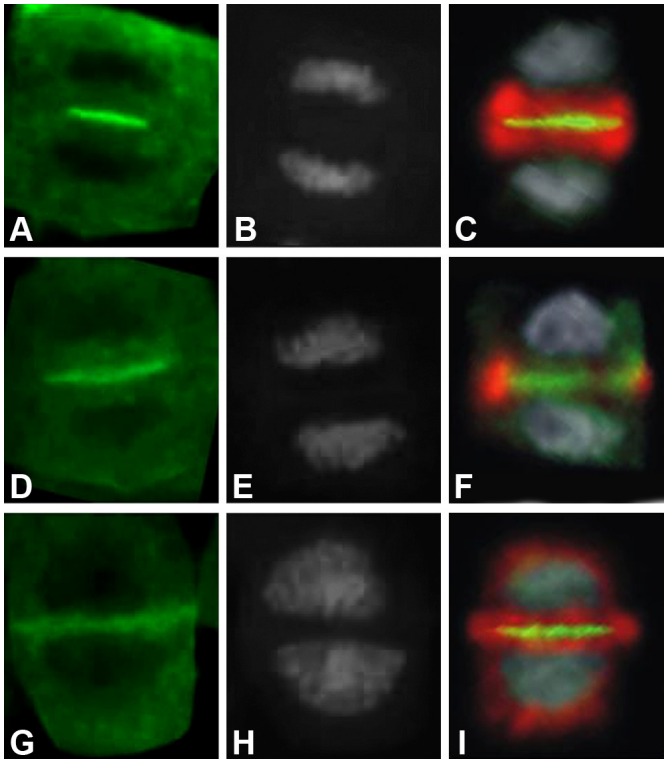

Figure 6. Results of the simultaneous immunolocalization of Mob1- like proteins (green fl uorescence, Panels A, D and G) and alpha tubulin (red fl uorescence, Panels C, F and I) in alfalfa cells during three successive stages of cytokinesis (the yellow fl uorescence represents tubulin and Mob1-like protein co-localization). DNA was also stained with DAPI (gray signal, B, E and H). Mob1-like proteins are localized to the cell division midplane during cytokinesis, marking the progressive formation of the phragmoplast (for additional information, see Citterio *et al*. 2006).

Apoptosis and programmed cell death

In a multicellular organism, the maintenance and surveillance of organ size is essential. Any imbalance in the relationship between cell size, cell proliferation and cell death must be prevented to allow proper organ development and to maintain the integrity of organ tissue over time. Failure to coordinate the creation of new cells (proliferation) and the elimination of excess ones (by apoptosis) can lead to diseases (Green and Evan, 2002). Mob proteins are involved in the control of cell death and its coordination with cell proliferation, being direct co-activators of NDR (nuclear Dbf2-related) kinases. Recent advances using *D. melanogaster* lead to the identification of a pathway that participates in the control of tissue growth (Harvey *et al*., 2003; Jia *et al*., 2003; Pantalacci *et al*., 2003; He *et al*., 2005; Huang *et al*., 2005). The control of cell death and proliferation by the

Hippo (hpo)-Large tumor suppressor (Lats) pathway was demonstrated and a similar pathway was also postulated in mammals (Figure 7). In *Drosophila*, four factors that induce tissue overgrowth without affecting pattern formation were identified: Sav, Hpo, Lats and dMob1/Mats (reviewed by Hergovich *et al*., 2006). Loss of any of these factors results in tissue overgrowth which is associated with increased cell proliferation and decreased cell death, indicating that Sav, Hpo, Lats and dMob1 all function as tumour suppressors. Genetic and biochemical independent studies indicate that Hpo interacts with Sav, which acts as a scaffold protein, and phosphorilates Warts-Mats. The association of Mats with Warts is essential in this regulatory process, as flies that carry mutation in Mats are unable to control tissue growth, despite having a functional Warts. Activated Warts has been proposed to negatively regulate the transcription of cell cycle and cell death regulators. Interestingly, the tissue overgrowth phenotype in *Drosophila* is accompanied by elevated levels of an important regulator of S-phase entry (i.e. cyclin E) and Diap1 (*Drosophila* inhibitor of apoptosis protein-1), an inhibitor of apoptosis. Moreover, *Drosophila* Salvador (Sav) interacts biochemically with Hpo, thereby facilitating the activation of Lats by phosphorylation (Harvey *et al*., 2003; Pantalacci *et al*., 2003; Wu *et al*., 2003). The activated Lats-dMob1 (*Drosophila* Mps1-one binder-1) complex then inactivates Yorkie (Yki) by phosphorylation (Huang *et al*., 2005). Phosphorylated Yki can not stimulate the expression of cyclin E and Diap1, which results in decreased cell proliferation (low cyclin E) and increased cell death (low Diap1). It is worth noting that the association of dMob1 with Lats is essential in this regulatory process, as flies that carry mutations in dMob1 are unable to control tissue growth, despite having a functional Lats (Lai *et al*., 2005). Therefore, Lats that is phosphorylated by Hpo needs to bind to its co-activator dMob1 to properly coordinate cell death and proliferation (Figure 7). As a matter of fact, cells that carry mutations in Hpo, Sav, Lats and dMob1 show an accelerated proliferation, but maintain a normal size. As a consequence, loss of these genes must stimulate cell growth and reduce cell death. In mammals, a similar pathway was postulated (Figure 7). Several human orthologs of the Hpo–Sav–Lats–dMob1–Yki pathway have emerged as putative tumour suppressors (Tapon *et al*., 2002; Lai *et al*., 2005; Takahashi *et al.*, 2005; Jimenez-Velasco *et al* ., 2005). Human mammalian sterile

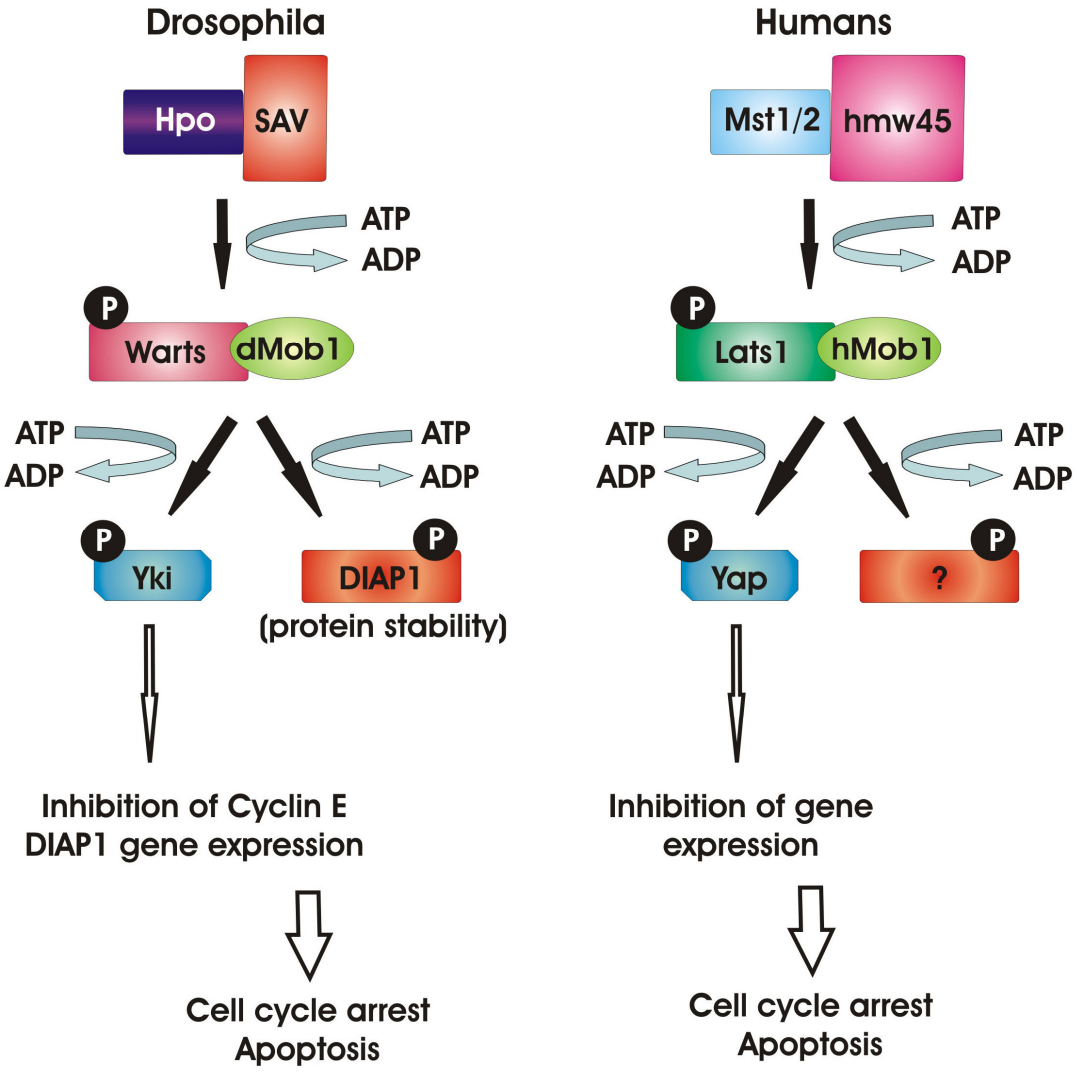

Figure 7. The HIPPO (hpo)-Large tumor suppressor (Lats) pathway validated in *Drosophila melanogaster* and its similar pathway recently postulated in mammals. The network involves Hippo (Hpo), Salvador (Sav), Lats1/Warts (dNDRs), Mats (Mob as tumor suppressor, dMob1) and Yorkie (Yki) factors, and participates to the control of tissue growth by regulating cell cycle arrest and cell death. In *Drosophila* Hpo interacts with Sav, which acts as a scaffold protein, and phosphorilates Warts-Mats. Activated Warts can negatively regulate the transcription of cell cycle and cell death regulators such as cyclin E and the apoptosis inhibitor DIAP1, through the phosphorilation of the non DNA binding transcriptional co-activator Yorkie. All components of the HIPPO pathway are well conserved in mammals and they have a similar function in humans since Lats1 (Warts), Mob1A (Mats), MST2 (Hippo) and Yap (Yorkie) genes can all functionally rescue their correspondent *Drosophila* mutants.

20-like kinase (MST1/2) associates with hWW45 (the human ortholog of Sav) and activates LATS1/2 by phosphorylation (Chan *et al*., 2005).The LATS–hMOB1 complex then potentially activates specific gene expression programs through YES-associated protein (YAP). Similar to large tumour suppressor (Lats) in invertebrates, several findings point to LATS functioning as a tumour suppressor in mammals (St John *et al.*, 1999; Hisaoka *et al*, 2002; Takahashi *et al*., 2005; Jimenez-Velasco *et al*., 2005). The significance of functional conservation is further strengthened by the fact that human MST2, hMOB1A and LATS1 can rescue the tissue-overgrowth phenotype of Hpo, dMob1/Mats and Lats mutants in *D. melanogaster* (Wu *et al*., 2003; Lai *et al*., 2005). Moreover HIPPO components, including Mob1A are mutated in mammalian tumors.

Overall, LATS seems to be a tumour-suppressor protein that is conserved in flies and humans, whereas the roles of mammalian NDR1/2 and their co-activators MOBs are yet to be fully established. Existing findings indicate that mammalian NDR1/2 could function as proto-oncogenes (Hergovich *et al*., 2006).

Like in animals, also in plants specific cell types undergo programmed cell death (PCD) as part of their developmental and differentiation program (Vaux and Korsmeyer, 1999). From embryogenesis to fertilization, cell and tissue death is an integral part of plant development and morphogenesis as well as a response to the environment (Barlow, 1982; Buckner *et al.*, 1988). Even though the cellular deterioration patterns described in plant tissues are in some cases similar to those observed in animal tissues, little is known of the mechanisms that control programmed cell death (PCD) in plants (Pennell and Lamb, 1997; Allen *et al*., 1998; Vaux and Korsmeyer, 1999). In angiosperms, PCD occurs late in the degenerative stage of the reproductive phase in both anther and pistil (Wu and Cheung, 2000). Production of functional male gametes depends largely on the deterioration and death of the anther tapetum, whose main functions appear to be the nurturing of microspores with cortical surface molecules and allowing pollen dispersion at maturity. The pathway of female gametogenesis frequently begins with the death of all but one reduced megaspores, while surrounding nucellar cells degenerate in concert with embryo sac expansion (Reiser and Fisher, 1993; McCormick, 1993; Barcaccia *et al*., 2003).

Mob1 may be a component of a complex of proteins with multiple functions, not only involved in cytokinesis, cell proliferation and morphogenesis, but also operatively

associated with cell death. Database searches revealed that MOB domain (pfam03637) can be combined in complex proteins with elements of the NB-ARC domain (pfam00931), a signaling motif shared by animal cell death gene regulators. Proteins containing a highly conserved Mob1 domain include also receptors for ubiquitination targets (F-Box), Ser/Thr and Tyr kinases as well as CBL (Calcineurin B-Like)-interacting kinases which may be implicated in either cell proliferation or cell death. The possible involvement of Mob1 proteins in PCD is also supported by our recent analysis of Mob1-like expression in alfalfa reproductive tissues (Figure 8). In the ovules during gametogenesis, both transcripts and proteins were mainly visualized in the reduced megaspores undergoing PCD or in the remnants of degenerated megaspores, whereas in the anthers, Mob1-like gene products were specifically found at the end of gametogenesis in tapetum cells naturally undergoing PCD to allow pollen grain dispersal (Citterio *et al.*, 2005). Moreover, localization of MOB-domain containing proteins was also documented in alfalfa meristematic tissues of the plant roots. Ii is known that the root cap consists in living parenchyma cells derived continuously from the apical meristem and programmed to die: as new cells are produced in the interior, those on the root periphery are shed in an orderly manner. Hybridization signals were detected in a thin cell layer of the root apex where meristematic root tip cells divide and differentiate in root cap. Such finding further supports the concept that Mob proteins are related to the onset of programmed cell death in plants (Citterio *et al*., 2006). Further experiments will help clarifying the function of Mob1-like proteins in both cell proliferation and PCD. The challenge will be to dissect the roles of each Mob1-like gene in different tissues. The production and exploitation of specific antibodies against each of the Mob1-like gene products encoded by a specific member of the MOB family should aid in determining whether a multi-domain protein component with distinct functions is operative during cell proliferation and PCD.

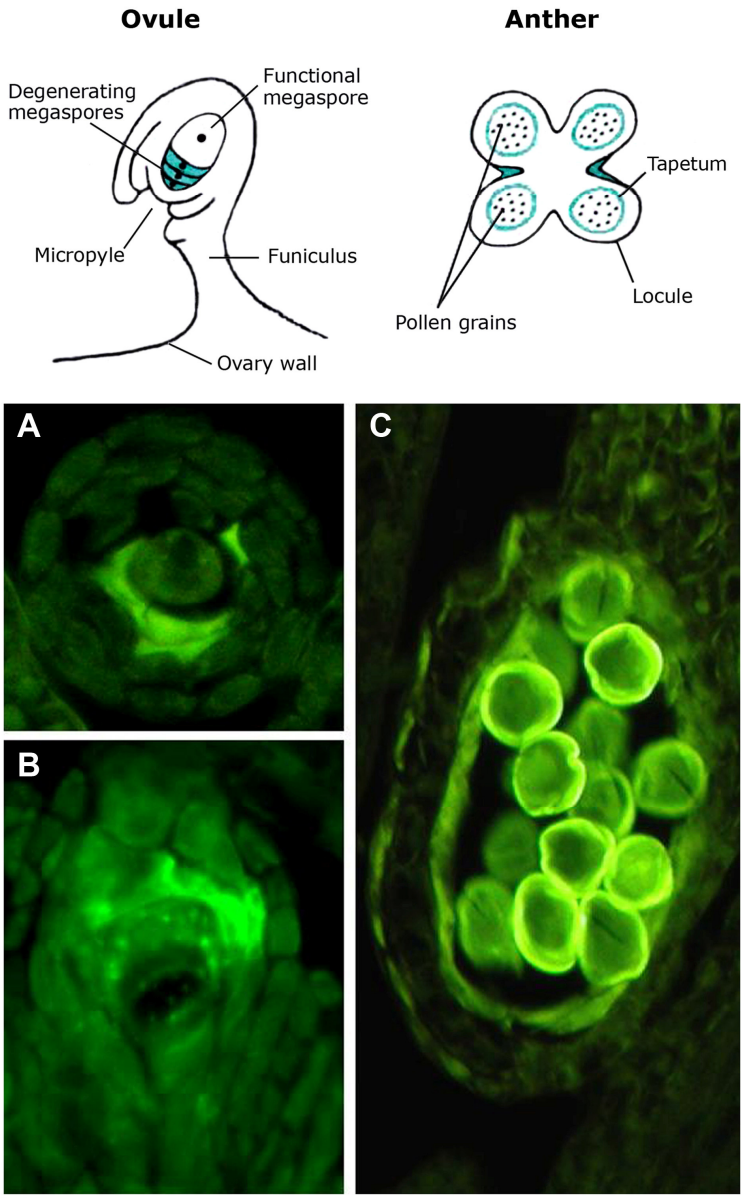

Figure 8. Mob1-like expression patterns in plant reproductive tissues, with particular reference to alfalfa (*Medicago sativa* L.). The cartoons show spores and cells that most prominently undergo programmed cell death (PCD) in ovules and anthers (adapted from Wu and Cheung, 2000). In ovules at the end of sporogenesis, proteins are mainly visualized in the reduced megaspores undergoing PCD or the remnants of degenerated megaspores, whereas in anthers, proteins are specifi cally found at the end of gametogenesis in tapetum cells naturally undergoing PCD to allow pollen grain dispersal. Bar: 20 μm

Cell polarity and morphogenesis

The MOB2-NDR proteins are central factors of the RAM (Regulation of *Ace2* Activity and Morphogenesis) network in cell separation and polarity establishment. In this section we will briefly review on the progress made so far on the elucidation of the role played by MOB proteins and NDR kinases in regulating cell morphology in co-ordination with the mitotic exit. Co-ordinating asymmetric cell division, and establishment and maintenance of cell polarity are essential processes in growth and differentiation. Polarised morphogenesis is necessary for proper functioning of specific cell types such as neurons, epithelial cells, plant root hairs and pollen tubes and fungal hyphae and its core elements are substantially conserved across eukaryotes. Cell intrinsic polarity is established early during cell division and factors governing cell separation and cell polarity are tightly controlled and co-ordinated.

Studies carried out on yeast, have led to the identification of the so-called RAM network of proteins as a central element involved in the early phases of polar morphogenesis during cell separation (Nelson *et al.*, 2003). The core components of the yeast RAM network are the LATS/NDR kinase CBK1p and its upstream regulator MOB2p, which play a dual role in controlling mother-daughter cell separation and establishment of cell polarity. Cell separation in yeast relies on the daughter cell specific expression of genes necessary for septum degradation, shown to be dependent on the specific localisation and activation of the ACE2 transcription factor in the daughter cell nucleus together with MOB2p and CBK1p at the end of mitosis (Colman-Lerner *et al*., 2001; Weiss *et al*., 2002). Loss of function strains mob2pΔ and cbk1pΔ as well as ace2pΔ show defects in the cell separation process resulting in clumps of cells. However, interestingly, the mob2pΔ and cbk1pΔ cells, but not the ace2pΔ, display loss of polar growth suggesting that the MOB2p-CBK1p complex regulates cell morphology through a specific pathway that is independent from Ace2 activity (Weiss *et al.*, 2002; Nelson *et al.*, 2003). Cells deleted for either CBK1 or MOB2 or expressing a catalytically inactive form of Cbk1p in *S. cerevisiae* (Racki *et al*., 2000; Bidlingmaier *et al*., 2001; Colman-Lerner *et al*., 2001; Weiss *et al*., 2002) or lacking CBK1 and MOB2 orthologs in *S. pombe* (Verde *et al*., 1998; Hou *et al*., 2003) are round and lack axial polarization, proper bud selection and mating projections. In addition cells lacking a functional MOB2p-CBK1p machinery

display multiple sites of bud selection and growth suggesting a general role for these proteins in determining early events for cell polarity establishment (Nelson *et al*., 2003). A schematic representation of the *S. cerevisiae* RAM network is reported in Figure 9. Based on genetic and biochemical studies in yeast, MOB2p–CBK1p activity is placed downstream of and dependent on the functional presence of the other RAM proteins KIC1p, HIM1p, TAO3p and SOG2p with KIC1p, HIM1p and SOG2p forming a functional complex required for MOB2p–CBK1p phosphorylation and activation (Nelson *et al.*, 2003). The KIC1p kinase, the second kinase of the RAM signaling network together with CBK1, displays significant sequence similarity to the MEN kinase Cdc15p, involved in the activation of the MEN MOB1p–DBF2p kinase complex directly (Mah *et al*., 2001), and it has been shown to activate Mob2p-Cbk1p for regulating Ace2p and cellular morphogenesis (Nelson *et al.* 2003). These data suggest the conservation of the core interaction of MOB and NDR proteins in both MEN and RAM networks and of their mode of regulation by immediate upstream factors. Furthermore, the role of the MOB2-NDR complex in establishing cell polarity seems to be conserved throughout eukaryotes, since loss of function of CBK1/ORB6-related NDR kinases leads to defects in cell axialisation and cell spreading and/or branching also in *Drosophila*, *C. elegans* and in mammalian cells. However, while loss of CBK1 function in yeast leads to a failure in axialisation and bud selection of cells (Racki *et al*., 2000; Bidlingmaier *et al*., 2001; Colman-Lerner *et al*., 2001; Du and Novick, 2002; Weiss *et al*., 2002; Nelson *et al*., 2003) the inactivation of the *Drosophila* NDR encoding gene *tricornered* (*trc*) leads to split epidermal hairs and bristles (Geng *et al*., 2000) and augmented dendritic branching (Emoto *et al*., 2004). Similar defects in dendritic branching are observed in the presence of mutations of the *C. elegans* NDR encoding gene *Sax1* (Zallen *et al.*, 2000) suggesting a negative role exerted by NDR kinases in the control of cell axialisation and branching in higher eukaryotes opposite to the positive role played by the MOB2p-CBK1p complex of yeast. Hyperpolarisation instead of loss of polarization has also been shown following systematic mutagenesis of components of the RAM network in the pathogenic fungus *Cryptococcus neoformans* (Walton *et al.*, 2006). This was observed in the presence of substantial conservation of subcellular localization and protein-protein interactions

between MOB2p and CBK1 homologs and upstream components (Walton *et al.*, 2006), further suggesting a general

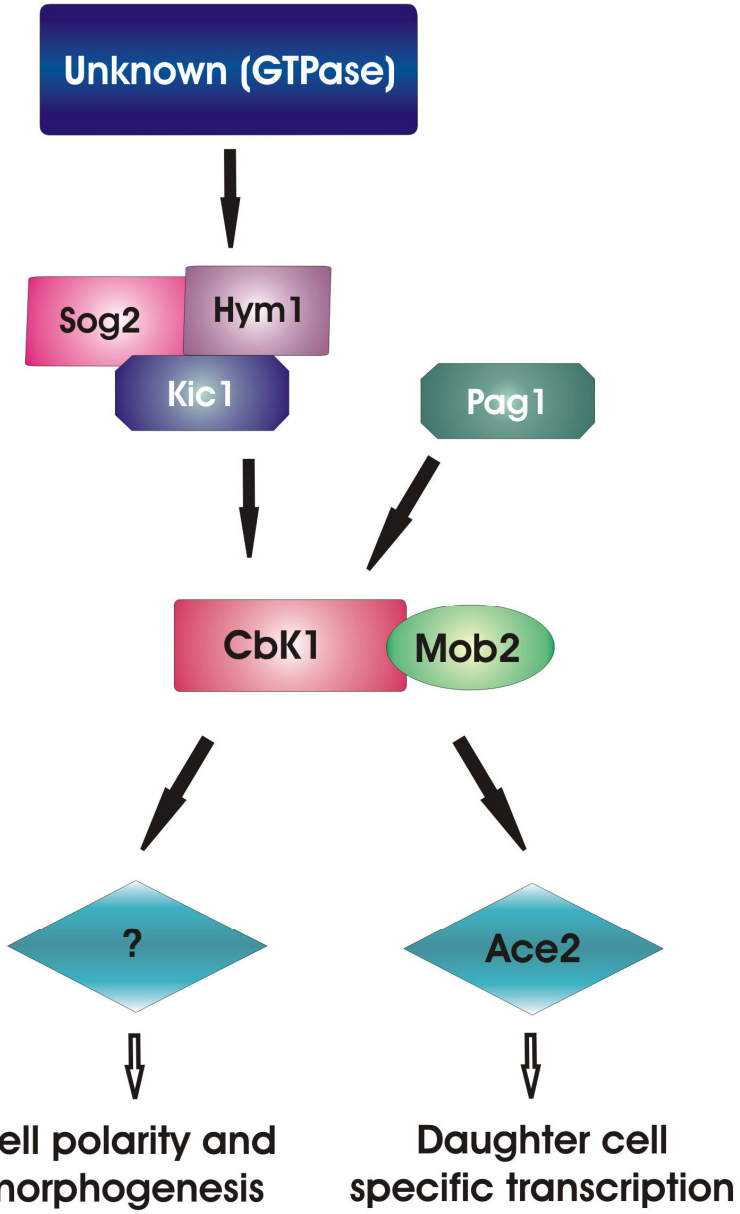

Figure 9. Schematic representation of the S. cerevisiae RAM network. The protein kinase Kic1 associates with the proteins Sog2 and Hym1 to form a complex necessary for proper localisation and function of Cbk1. In analogy to its counterpart Cdc15 in the MEN network, Kic1 likely activates Cbk1 directly. Pag1 interacts with Kic1 and Cbk1 facilitating its activation. Cbk1 requires the interaction with Mob2 for activation and to regulate the transcription factor Ace2, essential for cell separation to occur, through the transcription of genes involved in cell wall synthesis in a daughter cell specifi c way. The Cbk-Mob2 complex also regulates polarised growth of cells, proper bud site selection and

formation of mating projections through a largely uncharacterised Ace2 independent pathway.

conservation of the central role of the MOB2p-CBK1p/NDR complex in directing cell polarity in eukaryotes, but pointing to a probable divergence of downstream components leading to opposite cell polarity phenotypes. This may reflect different mechanisms of cell shape control via the re-organization of the cytoskeleton through assembly of actin cables, controlled for example in yeast by formin (Burns *et al*., 1994; Evangelista *et al*., 2002), or via alternative systems. Interestingly, the MOB2p-CBK1p complex seems to regulate cell polarity through a mechanism that is at least partly independent from the actin cables assembly since in RAM mutants actin organization has been reported to be not substantially affected (Weiss *et al.*, 2002; Nelson *et al.*, 2003). In addition MOB2 or CBK1 mutations result in additive phenotypes when combined with mutations affecting the formin encoding gene Bni1 (Du and Novick 2002; Weiss *et al.*, 2002; Nelson *et al.* 2003). This together with the finding that Cbk1p has been shown to bind Sec2p, a guanine nucleotide exchange factor involved in vesicle transport and exocytosis (Racki *et al*., 2000), have lead to the hypothesis that the RAM network may act in cell polarity through regulation of vesicle transport (Terbush *et al*., 1996; Lipschutz and Mostov, 2002). On the contrary, the Drosophila *Trc* gene functions altering actin and microtubule organization (He *et al.*, 2005) and has been placed on the same genetic pathway of RhoA GTPase since loss of *Trc* function and expression of a dominant negative form of RhoA result in similar non additive phenotypes (He *et al.*, 2005). Rho GTPases are well known players in cell polarity establishment through the regulation of actin dynamics, however even though it has been suggested that they may be downstream components of NDR kinases in *Drosophila* (He *et al.*, 2005) and in *C. elegans* (Zallen *et al.*, 2000), definitive biochemical evidence is needed to fully clarify their exact hierarchical relationships. In fact, it cannot be excluded that the MOB-NDR complex may be a downstream component of Rho GTPases, also considering the similarity of NDR kinases with Rho kinases, the immediate downstream components of Rho signaling.

General discussion and concluding remarks

The MOB family includes a group of cell cycle-associated, non-catalytic proteins highly conserved in eukaryotes, whose founding members are implicated in mitotic exit and co-ordination of cell cycle progression with cell polarity and morphogenesis (Luca *et al*., 2001; Stegmeier *et al*., 2002; Nelson *et al.*, 2003).

An HMM search for Mob-like domain containing proteins in 43 completed and ongoing eukaryotic genomes highlights the universal distribution of this protein family in the so-far sequenced organisms, suggesting its prominent biological function. The phylogenetic analysis reveals five distinct classes of the Mob domain, resulting in the necessity of a reassessment of the relationship existing among the proteins found in different taxa. As an example, in our analysis the founding member ScMob1 does not cluster within the Mob1 group, as previously reported in various papers (Stavridi *et al.*, 2003; Mrkobrada *et al.*, 2006).

Analysis on Mob domain distribution reveals a progressive expansion of this family from unicellular to multicellular organisms, reaching the highest number in mammals. Moreover, phylogenetic analysis shows that the Mob4 genes form a peculiar class of the invertebrata taxa, that underwent an expansion in vertebrata giving origin to Mob4a and Mob4b classes. Plant Mob genes appear to have evolved from a single ancestor, most likely due to the loss of one or more genes during the early stage of Viridiplantae evolutionary history. Finally Mob1, Mob2 and Mob3 classes are widespread among almost all analyzed organisms. Mob3 class is the most divergent one, suggesting a possible different function for the genes belonging to this class. Mob2 class, compared to the other Mob classes, presents lower gene identity percentage homogeneity, revealing the possible presence of other subgroups belonging to this class.

Different distribution and phylogenetic relationship among genes of the same organism and/or different organisms suggest that the Mob gene family evolves under a birth-and-death evolution model (Nei and Rooney, 2005).

Two distinct Mob proteins, Mob1 and Mob2, are known in fungi, while an expansion in metazoans gives rise to six (seven) in human, four in *D. melanogaster*, and four in *C. elegans* (Mrkobrada *et al*., 2006). Mob1 proteins have been demonstrated to be important for both mitosis completion and cell plate formation in yeast (Luca and Winey, 1998).

Moreover, the Mob1-related proteins Mob2 physically associate with specific kinases throughout the cell cycle, being required and periodically activated in yeast to promote polarized growth (Weiss *et al*., 2002). Mob1-like proteins have been also found in animals (Stavridi *et al*. 2003; Ponchon *et al*., 2004; Devroe *et al*., 2004). Plant genomes such as alfalfa, rice and *Arabidopsis* contain uncharacterized Mob1-related genes (Van Damme *et al*., 2004; Citterio *et al*., 2005; 2006). Although there are data to suggest that Mob1 proteins act as kinase activating subunits in higher eukaryotes, their function remains to be proved. Present findings suggest that animal and yeast Mob1 may have similar functions.

That Mob1 proteins play a crucial role in cytokinesis has been demonstrated in yeast (Luca and Winey, 1998). The study of a spontaneous lethal mutation in a *Drosophila* Mob1 gene has recently implicated the MOB-domain containing proteins in the control of animal cell proliferation and apoptosis (Lai *et al*., 2005). Moreover, the identification of the animal Dbf2 homologous proteins NDR (Nuclear Dbf2-Related) interacting with Mob1-related proteins, and the determination of the human and *Xenopus laevis* Mob protein tridimensional structures, may mean that Mob proteins act as kinase activating subunits even in higher eukaryotes. The functional co-dependence and cell cycle regulation of the Mob and Dbf2-like proteins is reminiscent of how cyclins bind and regulate cyclin-dependant kinases (Morgan, 1996; Mah *et al*., 2001).

MOB-domain containing proteins represent essential regulators of the localization and activity of nuclear Dbf2-related (NDR) protein kinases, components of the mitotic exit network (MEN) in yeast and MEN-like in human. Several lines of research in mammals are now in progress to define the precise roles of NDR interactors, particularly the regulation of Mob activators and MST kinases. A general regulation scheme at the molecular level, probably valid for all NDR family members, has recently been established (see Hergovich *et al*., 2006). The binding of the co-activator MOB-domain containing proteins to the N terminus of NDR kinases seems crucial for activation and function. It is known that Mob proteins interact with NDR-type kinases by binding a conserved stretch of primary sequence at their N-terminal regulatory domain. The interaction of Mob proteins with the NTR activation site is a conserved feature of all members of the NDR kinase family that have been tested so far in yeasts, flies and humans. Interestingly, Mob proteins do not function solely as co-activators of NDR

kinases, but are also required for the localization of yeast NDR kinases. As a matter of fact, members of the NDR family are essential genes in both uni- and multi-cellular organisms. Dbf2p and Sid2p regulate mitotic exit and cytokinesis in yeasts, and their counterparts in mammals and plants could also have a similar role.

Recent advances lead to the identification of the Hippo signaling pathway that controls the coordination of apoptosis and cell proliferation, and tissue growth in *D. melanogaster* (see Hergovich *et al*., 2006). The association of Mob1p with Lats (Large tumor suppressor) is essential in this regulatory process since flies that carry mutations in dMob1 are unable to control tissue growth, despite having a functional Lats (Lai *et al*., 2005). Therefore, Lats that is phosphorylated by Hpo needs to bind to its co-activator dMob1 to properly coordinate cell death and proliferation. Interestingly, conserved key components of this pathway have been found to be mutated in human cancer samples, which indicates that a kinase network is probably conserved from flies to humans.

In plants, signaling mechanisms co-ordinate mitosis spatially and temporarily with cytokinesis to ensure integrity of genetic transfer during the cell cycle (Guertin *et al.*, 2002), and important genes required for cytokinesis have recently been discovered. The involvement of plant Mob genes in cell cycle control is supported by recent data collected in *Arabidopsis* and *Medicago sativa* (Van Damme *et al.*, 2004; Citterio *et al*., 2006). For instance, in *Arabidopsis* several putative cell cycle associated components (e.g. Mob1-like proteins) were targeted to the cell division plane and to the nucleus, suggesting that this organelle operates as a coordinating hub for cytokinesis (Van Damme *et al.*, 2004). Moreover, in *M. sativa* Mob1-like proteins were proven to appear during late telophase and to localize across the entire cell division midplane, thus marking the progressive formation of the phragmoplast (Citterio *et al*., 2006). Nevertheless, the key role of MOB-domain containing proteins in plants is still poorly understood.

The greater amount of Mob1-like proteins in proliferating than in non-proliferating tissues, together with their cell cycle-regulated subcellular localization and their presence at the cleavage site suggest that these proteins may have a function in cell division similar to that of yeast Mob1 essential for mitotic exit and septum formation. In yeast, the spindle pole body operates as a signaling center during cytokinesis (Simanis, 2003). MEN/SIN regulators such as Sid kinases and Dbf2/Mob1 temporarily associate with the spindle pole

body at some point in the cell cycle. For instance, in *S. cerevisiae*, Mob1 mobilizes to the spindle pole body (SPB) at anaphase and localizes to the bud neck, the future site for cell division, during cytokinesis (Hou *et al.*, 2003). In analogy to this function, centrosomes have been implicated in completing cytokinesis in animals and human cells (Doxsey, 2001). In higher plant cells, microtubules (MTs) show dynamic structural changes during cell cycle progression and play significant roles in cell morphogenesis (Hasezawa and Kumagai, 2002). In addition to the cortical microtubules (CMT) that control the cell shape, the preprophase band (PPB) and the phragmoplast are other plant-specific structures which can be observed from late interphase to prophase, and from anaphase to telophase, respectively. How plant MT arrays reorganize during the cell cycle is an unanswered question. Plants lack conventional animal centrosomes and yeast SPBs seem to possess flexible centrosomes from which nucleating material disperses at different cell cycle stages (Chan *et al.*, 2003).

Despite differences between plant and yeast in mitotic entry and progression, the localization pattern in plant cells of Mob proteins shares many features with yeast (Van Damme *et al*., 2004; Citterio *et al*., 2006). In plant cells, Mob1-like proteins form grains in the cytoplasm from which fibrillar structures radiate in all directions, preferentially toward the cell midplane. These grains likely correspond to sites in which microtubules are reorganized during cell cycle progression. Proteins, barely visible in G_1 and S, are clearly seen in G_2 forming a ring around the nucleus, whereas during mitosis they preferentially localize as punctuate clusters at the two opposite cellular poles. Differently from yeast, in plants cells undefined fibrillar structures are formed. In cytokinesis besides the progressive labeling of the septum, Mob1-like proteins form fibrillar structures that partially co-localize with phragmoplast microtubules and partially form an aster, radiating from the growing septum poles. An interesting possibility is that Mob1-like proteins participate in cell plate orientation during cytokinesis, interacting with cytoskeletal structures and coupling the establishment of the division site, marked by PPB before the onset of mitosis, with septum formation. The interaction between MTs and Mob1p is emphasized by the characterization of haploid *mob1* yeast mutants, which display a complete increase in ploidy at permissive temperature, caused by cytokinetic defects (Luca *et al.*, 2001). However, although it is well demonstrated that yeast Mob1 is essential

for the exit from mitosis and for septum formation, its exact function is still to be known even in this simple organism. Mob1 has been proposed to activate the mitotic exit network acting as an activating subunit of the Dbf2 protein kinase (Stavridi *et al.*, 2003). In animal cells Dbf2 homologs interacting with Mob1-like proteins have been discovered (Ponchon *et al.*, 2004; Devroe *et al.*, 2004), suggesting a conserved function between yeast and higher eukaryotes. Nevertheless, Dbf2 homologs have not yet been characterized in plants. The control of cell proliferation and cell death are central points of ongoing research programs in cell cycle control of all eukaryotes and, particularly, in human diseases by using model organisms. Basic studies addressed to the understanding of the mitotic events and its alterations will be crucial for practical applications in cell biology and medicine.

References

Abascal F, Zardoya R, and Posada D (2005) ProtTest: Selection of best-fit models of protein evolution. Bioinformatics, 21: 2104-2105.

Allen RT, Cluck M.W, and Agrawal DK (1998) Mechanisms controlling cellular suicide: role of Bc11 and caspases. Cell Mol. Life Sci., 54: 427-445.

Baillat G, Moqrich A, Castets F, Baude A, Bailly Y, Benmerah A, and Monneron A (2001) Molecular cloning and characterization of phocein, a protein found from the Golgi complex to dendritic spines. Mol. Biol. Cell, 12: 663-673.

Baillat G, Gaillard S, Castets F, and Monneron A (2002) Interactions of phocein with nucleoside-diphosphate kinase, Eps15, and Dynamin I. J. Biol. Chem., 277: 18961-18966.

Barcaccia G, Tavoletti S, Mariani A and Veronesi F (2003) Occurrence, inheritance and use of reproductive mutants of alfalfa (*Medicago* spp). Euphytica, 133: 37-56.

Barlow PW (1982) Cell death: an integral part of plant development. In: M.B. Jackson, B. Grout, I.A. Mackenzie (Eds.), Growth regulators in plant senescence. Oxon British Plant Growth Regulator Group, Wantage. pp. 27-45.

Bichsel SJ, Tamaskovic R, Stegert MR and Hemmings BA (2004) Mechanism of activation of NDR (Nuclear Dbf2-related) protein kinase by the hMOB1 protein. J. Biol. Chem., 279: 35228-35235.

Bidlingmaier S, Weiss EL, Seidel C, Drubin DG, and Snyder M (2001) The Cbk1p pathway is important for polarized cell growth and cell separation in *Saccharomyces cerevisiae*. Mol. Cell. Biol., 21: 2449-2462.

Bothos J, Tuttle RL, Ottey M, Luca FC, and Halazonetis TD (2005) Human LATS1 is a mitotic exit network kinase. Cancer Res., 65: 6568-6575.

Buckner B, Janick-Buckner D, Gray J, and Johal GS (1998) Cell death mechanisms in maize. Trends Plant Sci., 3: 218-223.

Burns N, Grimwade B, Ross-Macdonald PB, Choi EY, Finberg K, Roeder GS, and Snyder M (1994) Large-scale analysis of gene expression, protein localization, and gene disruption in *Saccharomyces cerevisiae*. Genes Dev., 8: 1087-1105.

Citterio S, Varotto S, Albertini E, Feltrin E, Soattin M, Marconi G, Sgorbati S, Lucchin, M and Barcaccia G (2005) Alfalfa Mob1-like proteins are expressed in reproductive organs during meiosis and gametogenesis. Plant Mol. Biol., 58: 789-808.

Citterio S, Piatti S, Albertini E, Aina R, Varotto S and Barcaccia G (2006) Alfalfa Mob1-like proteins are involved in cell proliferation and localize in the cell division midplane during cytokinesis Exp. Cell Res., 312: 1050-1064.

Chan J, Calder GM, Doonan JH and Lloyd CW (2003) EB1 reveals mobile microtubule sites in *Arabidopsis*. Nat. Cell Biol., 5: 967-971.

Chan EH, Nousiainen M, Chalamalasetty RB, Schafer A, Nigg EA and Sillje HH (2005) The Ste20-like kinase Mst2 activates the human large tumour suppressor kinase Lats1. Oncogene, 24: 2076-2086.

Colman-Lerner A, Chin TE and Brent R. (2001). Yeast Cbk1 and Mob2 activate daughter-specific genetic programs to induce asymmetric cell fates. Cell, 107: 739-750.

Danial NN and Korsmeyer SJ (2004) Cell death: critical control points. Cell 116: 205-219.

Devroe E, Erdjument-Bromage H, Tempst P and Silver PA (2004) Human Mob proteins regulate the NDR1 and NDR2 serine-threonine kinases, J. Biol. Chem. 279: 24444-24451.

Doxey S (2001) Re-evaluating centrosome function. Nat. Rev. Mol. Cell. Biol. 2: 688-698.

Du LL and Novick P (2002) Pag1p, a novel protein associated with protein kinase Cbk1p, is required for cell morphogenesis and proliferation in *Saccharomyces cerevisiae*. Mol. Biol. Cell, 13: 503-514.

Durbin R, Eddy S, Krogh A and Mitchison G (1998) Biological sequence analysis: probabilistic models of proteins and nucleic acids. Cambridge University Press, UK.

Edgar BA (2006). From cell structure to transcription: Hippo forges a new path. Cell, 124(2): 267-73.

Emoto K, He Y, Ye B, Grueber W B, Adler PN, Jan LY and Jan, YN (2004) Control of dendritic branching and tiling by the Tricornered-kinase/Furry signaling pathway in *Drosophila* sensory neurons. Cell, 119: 245-256.

Evangelista M, Pruyne D, Amberg DC, Boone C and Bretscher A (2002) Formins direct Arp2/3-independent actin filament assembly to polarize cell growth in yeast. Nat. Cell Biol., 4: 260-269.

Frenz LM, Lee SE, Fesquet D and Johnston LH (2000) The budding yeast Dbf2 protein kinase localises to the centrosome and moves to the bud neck in late mitosis. J. Cell Sci., 113: 3399-3408.

Geng W, He B, Wang M and Adler, P.N. (2000) The tricornered gene, which is required for the integrity of epidermal cell extensions, encodes the *Drosophila* nuclear DBF2-related kinase. Genetics, 156: 1817-1828.

Green DR and Evan, G.I. (2002) A matter of life and death. Cancer Cell, 1: 19-30.

Guertin DA, Trautmann S and McCollum D (2002) Cytokinesis in eukaryotes. Microbiol. Mol. Biol. Rev., 66: 155-178.

Guindon S and Gascuel O (2003) A simple, fast, and accurate algorithm to estimate large phylogenies by maximum likelihood. Syst. Biol., 52: 696-704.

Hammarton TC, Lillico SG, Welburn SC and Mottram JC (2005) *Trypanosoma brucei* MOB1 is required for accurate and efficient cytokinesis but not for exit from mitosis. Mol. Microbiol., 56: 104-116.

Hasezawa S and Kumagai F (2002). Dynamic changes and the role of the cytoskeleton during the cell cycle in higher plant cells. Academic Press, Tokio, Japan. pp. 161-191.

Harvey KF, Pfleger CM and Hariharan, I.K. (2003). The *Drosophila* Mst ortholog, *hippo*, restricts growth and cell proliferation and promotes apoptosis. Cell, 114: 457-467.

He Y, Emoto K, Fang X, Ren N, Tian X, Jan YN and Adler PN. (2005) *Drosophila* Mob family proteins interact with the related tricornered (Trc) and warts (Wts) kinases. Mol. Biol. Cell, 16: 4139-4152.

Hennebold JD, Tanaka M, Saito J, Hanson BR and Adashi EY (2000) Ovary-selective genes I: the generation and characterization of an ovary-selective complementary deoxyribonucleic acid library. Endocrinology, 141: 2725-2734.

Hergovich A, Bichsel SJ and Hemmings BA (2005) Human NDR kinases are rapidly activated by MOB proteins through recruitment to the plasma membrane and phosphorylation. Mol. Cell Biol., 25: 8259-8272.

Hergovich A, Schmitz D and Hemmings BA (2006) The human tumour suppressor LATS1 is activated by human MOB1 at the membrane. Biochem. Biophys. Res. Comm., 345: 50-58.

Hergovich A, Stegert MR, Schmitz D and Hemmings BA (2006) NDR kinases regulate essential cell processes from yeast to humans. Nature Reviews, 7: 253-264.

Higgins DG, Bleasby AJ and Fuchs R (1992) CLUSTAL: a package for performing multiple sequence alignments on a micro-computer. Comput. Appl. Biosci., 8: 189-191.

Hisaoka M, Tanaka A and Hashimoto H (2002) Molecular alterations of h-warts/LATS1 tumor suppressor in human soft tissue sarcoma. Lab Invest., 82: 1427-1435.

Hou MC, Wiley DJ, Verde F and McCollum D (2003) Mob2p interacts with the protein kinase Orb6p to promote coordination of cell polarity with cell cycle progression. J. Cell Sci., 116: 125-135.

Hou MC, Guertin DA and McCollum D (2004) Initiation of cytokinesis is controlled through multiple modes of regulation of the Sid2p-Mob1p kinase complex. Mol. Cell Biol., 24: 3262-3276.

Huang J, Wu S, Barrera J, Matthews K and Pan D (2005) The Hippo signaling pathway coordinately regulates cell proliferation and apoptosis by inactivating Yorkie, the *Drosophila* homolog of YAP. Cell, 122: 421-434.

Jia J, Zhang W, Wang B, Trinko R and Jiang J (2003) The Drosophila Ste20 family kinase dMST functions as a tumor suppressor by restricting cell proliferation and promoting apoptosis. Genes Dev., 17: 2514-2519.

Jimenez-Velasco A Roman-Gomez J, Agirre X, Barrios M, Navarro G, Vazquez I, Prosper F, Torres A and Heiniger A (2005) Downregulation of the large tumor suppressor 2 (*LATS2/KPM*) gene is associated with poor prognosis in acute lymphoblastic leukemia. Leukemia, 19: 2347-2350.

Justice RW, Zilian O, Woods DF, Noll M and Bryant, P.J. (1995). The *Drosophila* tumor suppressor gene *warts* encodes a homolog of human myotonic dystrophy kinase and is required for the control of cell shape and proliferation. Genes Dev., 9: 534-546.

Komarnitsky SI, Chiang YC, Luca FC, Chen J, Toyn JH, Winey M, Johnston LH and Denis CL (1998) DBF2 protein kinase binds to and acts through the cell cycle-regulated MOB1 protein. Mol. Cell Biol., 18: 2100-2107.

Krapp A, Gulli MP and Simanis V (2004) SIN and the art of splitting the fission yeast cell. Curr. Biol., 14: R722-R730.

Lai ZC, Wei X, Shimizu T, Ramos E, Rohrbaugh M, Nikolaidis N, Ho LL and Li Y (2005) Control of cell proliferation and apoptosis by mob as tumor suppressor, mats. Cell, 120: 675-685.

Lee SE, Frenz LM, Wells NJ, Johnson AL and Johnston L.H. (2001) Order of function of the budding-yeast mitotic exit-network proteins Tem1, Cdc15, Mob1, Dbf2, and Cdc5. Curr. Biol. 11: 784-788.

Lippincott J, Shannon KB, Shou WY, Deshaies J and Li R (2001) The Tem1 small GTPase controls actomyosin and septin dynamics during cytokinesis. J. Cell Sci., 114: 1379-1386.

Lipschutz JH and Mostov KE (2002) Exocytosis: the many masters of the exocyst. Curr. Biol., 12: R212-R214.

Luca FC and Winey M(1998) MOB1, an essential yeast gene required for completion of mitosis and maintenance of ploidy. Mol. Biol. Cell, 9: 29-46.

Luca FC, Mody M, Kurischko C, Roof DM, Giddings TH and Winey M (2001) *Saccharomyces cerevisiae* Mob1p is required for cytokinesis and mitotic exit. Mol. Cell Biol, 21: 6972-6983.

Mah AS, Jang J and Deshaies RJ (2001) Protein kinase Cdc15 activates the Dbf2-Mob1 kinase complex. Proc. Natl. Acad. Sci. USA, 98: 7325-7330.

Mah AS, Elia A EH, Devgan G, Ptacek J, Schutkowski M, Snyder M, Yaffe MB and Deshaies RJ (2005) Substrate specificity analysis of protein kinase complex Dbf2-Mob1 by peptide library and proteome array screening. BMC Biochem., 6: 22.

Manning G, Whyte DB, Martinez R, Hunter T and Sudarsanam S (2002) The protein kinase complement of the human genome. Science, 298: 1912-1934.

McCormick S (1993) Male gametophyte development. Plant Cell, 5: 1265-1275.

McPherson JP, Tamblyn L, Elia A, Migon E, Shehabeldin A, Matysiak-Zablocki E, Lemmers B, Salmena L, Hakem A, Fish J, Kassam F, Squire J, Bruneau BG, Hande MP, Hakem R (2004) Lats2/Kpm is required for embryonic development, proliferation control and genomic integrity. EMBO J., 23: 3677-3688.

Morgan DO (1996) The dynamics of cyclin dependent kinase structure. Curr. Opin. Cell Biol., 8: 767-772.

Moreno CS, Lane WS and Pallas DC (2001) A mammalian homolog of yeast MOB1 is both a member and a putative substrate of striatin family-protein phosphatase 2A complexes. J. Biol. Chem., 276: 24253-24260.

Mrkobrada S, Boucher L, Ceccarelli DFJ, Tyers M and Sicheri F (2006) Structural and functional analysis of *Saccharomyces cerevisiae* Mob1. J. Mol. Biol., 362: 430-440.

Murray AW (2004) Recycling the cell cycle: cyclins revised. Cell, 116: 221-234.

Nei M and Rooney AP (2005) Concerted and Birth-and-Death Evolution of Multigene Families. Annu. Rev. Genet., 39:121-52.

Nelson B, Kurischko C, Horecka J, Mody M, Nair P, Pratt L, Zougman A, McBroom L, Hughes T, Boone C and Luca F (2003) RAM: a conserved signaling network that regulates Ace2p transcriptional activity and polarized morphogenesis. Mol. Biol. Cell, 14: 3782-3803.

Pantalacci S, Tapon N and Leopold P (2003) The Salvador partner Hippo promotes apoptosis and cell-cycle exit in *Drosophila*. Nature Cell Biol., 5: 921-927.

Park CJ, Song SG, Lee PR, Shou WY, Deshaies RJ and Lee KS (2003) Loss of CDC5 function in *Saccharomyces cerevisiae* leads to defects in Swe1p regulation and Bfa1p/Bub2p-independent cytokinesis. Genetics, 163: 21-33.

Pennell RI and Lamb C (1997) Programmed cell death in plants. Plant Cell, 9: 1157-1168.

Ponchon L, Dumas C, Kajava AV, Fesquet D and Padilla A (2004) NMR solution structure of Mob1, amitotic exit network protein and its interaction with an NDR kinase peptide, J. Mol. Biol., 337: 167-182.

Racki WJ, Becam AM, Nasr F and Herbert CJ (2000) Cbk1p, a protein similar to the human myotonic dystrophy kinase, is essential for normal morphogenesis in *Saccharomyces cerevisiae*. EMBO J., 19: 4524-4532.

Reiser L and Fisher RL (1993) The ovule and the embryo sac. The Plant Cell, 5: 1291-1301.

Salimova E, Sohrmann M, Fournier N and Simanis V (2000) The *S. pombe* orthologue of the *S. cerevisiae* MOB1 gene is essential and functions in signaling the onset of septum formation. J. Cell Sci., 113: 1695-1704.

Sherr CJ (2004) Principles of tumor suppression. Cell 116: 235-246.

Shou WY, Seol JH, Shevchenko A, Baskerville C, Moazed D, Chen ZWS Jang J, Shevchenko A, Charbonneau H and Deshaies RJ (1999) Exit from mitosis is triggered by Tem1-dependent release of the protein phosphatase Cdc14 from nucleolar RENT complex. Cell, 97: 233-244.

Simanis V (2003) Events at the end of mitosis in the budding and fission yeasts. J. Cell Sci., 116: 4263-4275.

Stavridi ES, Harris KG, Huyen Y, Bothos J, Verwoerd PM, Stayrook SE, Pavletich NP, Jeffrey PD and Luca FC (2003) Crystal structure of a human Mob1 protein: toward understanding Mob-regulated cell cycle pathways. Structure, 11: 1163-1170.

Stegert MR, Hergovich A, Tamaskovic R, Bichsel SJ and Hemmings BA (2005) Regulation of NDR protein kinase by hydrophobic motif phosphorylation mediated by the mammalian Ste20-like kinase MST3. Mol. Cell Biol., 25: 11019-11029.

Stegmeier F, Visintin R and Amon A (2002) Separase, polo kinase, the kinetochore protein Slk19, and Spo12 function in a network that controls Cdc14 localization during early anaphase. Cell, 108: 207-220.

Stegmeier F and Amon A (2004) Closing mitosis: the functions of the Cdc14 phosphatase and its regulation. Annu. Rev. Genet., 38: 203-232.

Stoepel J, Ottey MA, Kurischko C, Hieter P and Luca FC (2005) The mitotic exit network Mob1p-Dbf2p kinase complex localizes to the nucleus and regulates passenger protein localization. Mol. Biol. Cell, 16: 5465-5479.

Sonnhammer ELL, Eddy SR, Birney E, Bateman A and Durbin R (1998) Pfam: multiple sequence alignments and HMM-profiles of protein domains. Nucleic Acids Res., 26: 320-322.

St John MA, Tao W, Fei X, Fukumoto R, Carcangiu ML, Brownstein DG, Parlow AF, McGrath J and Xu T (1999) Mice deficient of *Lats1* develop soft-tissue sarcomas, ovarian tumours and pituitary dysfunction. Nature Genet., 21: 182-186.

Takahashi Y, Miyoshi Y, Takahata C, Irahara N, Taguchi T, Tamaki Y and Noguchi S (2005) Down-regulation of *LATS1* and *LATS2* mRNA expression by promoter hypermethylation and its association with biologically aggressive phenotype in human breast cancers. Clin. Cancer Res., 11: 1380-1385.

Tapon N, Harvey KF, Bell DW, Wahrer DC, Schiripo TA, Haber DA, Hariharan IK (2002) Salvador promotes both cell cycle exit and apoptosis in *Drosophila* and is mutated in human cancer cell lines. Cell, 110: 467-478.

Terbush DR, Maurice T, Roth D and Novick P (1996) The Exocyst is a multiprotein complex required for exocytosis in *Saccharomyces cerevisiae*. EMBO J., 15: 6483-6494.

Van Damme D, Bouget FY, Van Poucke K, Inzé D and Geelen D (2004) Molecular dissection of plant cytokinesis and phragmoplast structure: a survey of GFP-tagged proteins. Plant J., 40: 386-398.

Vaux DL and Korsmeyer SJ (1999) Cell death in development. Cell, 96: 245-254.

Verde F, Wiley DJ and Nurse P (1998) Fission yeast Orb6, a ser/thr protein kinase related to mammalian rho kinase and myotonic dystrophy kinase, is required for maintenance of cell polarity and coordinates cell morphogenesis with the cell cycle. Proc. Natl. Acad. Sci. USA, 95: 7526-7531.

Walton F, Heitman J and Idnurm A (2006) Conserved elements of the RAM signaling pathway establish cell polarity in the Basidiomycete *Cryptococcus neoformans* in a divergent fashion from other fungi. Mol. Biol. Cell Vol., 17: 3768-3780.

Weiss EL, Kurischko C, Zhang C, Shokat K, Drubin DG and Luca FC (2002) The *Saccharomyces cerevisiae* Mob2p-Cbk1p kinase complex promotes polarized growth and acts with the mitotic exit network to facilitate daughter cell-specific localization of Ace2p transcription factor. J. Cell Biol., 158: 885-900.

Wolfe BA and Gould KL (2005) Split decisions: coordinating cytokinesis in yeast. Trends Cell Biol., 15 (1): 10-18.

Wu HM and Cheung AY (2000) Programmed cell death in plant reproduction. Plant Mol. Biol., 44: 267-281.

Wu S, Huang J, Dong J and Pan D (2003) *Hippo* encodes a Ste-20 family protein kinase that restricts cell proliferation and promotes apoptosis in conjunction with *salvador* and *warts*. Cell, 114: 445-456.

Xu T, Wang W, Zhang S, Stewart RA and Yu W (1995) Identifying tumor suppressors in genetic mosaics: the *Drosophila* lats gene encodes a putative protein kinase. Development, 121: 1053-1063.

Zallen JA, Peckol EL, Tobin DM and Bargmann CI (2000) Neuronal cell shape and neurite initiation are regulated by the Ndr kinase *SAX-1*, a member of the Orb6/COT-1/warts serine/threonine kinase family. Mol. Biol. Cell, 11: 3177-3190.

Capitolo II

The Mob1-like gene is responsible for defective female meiosis and gametogenesis in *Arabidopsis thaliana* L.

Abstract

Angiosperm life cycle is determined through alternation of a large diploid sporophytic and a few celled haploid gametophytic generations. Meiosis represents the transition process from the sporophyte to the male and female gametophytes as it results in the production of haploid, normally reduced micro- and mega-spores. Ovule development and the onset of embryo sac formation and its maturation have been analyzed in great detail in *Arabidopsis* during the last decades. Several sterile mutants defective in meiotic and post-meiotic stages have been isolated and characterized in the model *A. thaliana* and other crop plants. The alfalfa *Mob1*-like gene was reported to be expressed in a 2*n* egg cell producer of *Medicago* spp., specifically in enlarged megaspore mother cells and embryo sacs of apomeiotic ovules. Gene products were also found in microspore tetrads at the beginning of pollen development as well as in tapetum cells of anthers undergoing programmed cell death. To further elucidate the role of the *Mob1*-like gene, a reverse genetic approach was attempted using *Arabidopsis* as biological system. Temporal and spatial gene expression patterns of the *AtMob1*-like gene (locus At5g45550) were analyzed at both transcript and protein level within plant tissues and reproductive organs. Furthermore, silenced lines were investigated on the basis of plant morphological traits and cyto-histological observations of male and female meiosis and gametogenesis. Our data support a strongly reduced seed set in *AtMob1*-interfered plants, along with a faster development of plants, thinner shoots and smaller flowers and siliques. Moreover, ovules were shown to contain bi-nucleated megaspores and non-polarized or abnormally cellularized embryo sacs. To confirm the possibility of apomeiotic megaspores to give rise to unreduced embryo sacs containing functional egg cells, a FCSS analysis of three distinct RNAi lines was attempted. Overall results in terms of transcript expression and protein localization within flowers along with plant morphology and seed ploidy are reported and critically discussed.

Introduction

Transition from the diploid sporophytic to the haploid gametophytic generations takes place during meiosis. Ovule development and the onset of processes leading to embryo sac formation have been analyzed in great detail in *Arabidopsis* and other model species during the last decades (Mansfield *et al*., 1991; Robinson-Beers *et al*., 1992; Schneitz *et al*., 1995; Christensen *et al*., 1997). After a single round of DNA replication, two rounds of nuclear division occur: meiosis I, which involves the segregation of homologous chromosomes, and meiosis II, which leads to the segregation of sister chromatids being similar to mitosis. At the end of meiosis, four haploid spores are formed upon cytokinesis (Webb and Gunning, 1990; Schneitz *et al*., 1995). Soon after the programmed cell death of three of the four meiotic megaspores, the onset of gametogenesis throughout three successive mitotic divisions transforms the functional megaspore into the embryo sac. Although the goal of cytokinesis is generally conserved between sporophytic and gametophytic tissues, genes required for cytokinesis in somatic cells were reported to be partially distinct from those required during gametophytic development (Lauber *et al*., 1997; Otegui and Staehelin, 2000; Söllner *et al*., 2002). Indeed, within systems exhibiting non-conventional cytokinetic mechanisms, *e.g*. megasporogenesis, nuclear divisions and cytokinesis are uncoupled (Otegui and Staehelin, 2000), frequently leading to the formation of multinucleate or syncytial cells. Similarly, cellularization of the mature embryo sac involves the simultaneous formation of cell walls between sister and non-sister nuclei at sites determined by a cytoskeleton machinery (Otegui and Staehelin, 2000). On the whole, the proper embryo sac development requires the progression of several fundamental processes, such as nuclear division, migration and fusion, cell wall production, vacuole formation, and cell death (Christensen *et al*., 2002). Mutations of one of the genes that control these processes usually affect the formation and/or organization of the embryo sac and consequently exhibit a hampered inheritance through the gametophytes as well as the corresponding mutants show a low or null occurrence among the sporophytes of their progeny. Numerous sterile mutants defective in sporogenic cell specification (Sheridan *et al*., 1999, Schiefthaler *et al*., 1999), along with alteration of chromosome behaviour during meiosis (Yang *et al*., 1999; Siddiqui *et al*., 2000),

cytokinesis (Jingjing Liu and Lia-Jia Qu, 2008) and gametogenesis (Yang and Sundaresan, 2000) have been isolated and characterized in *Arabidopsis*, maize and other crop plants.
Two distinct signaling networks, namely MEN and HIPPO (Bothos *et al.*, 2005; Edgar, 2006), controlling cell proliferation and involving Mob1-like proteins have been recently proposed in *Saccharomyces* spp., *Drosophyla* and mammalian cells (see Hergovich *et al*., 2006). Components of the mitosis exit network are conserved throughout evolution and, in particular, Mob1 along with Dbf2-related proteins have been found in both animal (Stavridi *et al.*, 2003; Ponchon *et al.*, 2004; Devroe *et al.*, 2004) and plant cells (Van Damme *et al.*, 2004; Citterio *et al.*, 2005, 2006, Bedhomme *et al*., 2008), suggesting that their role in controlling cell cycle progression might be conserved in higher eukaryotes. Nevertheless, most of the available information on the biological role of *Mob1*-like genes in the cell cycle and cytokinesis refers to studies performed using *S. cerevisiae* and *S. pombe* as model species. In eukariotes it is becoming clear that Mob1p is an essential regulator of the localization and activity of Dbf2 protein kinase. The MEN pathway has been described in fixing yeast and is composed by the RAS-like GTPase Tem1, the protein kinase cdc15 and Dbf2, the Dbf2-associated factor Mob1 and a scaffold protein Nud1 (reviewed by Vitulo *et al*., 2008). In this network, the activated form of Tem1 is thought to propagate a signal to the protein kinase cdc15 which, in turns, activate the protein kinase Dbf2. It is known that Dbf2 kinase activity requires the Dbf2-associated factor Mob1. The Mob1p-Dbf2 interaction leads to the release from the nucleolus and subsequent activation of the Cdc14p phosphatase during anaphase (Luca *et al.*, 2001; Stegmeier and Amon, 2004). It has been extensively reported that release of cdc14 from its inhibitor complex (Shou *et al*., 1999; Visintin *et al*., 1999) promotes the inactivation of the mitotic CDK1-cyclin B complex finally driving to mitosis exit. Consistent with these functions, the MEN protein kinase complex Mob1p-Dbf2p localizes to mitotic nuclei and partially co-localizes with Cdc14p and kinetochore proteins (Van Damme *et al*., 2005. Vitulo *et al*., 2008). Yeast Mob1 proteins do not function solely as activators of Dbf2/Sid2, but are also required for Dbf2/Sid2 localization to activation sites (Frenz *et al.*, 2000; Lee *et al.*, 2001). Indeed, in agreement with their functions in mitosis exit and cytokinesis, Dbf2/Sid2-Mob1 complexes localize to the spindle pole body in anaphase and move to the division site in late mitosis (Stegmeier and Amon, 2004). Recent findings also

suggest an involvement of Mob1p in coordinating chromosome separation and/or spindle integrity with mitosis exit and cytokinesis via regulation of chromosomal passenger proteins. Moreover, Mob1p has been demonstrated to be essential for maintaining the localization of Aurora, INCENP, and Survivin chromosomal passenger proteins on anaphase spindles and for dissociating Aurora from the kinetochore region (Stoepel *et al.*, 2005). Recent advances in *Drosophila* led to the recognition of Mats (Mob as tumor suppressor, dMob1) as a factor that induces tissue overgrowth without affecting pattern formation. Along with Mats, the Hippo (Hpo), Salvador (Sav), Lats/Warts (dNDRs) factors were reported to be part of a pathway that participates in the control of tissue growth and cell death (Harvey *et al*., 2003; Jia *et al*., 2003; Pantalacci *et al*., 2003; He *et al*., 2005; Huang *et al*., 2005). It is worth noting that the association of dMob1 with Lats is essential in this regulatory process, as flies that carry mutations in dMob1 are unable to control tissue growth, despite having a functional Lats (Lai *et al*., 2005). Therefore, Lats that is phosphorylated by Hpo needs to bind to its co-activator dMob1 to properly coordinate cell death and proliferation. As a matter of fact, cells that carry mutations in Hpo, Sav, Lats and dMob1 show an accelerated proliferation, but maintain a normal size. As a consequence, loss of these genes must stimulate cell growth and reduce cell death.

Overall, LATS seems to be a tumour-suppressor protein that is conserved in flies and humans, whereas the roles of mammalian NDR1/2 and their co-activators MOBs are yet to be fully established. Existing findings indicate that mammalian NDR1/2 could function as proto-oncogenes (Hergovich *et al*., 2006). Like in animals, also in plants specific cell types undergo programmed cell death (PCD) as part of their developmental and differentiation program (Vaux and Korsmeyer, 1999). From embryogenesis to fertilization, cell and tissue death is an integral part of plant development and morphogenesis as well as a response to the environment (Barlow, 1982; Buckner *et al.*, 1988). Even though the cellular deterioration patterns described in plant tissues are in some cases similar to those observed in animal tissues, little is known of the mechanisms that control PCD in plants (Pennell and Lamb, 1997; Allen *et al*., 1998; Vaux and Korsmeyer, 1999). In angiosperms, PCD occurs late in the degenerative stage of the reproductive phase in both anther and pistil (Wu and Cheung, 2000). Production of functional male gametes depends largely on the deterioration and death of the anther

tapetum, whose main functions appear to be the nurturing of microspores with cortical surface molecules and allowing pollen dispersion at maturity. The pathway of female gametogenesis frequently begins with the death of all but one reduced megaspores, while surrounding nucellar cells degenerate in concert with embryo sac expansion (Reiser and Fisher, 1993; McCormick, 1993; Barcaccia *et al*., 2003).

Mob1 may be a component of a complex of proteins with multiple functions, not only involved in cytokinesis, cell proliferation and morphogenesis, but also operatively associated with cell death. The possible involvement of Mob1 proteins in PCD is also supported by recent analysis of Mob1-like expression in alfalfa reproductive tissues. In the ovules during gametogenesis, both transcripts and proteins were mainly visualized in the reduced megaspores undergoing PCD or in the remnants of degenerated megaspores, whereas in the anthers, Mob1-like gene products were specifically found at the end of gametogenesis in tapetum cells naturally undergoing PCD to allow pollen grain dispersal (Citterio *et al.*, 2005). Moreover, localization of MOB-domain containing proteins was also documented in alfalfa meristematic tissues of the plant roots. It is known that the root cap consists in living parenchyma cells derived continuously from the apical meristem and programmed to die: as new cells are produced in the interior, those on the root periphery are shed in an orderly manner. Hybridization signals were detected in a thin cell layer of the root apex where meristematic root tip cells divide and differentiate in root cap. Such finding further supports the concept that Mob1-like proteins are related to the onset of programmed cell death in plants (Citterio *et al*., 2006).

Differential display analyses performed on an apomeiotic mutant of *Medicago sativa* L. (Barcaccia *et al*., 2000) enabled the identification and characterization of a *Mob1*-like gene that resulted to be differentially expressed between the 2*n* egg cell producer and wild type progenies (Barcaccia *et al*., 2001). To further elucidate the role of the *Mob1*-like gene during sporogenesis and gametogenesis, a reverse genetics approach was followed using *Arabidopsis* as biological system. Data collected on plant fertility traits along with megasporogenesis and embryo sac formation patterns in RNAi lines are reported and critically discussed.

Materials and Methods

Construction of the binary vectors and plant transformation

For the production of a RNAi construct specific of the Arabidopsis *Mob1*-like gene (*At5g45550*), a 158 bp long cDNA unique fragment was amplified using specific primers designed in the 3'-UTR: RNAMOB1FOR (5'-CACCTTGAGCAAAAGACCATTTCTG-3') RNAMOB1REV (5'-TACATAGTAAATGTTTAAATTTTACAG-3'). The forward primer contained four additional bases at the 5' end, not present in the native sequence, which were required for directional cloning. The PCR product was cloned into pENTR™/D-TOPO_vector (Invitrogen, Carlsbad, CA), according to the recommendations of the supplier. This vector was sequenced to confirm the absence of errors and then used for LR recombination reaction performed with the RNAi Gateway destination vector pK7GWIWG2(II) (Karimi *et al*., 2002), producing the *Mob1-RNAi* vector.

For the *GFP-MOB1* construct, the *Mob1* coding region was PCR-amplified from a leaf cDNA using specific primers: ESMOB1FOR (5'-CACCATGAGTCTCTTTGGGTTAGG-3') and ESMOB1AREV (5'-TCAATAAGGTGAAATGATAGATT-3') The PCR product was cloned into pENTR™/D-TOPO_vector and subsequently transferred into the destination vector pK7FWG2 (Karimi *et al*., 2002), producing the *GFP-MOB1* vector using the strategy as described above. Constructs were transformed into the *Agrobacterium tumefaciens* strain EHA105 by electroporation.

Plant materials and growth conditions

The Columbia (Col-0) ecotype of *Arabidopsis thaliana* was used in all experiments. Surface-sterilization of wild-type (WT) and silenced lines (4G, 6M and 2F) seeds was achieved with a treatment based on an immersion in 70% ethanol for 2 min followed by a 10 min in a 30% (v/v) commercial bleach solution and 5 rinses with sterile water. Sterile seeds were then plated in Petri dishes (Ø 10cm) containing 0.5 X Murashige and Skoog (1962) salts, 0.5% (w/v) sucrose (Sigma), 1% agargel (Sigma), and left for 3 days at 4° C in a dark chamber to synchronize their germination. Kanamicin (50 mg/ml) was added for selecting silenced lines and plates were incubated at 22° C in a growth chamber with a

daylight cycle of 16 h of light and 8 of dark for 10 to12 days. Seedlings were then transplanted and grown with the same environmental conditions.

Arabidopsis plants Col-0 ecotype were transformed by a modified version of the floral dip method (Clough and Bent, 1998), in which the *Agrobacterium* culture was applied directly to flower buds using a pipette.

For gene expression analysis, leaves and roots were collected 30 days after germination, whereas flowers were collected at S7-8, S12 and S13 developmental stages (Smyth *et al*., 1995), corresponding to flower buds, flower with visible petals and completely opened flowers, respectively. Siliques were collected at stage 1 (half of total elongation) and stage 2 (complete elongation), corresponding to early and late S17 flower developmental stage, respectively (Smyth *et al*., 1995).

RNA isolation and analysis

Total RNA was extracted and purified using the SIGMA-Aldrich RTN70 Mammalian RNA extraction Kit, following the manufacturer's instructions.

The samples were treated with RQ1 RNase-free DNase (Promega, Madison, WI) following the manufacturer's instructions. Reverse transcription was performed with the oligo(dT) primer using the ImProm-II Reverse Transcriptase system (Promega) according to the manufacturer's instructions.

Semi-quantitative Real-Time RT-PCR

Semi-quantitative Real-Time RT-PCR analyses were performed using Mx3000P QPCR (Stratagene, La Jolla, CA) with SYBR green PCR Master Mix reagent (Applera, Foster City, CA). Specific primers for *Mob1* were designed in the 3'-UTR: MOB1AFOR (5'-CGCCTCTACAAGAGCTCATA-3') and MOB1AREV (5'-ATTGGGGTTTTTAATCTGAA-3'). All Real-Time RT-PCR experiments were performed with two independent sets of RNA samples. Each analysis was performed in a final volume of 50 µL containing 1 µL of cDNA, 0,2 µM of each primer, and 25 µL of 2XSYBR Green PCR Master Mix according to the manufacturer's instructions. The following thermal cycling profile was used for all PCRs: 95°C for 10 min, ~50 cycles of

95°C for 10 s, 57°C for 15 s, 72°C for 15 s. All quantifications were normalized to actin cDNA fragments amplified in the same conditions by primers ACT5RT (5'-CTCATGCCATCCTCCGTCTT-3') and ACT3RT (5'-CAATTTCCCGCTCTGCTGTT-3'). Each real-time assay was tested by a dissociation protocol to ensure that each amplicon was a single product. Negative template controls were run in these experiments, and no signal was observed (data not shown). The amplification efficiency was calculated from raw data using LingRegPCR software (Ramakers *et al*., 2003). The relative expression ratio value was calculated for the first developmental stage of flowers according to the Pfaffl equation (Pfaffl, 2001).

Root and steam histological analysis

Cross sections of wild-type and *AtMob1*-RNAi *Arabidopsis* stems and vascular bundles were histologically analysed. Transverse vibratome sections of 80 µm at the basal internode of wild-type Col-0 and *AtMob1*-RNAi lines were performed five weeks after germination and stained with toluidine blue, phloroglucinol and aniline blue, in different preparations. For what concern the primary root, the effect of *Mob1* silencing was investigated in seedlings after 48h from imbibition. Image analysis (Image-Pro Express 6.0, Media Cybernetics) was applied to measure the length, diameter and area of the different primary root regions and the mean area of the meristematic cells.

Cytohistological observations of sporogenesis and gametogenesis by light microscopy

Ovules were dissected on a slide under a Zeiss Discovery.V20 (Carl Zeiss MicroImaging, Germany) stereomicroscope and cleared with chloral hydrate prior to observation. Alternatively, whole inflorescences were stain-cleared following the protocol reported by Stelly *et al*. (1984) with some minor modifications. Briefly, the tissues were fixed in FAA (3.7% formalin, 5% acetic acid, 50% ethanol) overnight at 4°C, and then progressively rehydrated for following staining steps. Samples were stained with pure Mayer's hemalum for 30 min, placed in acetic acid 2% for 30 min, then dehydrated with in 25%, 50% 70%, 95% and 100% progressive ethanol solutions for 20 min each. After dehydration, samples were cleared with mixtures of pure ethanol and methyl salicylate (2:1 and 1:2) and twice

with pure methyl salicylate (10 min per step). Ovules were dissected on a slide under a Zeiss Discovery.V20 (Carl Zeiss MicroImaging, Germany) stereomicroscope then mounted with one drop of pure methyl salicylate and coverslipped. Cytohistological observations were realized by means of a Zeiss Axioplan (Carl Zeiss MicroImaging, Germany) microscope under DIC optics, using 100X objective.

Whole-mount immunolocalizations and confocal laser scanning microscopy

Flowers were collected and dissected under a Zeiss Stemi SV11 Apo stereomicroscope (Carl Zeiss MicroImaging, Germany). Carpels were fixed with 4% paraformaldehyde/MTSB (pH 7.0) for 1 h and washed three times with ddH2O. Tissue clarification was obtained with two washings in methanol for 20 min and progressive substitution with distilled water. Permeabilization was achieved by 30 min incubation in 0.15% Driselase (Sigma), 0.15% Macerozyme (Sigma) in 10 mM MES (pH 5.3) at 37°C, followed by one washing in MTSB and successive treatment with 10% DMSO, 3% Nonidet P40 (Fluka). After two washings in MTSB, blocking was performed in 3% BSA (Carl Roth, Germany) in MTSB for one hour at RT. Rabbit anti-MOB primary antibody (1:200) in 3% BSA in MTSB was applied for 1.5 hours at RT, followed by two washings in MTSB. Goat anti-rabbit A555-conjugated (1:600) secondary antibody (Invitrogen) was applied for 1.5 h at RT, followed by three washings in MTSB. Carpels were mounted in Prolong Gold antifade reagent containing DAPI (Molecular Probes). Samples were analyzed with a Zeiss LSM 5 DUO scanning microscope. Excitation wavelengths were 405 nm for DAPI and 561 nm for A555. Emission was detected between 420 and 480 nm for DAPI and above 575 nm for A555. Images were acquired using multi-tracking in frame mode and successively analyzed using the LSM image browser (Carl Zeiss MicroImaging, Germany).

Flow cytometric screening of WT and RNAi seeds

Single seeds were grinded in 80 µl of staining buffer (Citric acid monohydrate 0.1 M, Tween 20, 0.5 %, pH adjusted to 2-3 and mercaptomethanol) by using the 2000

Geno/Grinder homogenizer (Spex Certiprep) (50 strokes/2 minutes, 1x RATE). After grinding, 250 µl of staining buffer were added to each sample and the obtained suspensions (160 µl out of the total) filtered through a 30 µm mesh width nylon tissue. A total of 80 µl of the filtrated was then transferred in to a new 96 well plate and 80 µl of buffer Otto II (Na2HPO4, 12 H2O, 0.4 M, 2 ml of DAPI solution, pH adjusted to 8.5) added to each sample. The fluorescence intensity of DAPI-stained nuclei was determined using the flow cytometer Ploidy Analyser PA II (Partec GmbH, Münster, Germany), equipped with HBO mercury lamp for UV excitation. Originated histograms were than evaluated using the Flomax software (Partec GmbH).

Results

Mob1-like transcript levels are reduced in the RNAi transgenic lines

A post-transcriptional silencing approach mediated by RNA interference was carried out to shed light on the biological function of *Mob1*-like in *Arabidopsis* within both sporophytic and gametophytic tissues.

A 158 bp long sequence specifically belonging to the 3'-UTR of the target *Mob1*-like gene (locus At5g45550) was preliminarily selected to produce the RNAi construct for gene silencing experiments. This sequence was cloned in both sense and antisense orientations in the pK7GWIWG2(II) vector, under control of the CaMV-35S promoter and terminator, and the originated construct allowed to successfully transform wild-type *Arabidopsis* (Col-0) plants. Twenty independent kanamycin-resistant lines were recovered, each carrying the *Mob1*-like RNAi construct. Several plants from all obtained transgenic lines were self-pollinated. Plants putatively bearing a single copy of the transgene were selected according to a 3:1 segregation pattern of resistant vs. susceptible plantlets of their progeny grown in a medium added with kanamicin (Table 1). The expression analysis of the *Mob1*-like gene was performed by Real-Time reverse transcriptase PCR in order to estimate the amount of transcripts in distinct plant organs (*i.e.*, flowers, stems, leaves and roots) and to evaluate the effectiveness of gene silencing in all selected transgenic plants.

Table 1. Segregation ratios observed in the selected T1 *Mob1*-like RNAi lines.

Line	Kan^R	Kan^S	Ratio
T1-2	90	24	3.75:1
T1-4	91	27	3.37:1
T1-6	102	32	3.19:1

Mob1-like transcripts were detected in all analyzed tissues with different expression levels. In particular, the absolute amount of transcripts in young flowers was significantly higher than in later stages of partially or fully open flowers. Siliques, leaves and roots were characterized by lower levels of expression with respect to the flowers (Figure 1). More specifically, the expression levels measured in T2, T4 and T6 lines proved to be decreased as much as 50%, 50% and 70% respectively, compared to the corresponding wild-type organ (Figure 1).

Mob1-like silenced plants showed defects in vegetative growth and reproductive behaviour

The effect of *Mob1*-like gene silencing was investigated in both sporophytic and gametophytic constitutive parts of the plant.

The silencing of the *Mob1*-like gene resulted in a marked reduction of the seed set in all analyzed RNAi lines. Transgenic plants showed smaller siliques and a much lower number of seeds per silique compared to wild-type plants, as reported in Table 2. In particular, line 4G showed a phenotype stronger than phenotypes of lines 6M and 2F, although clearly deviating from the wild-type phenotype (Figure 2). As an example, wild-type plants yielded, on average, 3,614 $\pm$382 seeds per plant (No. of seeds/silique 54 $\pm$ 5), whereas this number decreased to 1,785 $\pm$255 for line 6M (No. of seeds/silique 30$\pm$7) and to 2.067$\pm$290 for line 2F (No. of seeds/silique 36$\pm$4). The number of seeds per plant was dramatically low in line 4G (130$\pm$75 with a No. of seeds/silique as low as 10$\pm$5).

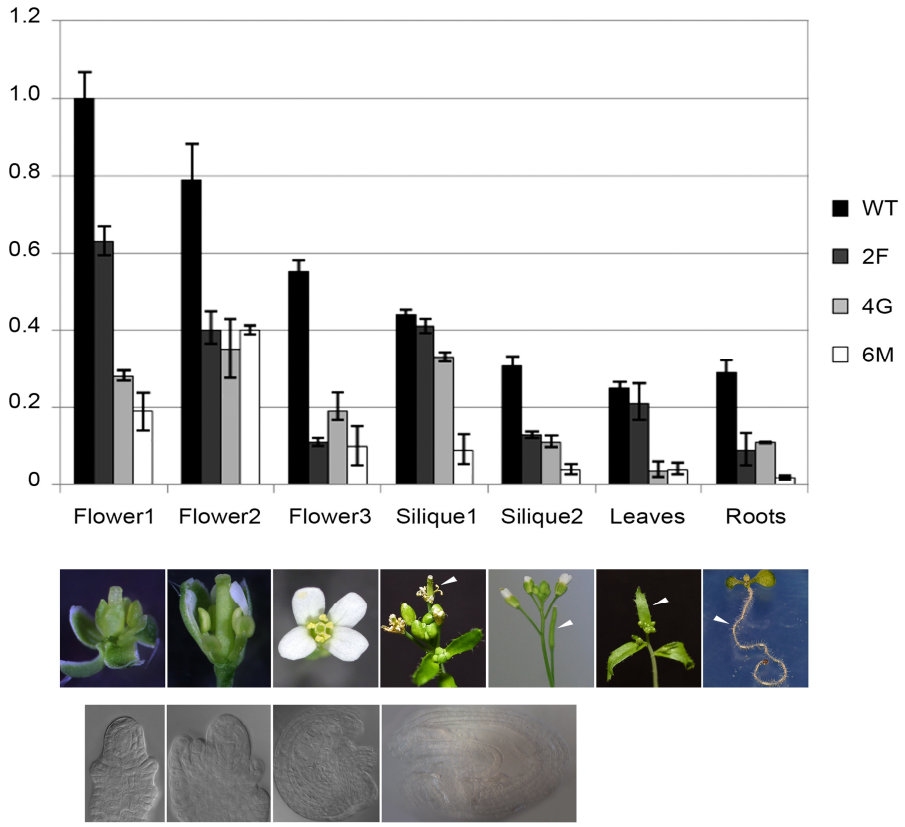

Figure 1. Expression analysis in *AtMob1*-like RNAi lines as assessed by Real-Time PCR. Three different stages of the flower were analyzed along with young and mature siliques, leaves and roots (bottom panels, white arrowheads). Flower and associated ovule stages are reported below the histograms. Dark grey, grey and light grey histograms refer to the expression levels recorded in 2F, 4G and 6M *AtMob1*-Like RNAi lines, respectively. The white histograms refer to the wild-type.

As far as the silique size is concerned, it was 47.9±6.3 mm in wild-type plants and as low as 31.0±3.5 mm and 33.0±3.0 in the lines 6M and 2F, respectively. Moreover, line 4G line produced siliques whose length was about one third compared to the wild-type ones (17.8±2.5 mm). Interestingly, for other morphological traits such as plant height, No. of stems per plant, siliques per plant, branches per stem, leaves per rosette and days to first open flower, line 4G differed significantly from wild-type plants, whereas lines 6M and 2F were comparable with the wild-types (Figure 2). Indeed, with the exception of some aberrant traits observed for the line 4G, lines 2M and 6F did not significantly differ from the wild-type for most of the considered morphological traits (Table 3).

Figure 2. Morphological traits of wild-type and *AtMob1*-like RNAi lines. The panel A shows the typical plant architecture along with flower morphologies and sizes recorded in wild-type and mutant lines. Panel B shows the silique sizes of WT and RNAi lines and the presence of aborted seeds observed in *AtMob1*-like silcenced lines. The arrow-head indicate the aborted seeds within siliques.

Table 2. Statistics on silique size and plant fertility related to WT and *AtMob1*-like RNAi lines.

	Silique size (mm)	Siliques/plant (No.)	Seeds/silique (No.)	Seeds/plants (No.)
WT	47.9±6.3	66.7±4.2	54.2±4.8	3614±382
2F	33.0±3.0	61.0±6.2	36.0±4.2	2067±290
4G	17.8±2.5	21.0±7.1	10.4±5.2	130±74
6M	31.0±3.5	60.0±5.8	30.0±6.7	1785±255

However, it is worth mentioning that stems proved to be much thinner in RNAi plants than wild-types. To further investigate structure and size of stem tissues, toluidine blue (Figure 3, A-D), phloroglucinol (Figure 3, E-H) and aniline blue (Figure 3, I-L) staining were performed on cross sections at the basal internode of stems of both wild-types and RNAi plants, five weeks after germination. Despite the largely conserved plant height, number of leaves per rosette and branching values, a marked reduction in terms of stem diameter was observed for all the RNAi independent lines (Figure 3, A-D). Moreover, a significant increment of the cell wall thickness restricted to the vascular vessels was recorded (Figure 3, E-H) using either phloroglucinol or aniline blue staining. A marked reduction of flower size was also observed in the silenced lines, associated with pistils and anthers much smaller than wild-type ones (Figures 2, 9). To characterize the RNAi plants as a whole, root length, diameter and area along with the mean area of the meristematic cells were measured with the use of a specific software for image analysis (Figure 4).

Table 3. Statistics on the main plant morphological traits related to wild-type and *AtMob1*-like RNAi lines

	Days to flowering	Plant height (cm)	Leaves/rosette (No.)	Stems/plant (No.)	Branches/stem (No.)	Germinability (%)
WT	30,5±1.4	40.3±2.7	13.4±0.8	3.0±1.1	2.9±0.6	98.5
2F	30,0±1.3	38.0±4.0	12.0±1.8	3.0±0.8	3.0±1.1	96.0
4G	24,9±2.1	28,6±2.8	9.0±1.7	10.6±2.5	5.4±1.1	78.3
6M	29,0±1.8	39.0±3.7	12.0±1.8	3.0±1.0	3.0±0.6	94.0

A detailed investigation of the primary root regions showed that only the area of the elongation region was clearly affected by the silencing of the *Mob1*-like gene as it was significantly (P<0,05) reduced in length (Figure 4C) but not in width (Figure 4D). The calculated size of root cap and meristem regions was similar in wild-type and RNAi line seedlings, whereas the hair region size was greater in silenced plants than in wild-types, although the difference was not statistically significant (Figure 4B). In the seedlings of RNAi lines, the greater hair region was balanced by the smaller elongation region and consequently the mean area of the whole root tended to be greater than in the wild-type plants (Figure 3A). Most importantly, RNAi lines were characterized by a significantly reduced size of the meristematic cells and consequently by an increased number of cells within the same area, as the size of this region was similar to that of the control.

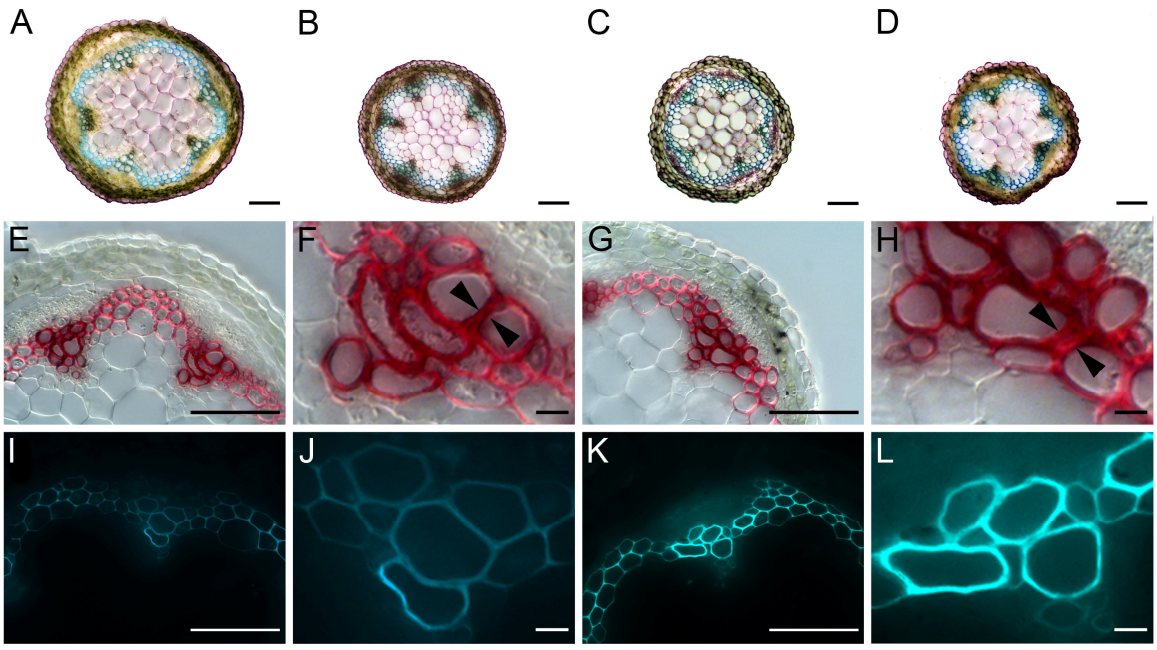

Figure 3. Organization and size of stems from WT and *Mob*1-like-RNAi individuals analyzed by staining of cross sections. Panels A-D: toluidine blue staining. Panels E-H: phloroglucinol staining. Panels I-L: aniline blue staining.

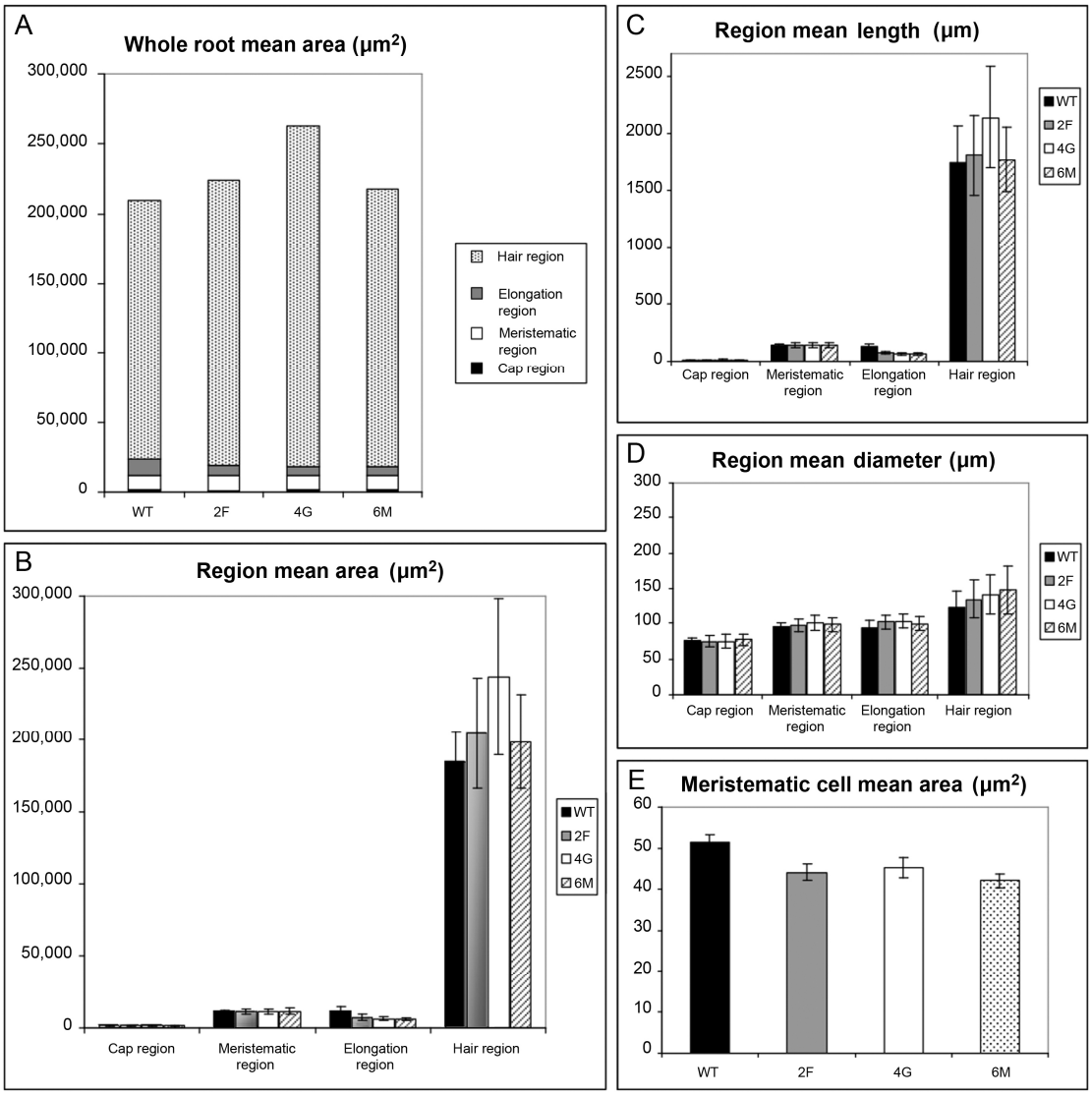

Figure 4. Histological analysis of the primary root in *Mob1*-like silenced plants in comparison with WT after 48 h from imbibition. Histogram A shows the mean area of the whole root, measured for two independent RNAi lines (4G and 6M) and for wild-types. Histograms C, B and D show the mean area, length and diameter (±SD) of the different root regions. The size of the meristematic cells (mean cell area ± SD) is reported in histogram E.

Mob1-like protein accumulates within the nucleus of somatic and sporogenic cells

The Arabidopsis sub-cellular localization of Mob1-like protein was attempted inducing the expression of a properly produced *GFP-Mob1* construct under the control of the CaMV-35S promoter and terminator. Strong and constitutive expression of the promoter allowed the visualization of the recombinant protein in root and leaf tissues and cells. Along with the sub-cellular localization of the protein, the specific localization of the Mob1-like protein was analyzed within wild-type ovules by means of immunolocalization and confocal laser scanning microscopy.

The sub-cellular localization within somatic tissues demonstrated the accumulation of the Mob1-like protein within the nucleus, according to a clear peri-nucleolar pattern.

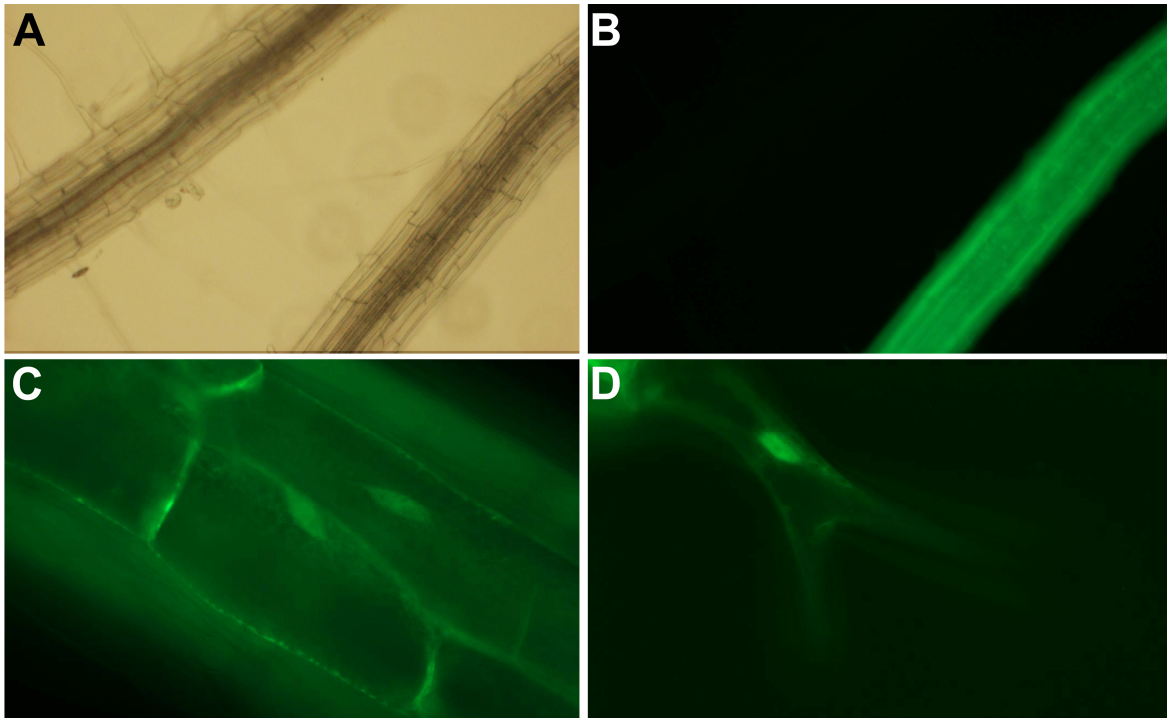

Figure 5. GFP::Mob1-like localization in *Arabidopsis* sporophytic cells. Panels A-B: GFP florescence is present in the mutant roots (right) but not in the wild-type roots (left). Panels C-D: Mob1-like localization within epidermal (C) and hair cells (D).

Figure 5 clearly shows the nuclear, specifically peri-nucleolar, localization of the Mob1-like protein within epidermal, root hair and stomata cells. Protein clusters were also visible in the most peripheral area of the cytoplasm, most likely in the plasma membrane.

A detailed analysis of Mob1-like protein domains and dynamics was also performed within wild-type ovules containing sporogenic cells and developing gametophytes (Figure 6). Protein immunolocalization within reproductive organs and specific cells was attempted in combination with DAPI staining of nuclear DNA contents by using

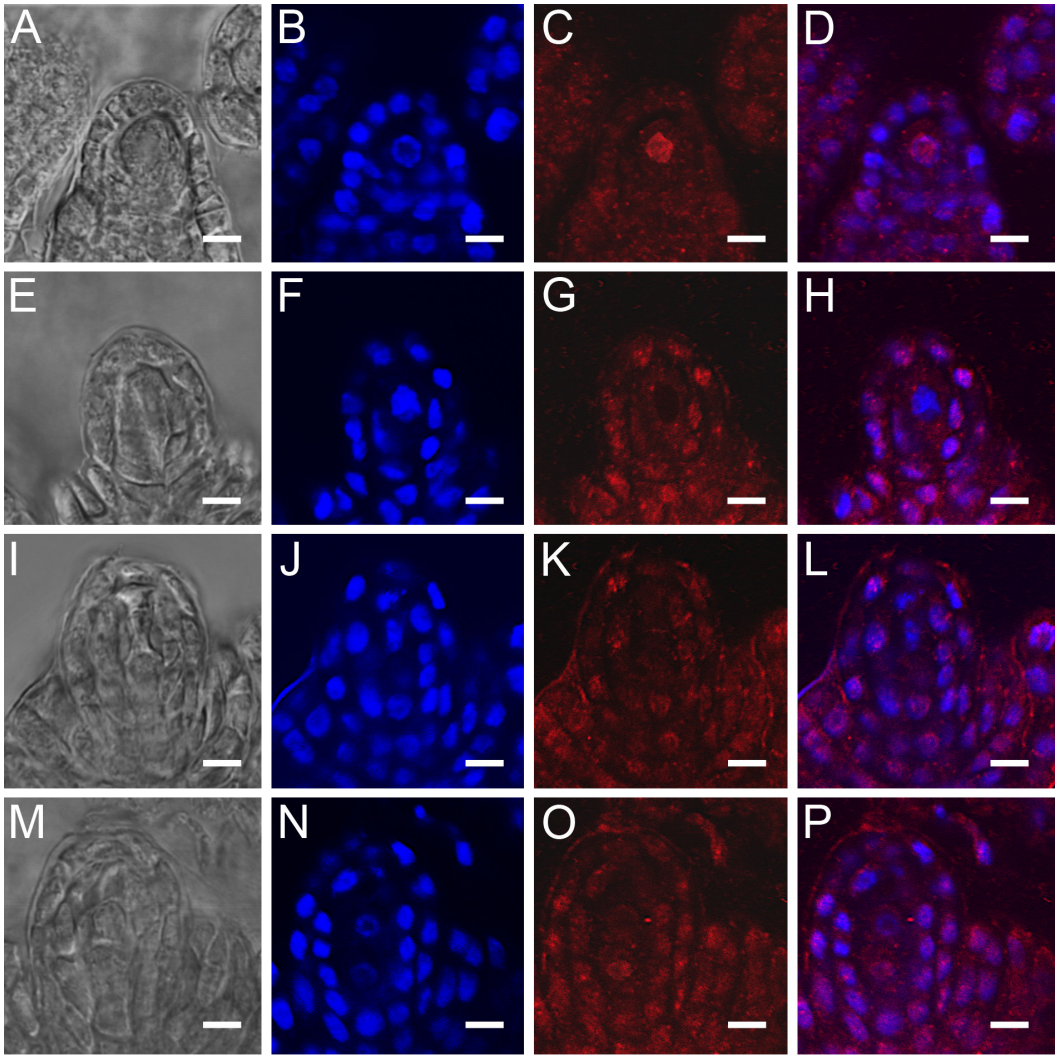

Figure 6. Whole-mount immunolocalization of Mob1-like in reproductive tissues at different developmental stages. Panels A, E, I, M: cleared tissues. Panels B, F, J, N: DAPI staining. C, G, K, O: Mob1-like immunolocalization. D, H, L, P: Merge of the DAPI and Mob1-like images. Panels A-D show ovules at pre-meiotic stages. Panels E-H show an ovule at MMC developmental stage. Panels I-L show an ovule in the tetrad stage. Panels M-P show an ovule at early two-nucleate embryo sac developmental stage.

whole-mount confocal laser scanning microscopy. This analysis was focused on pre-meiotic, meiotic and early post-meiotic ovules, corresponding to 2_I, 2-IV and 3-II stages, respectively (Schneitz *et al*., 1995). Results clearly demonstrated the localization of the protein within ovules at both meiotic and post-meiotic stages, thus confirming the physical presence of Mob1-like protein throughout female sporogenesis and early gametogenesis (Figure 6). In particular, the nuclear localization of Mob1 was observed in the megaspore mother cells (Figure 6, C) and early developing embryo sacs (Figure 6, O). In both sporophytic and gametophytic developmental stages, the Mob1 protein co-localized with the nuclear DNA as demonstrated by the overlapped signals generated by detecting the Mob1 protein with its specific antibody and the chromosomal DNA through DAPI staining (Figure 6, D-P). Interestingly, the Mob1-like protein was not detected within ovules at the meiotic stage (2-IV), undergoing nuclear division (Figure 6, G-K). Present findings clearly demonstrate, on one hand, the nuclear localization domain of the Mob1-like protein in sporogenic cells undergoing meiosis and, on the other, the accumulation dynamics of the Mob1-like protein in the gametophytic nuclei according to a cell cycle-dependent pattern.

Silencing of the *Mob1*-like gene causes defects of megasporogenesis and megagametogenesis leading to either unreduced megaspores and degenerated embryo sacs

Stain-clearing techniques combined with Differential Interference Contrast (DIC) microscopy were adopted to analyze dissected ovules of the *Mob1*-like-RNAi lines. A total of 81 ovules out of 183 totally considered (44%) revealed deviations from the regular female sporogenic developmental pattern at stage 2-IV/V. Besides the progression of normal megasporogenesis, 31 ovules out of 110 totally analyzed (28%) were characterized by premature degeneration of megasporocytes and megaspores at stages 2-III/IV. We found the proportion of degenerating pre-meiotic MMCs and meiotic megaspores to be highly variable among the three independent RNAi lines, being lower than 10% in line 4G

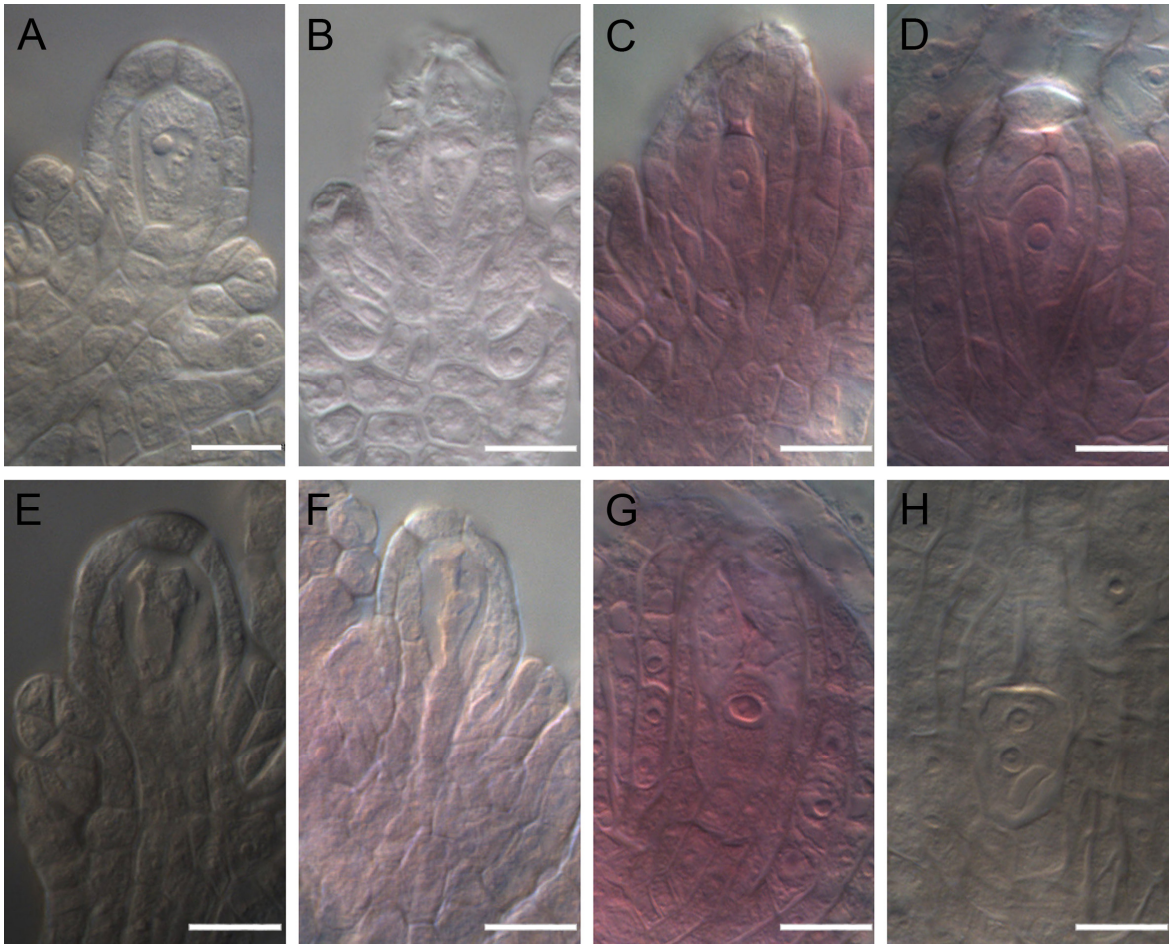

Figure 7. Female sporogenesis progression in *Arabidopsis* wild-type and *Mob1*-like RNAi lines. Panel A: MMC, B: tetrad, C, D: early and late functional megaspores. The degeneration of the micropylar meiotic megaspores is clear in D. E, F: megaspore degeneration at different developmental stages. G, H : unreduced megaspores.

and as high as 60% in line 6M. The abortion of megaspores in post-meiotic stages was frequently associated with the presence of two clearly detectable nuclei, enclosed within a centrally contracted cytoplasm. Moreover, 30 ovules out of 132 viable ones totally detected (23%) at stage 2-V proved to include bi-nucleate chalazal megaspores (Figure 7). The observed positioning of vacuoles within these unreduced megaspores deviated from the expected one as reported for FG1 and FG2 developing embryo sacs (Christensen *et al*., 1997). Many ovules bearing unreduced megaspores showed a delay of the most micropylar megaspore programmed death (Figure 7). In particular, such a delayed or missed degeneration of distal megaspores was observed in about 30% of ovules carrying unreduced chalazal megaspores and 20% of ovules bearing apparently reduced functional

Table 4. Megasporogenesis abnormalities in *AtMob1*-RNAi silenced lines.

	Developmental stages and number of ovules				Observed deviations	
	MMC	Dyad	Tetrad	FM	Degenerated	Unreduced
2F	4	0	0	9	17 (60.7%)	2 (7.1%)
4G	19	2	4	20	2 (7.1%)	2 (7.1%)
6M	60	9	22	47	32 (25.2%)	26 (20.5%)

megaspores (Figure 7, A-B). Surviving meiotic megaspores were also observed in ovules that contained developing embryo sacs: an average of 11% of ovules at stage FG2 were characterized by persistence of the micropylar megaspores, suggesting a failure of their cell death program.

The silencing of the *Mob1*-like gene affected also later stages of the embryo sac development. About 27% (50 ovules out of 183 totally analyzed) of ovules at FG6 stage showed gametogenesis abnormalities eventually leading to embryo sac degeneration (16% of the total number of embryo sacs considered).

Coherently with the degeneration events observed during early developmental stages, from 3.5% to 30.2% of the ovules completely lacked the embryo sac. This phenomenon was mainly observed in the RNAi lines 2F and 6M, being characterized by 21.0% and 30.2% of degenerated embryo sacs, respectively. The frequency of degenerated embryo sacs was much lower in the line 4G (4%).

Collapsed embryo sacs were observed in ovules at different developmental stages, ranging from FG2 to FG6. Frequently the cavity of these aborting ovules was filled by somatic cells showing heavily stained components.

Along with fully degenerated embryo sacs, a number of ovules clearly showed non-differentiated embryo sacs. Cytological evidences indicate that these ovules were characterized by a blocked development of embryo sacs at stage FG1. Most of the ovules completely lacked an embryo sac which cavity was apparently replaced by a tissue produced from an atypical proliferation of sub-epidermally localized cells. In these ovules, nucellar-derived tissues were typically composed by enlarged cells that often developed towards the most micropylar pole of the embryo sac cavity.

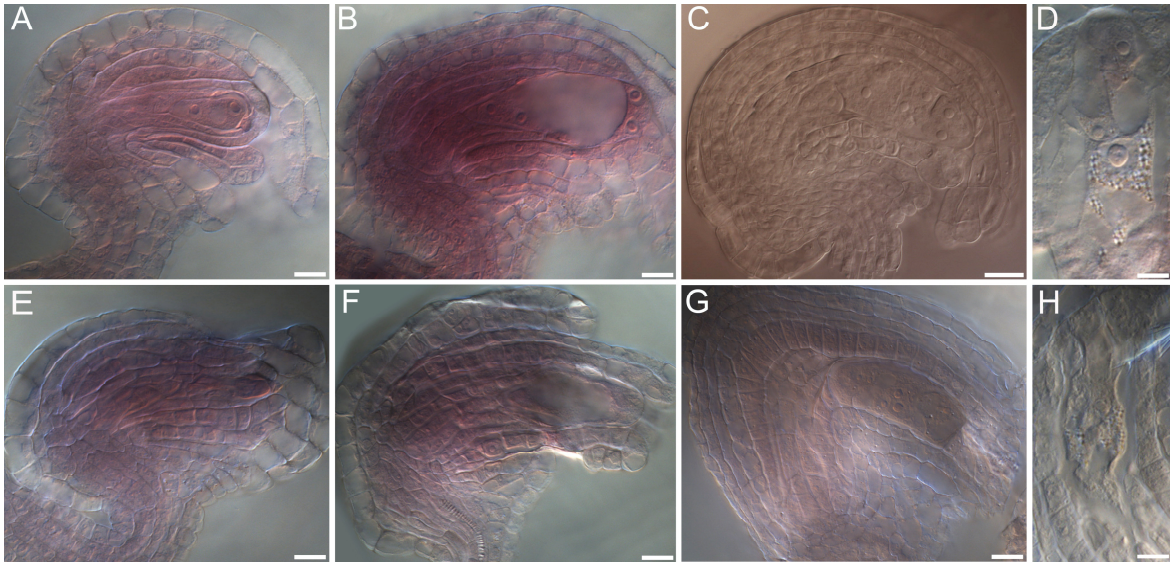

Figure 8. Arabidopsis wild-type megagametogenesis progression (upper panels) and most frequent deviations observed within ovules of RNAi lines (bottom panels). A: 2N embryo sac, B: 4N embryo sac, C: 8N embryo sac, D: mature embryo sac. E: embryo sac development arrest at 1N embryo sac developmental stage, F: overgrowing gametophyte, G: embryo sac degeneration and unregulated growth of the endothelium, H: lack of cellularization of the egg cell apparatus. (ES: embryo sac).

Moreover, about 30% of ovules bearing an FG6 embryo sac were characterized by cellularization abnormalities (Figure 8). In particular, from 26.4% to 28.4% (19 and 23 embryo sacs out of 72 and 81, respectively) of ovules bearing an FG6-like embryo sac showed a defective cellularization due to the mis-localization, often combined with an abnormal shape, of the egg cell and synergids prior to their degeneration (Figure 8).

A rare phenotype was observed in ovules lacking an embryo sac and it consisted in the presence of an abnormal coenocytic structure developing from the already formed endothelium (Figure 8). Such structure was observed only within ovules characterized by a complete lack of embryo sac at late developmental stages. Multinucleate cells were produced by either anticlinal or periclinal divisions of somatic cells belonging to the endothelium. Coenocytic structures included an atypical number of nuclei, up to 10 as a whole, characterized by a high variation in their size and distribution pattern within the cytoplasm.

Table 5. Megagametogenesis abnormalities in *AtMob1*-RNAi silenced lines.

	Developmental stages and number of ovules				Observed deviations	
	2N ES	4N ES	8N ES	Mature ES	Degenerated ES	Defective cell.
2F	3	9	21	72	26 (30.2%)	19 (26.4%)
4G	36	25	23	30	4 (5.0%)	8 (26.6%)
6M	29	26	31	81	29 (21.0%)	23 (28.4%)

Microsporogenesis abnormalities of *Mob1*-like silenced lines are responsible for the production of unreduced pollen

Pollen viability of *Mob1*-RNAi plants was compared with that of wild-types. The stainability of pollen produced by each RNAi line was regular and comparable with that of wild-type pollen, as demonstrated by the red staining of the cytoplasmic region in place of the green-blue staining expected for non-viable pollen grains (Figure 9). Furthermore, the aceto-carmyne staining of pollen grains collected from RNAi lines allowed the identification of a high variation in terms of pollen size. Similarly, DAPI staining of pollen grains collected from wild-type and RNAi individuals showed a high variation for the nucleus stainability (Figure 9). This observation strongly accounts for ploidy variation and production of unreduced pollen in the *Mob1*-like silenced lines.

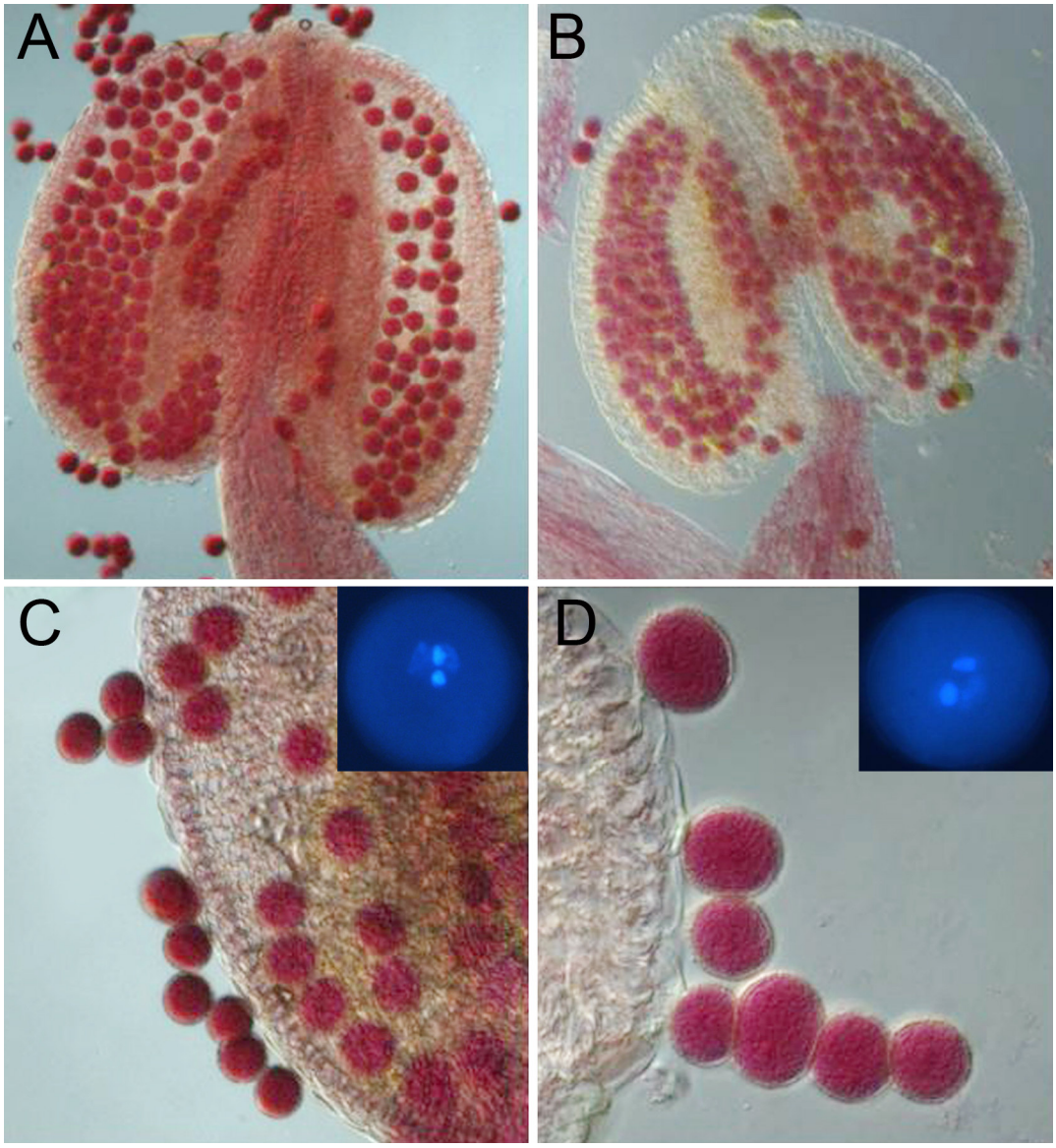

Figure 9. Alexander's staining and DAPI staining of dissected pollen from wild-type (A, C) and *Mob1*-like RNAi (B, D) individuals. Viable, red stained, pollen grains are visible in panels A-D. The panel D shows the high variation in pollen size recorded in the silenced lines, variation that was never observed for the wild-types (panel C). Panels C and D (upper right side) include a detail of DAPI stained pollen grains in which the different size of the vegetative nucleus in WT and RNAi plants can be clearly seen.

The production of tetraploid seeds supports the occurrence of bilateral sexual polyploidization events in the *Mob1*-like silenced plants likely mediated by unreduced gametes

Seed ploidy analysis was investigated by flow cytometric screening of single seeds originated by selfing *Mob1*-RNAi plants (Figure 10). Although no DNA peak corresponding to the endosperm was visualized, due to the very low amount of living cells in *Arabidopsis* seeds, this analysis allowed a clear detection of the DNA peak corresponding to the embryo. Wild-type samples and standard controls were run on all plates thus allowing the estimation of the nuclear DNA content of each single seed preparation (Figure 10). The flow cytometric seed screen revealed that *Mob1*-RNAi plants produced a low frequency of tetraploid progenies (about 2%, *i.e.* 6 tetraploids out of 300 seeds totally screened) (Figure 10), whereas only diploids were detected in the wild-types (250 seeds totally analyzed). Polyploid seeds were mainly recorded in the lines 2F and 6M, whereas in the line 4G they were never detected.

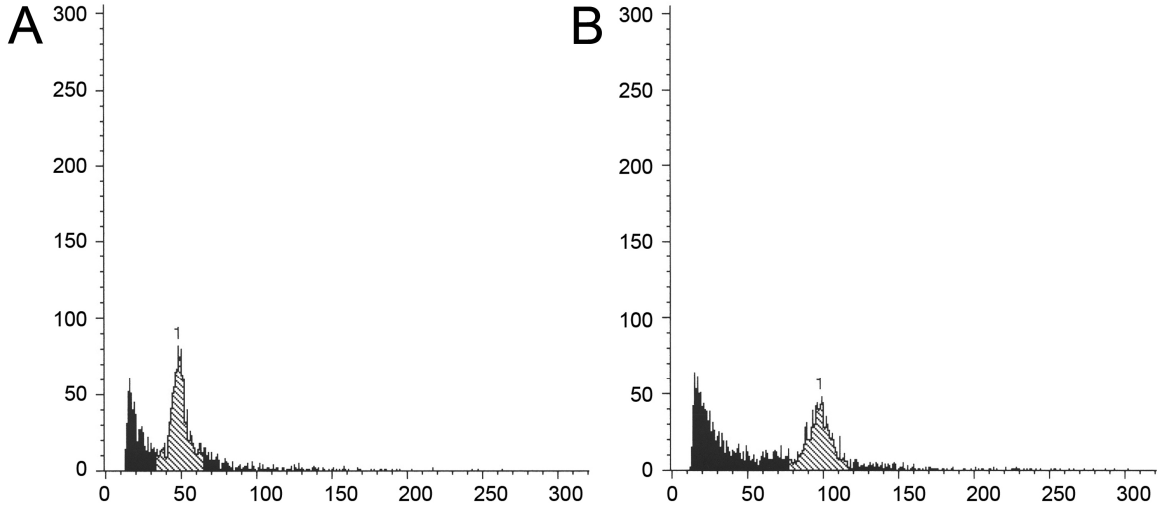

Figure 10. FCM Histograms of nuclear DNA content obtained by simultaneous analysis of nuclei isolated from WT and *AtMob1*-like single seed samples. Histograms corresponding to the diploid (left panel) and tetraploid (right panel) DNA contents are reported.

Discussion

A partial silencing of the *Mob1*-like gene associates to an altered plant growth in *Arabidopsis*

Abundant *Mob1*-like transcripts were detected in all analyzed tissues. It is however interesting to note that gene expression was predominant in flowers and much higher than levels recorded in siliques, leaves and roots, thus suggesting a major activity of the Mob1-like gene in reproductive organs. Concerning the effect of *Mob1*-like silencing with respect to the primary root, a significant reduction of the cell size along with an increment of the cell number was recorded in the meristematic area. Moreover, a significant reduction in size of the elongation region of the primary root was recorded. Since the elongation region is composed of cells originated from the meristematic area, which undergoes elongation prior to differentiation, it is likely that a close connection exists between the reduced cell size recorded for the meristematic area and the reduced size of the elongation region. As far as the green part of the plant is concerned, despite the largely conserved plant height, number of leaves per rosette and branches per plant, a marked reduction in terms of stem diameter was observed for all the RNAi independent lines. Furthermore, a marked reduction of flower size was also observed in the silenced lines, associated with pistils and anthers much smaller than wild-type ones. Present results on the effect of *Mob1*-like silencing with respect to the vegetative part of the plant are highly reminiscent of the results reported for several mutants of the HIPPO network in fly and mouse (Lai *et al*., 2005; St John *et al*., 1999). Present investigations of the primary root morphology further confirm the already postulated involvement of *Mob1*-like in cell proliferation (Citterio *et al*., 2006). Moreover, the increased cell proliferation observed in the root meristem confirmed the predominant biological role of *Mob1* in cell division rate and morphogenesis, probably due to the HIPPO regulation network.

Morpho-phenological analysis reveals that *Mob1*-like gene affects ovule fecundity and pollen ploidy

Female fertility of RNAi lines, characterized by a partial silencing of the *Mob1*-like gene within flowers, greatly differed from wild-types. In particular, all *Mob1*-like RNAi lines showed a low number of seeds per silique and, consequently, a low number of seeds per plant. Lines 2F and 6M revealed a very similar phenotype. In fact, they did not statistically differ one from another for the traits related to siliques and seeds. Line 4G showed an even more severe phenotype in terms of plant fertility. This line was characterized by a number of seeds per silique markedly lower than that scored in lines 2F and 6M.

Overall results indicate that Mob1-like gene could be involved in flower growth, pistil and anther development, and gamete fertility. As a matter of fact, all three *Mob1*-like silenced lines showed flowers, pistils and anthers much smaller than wild-type flowers, and their ability to set seeds was strongly affected compared to wild-types (the number of seeds per silique was, on average, 25 in silenced lines vs. 54 in wild-types). It is worth mentioning that in the three RNAi lines all siliques contained many aborted ovules and underdeveloped embryos. This behavior could be due not only to the documented meiotic and post-meiotic alterations during embryo sac development, but also to post-fertilization blocks because of endosperm unbalanced numbers determined by the fusion of an unreduced egg cell with a normally reduced sperm nucleus. Taking this into account, seed abortion was likely a consequence of endosperm unbalanced numbers, originated by unconventional maternal versus paternal genome contribution. Scott *et al*. (1998) have demonstrated that an increased dose of maternal genomes with respect to paternal contribution inhibits endosperm development and ultimately leads to smaller embryos. The finding of both bi-nucleate megaspores and jumbo pollen grains in the *Mob1*-like RNAi lines suggest that the development of the seed and in particular the endosperm may be abnormal in interploidy gamete unions, when a maternal or a paternal genomic excess takes place with fertilization.

Mob1-like gene expression is essential for a regular progression of megasporogenesis and megagametogenesis

Our combined cytological, molecular and immunological results support the hypothesis that the *Mob1*-like gene (At5g45550) is essential for the regular progression of megasporogenesis and the formation of functional embryo sacs in *Arabidopsis*. If it is true that the *Mob1*-like transcripts were particularly abundant in early stages of flower development, it is also true that the corresponding protein was mainly localized in the nucleus of enlarged MMCs in wild-type plants. This is not the first evidence of sub-cellular localization of the protein as the MEN protein kinase complex Mob1p-Dbf2p was already shown to be localized in the nucleus of diving cells during mitosis. Moreover, a partial co-localization of Mob1p with Cdc14p and kinetochore proteins was reported by Stegmeier and Amon (2004), Van Damme *et al*. (2005) and Vitulo *et al*. (2008). In agreement with their functions in mitosis exit and cytokinesis, it was reported that yeast Dbf2/Sid2-Mob1 complexes localize to the spindle pole body in anaphase and move to the division site in late mitosis (Stegmeier and Amon, 2004). As a matter of fact, localization of Mob1 protein in plants was reported for tobacco Bright Yellow-2 cells (Van Damme *et al*., 2004), while a cell cycle-regulated pattern with alternation of perinuclear and cytoplasmic localization, was described for synchronized alfalfa root tip cells (Citterio *et al*., 2005).

Two major considerations may be accounted for the localization of Mob1 proteins within ovules. First, the nuclear localization of this protein in enlarged megaspore mother cells entering meiosis is coherent with previously reported observations in somatic cells and the specific role played by Mob1p in the MEN network as well as Cdc14p localization was extensively documented to be nucleolar prior to FEAR and MEN mediated activation. Second, besides the involvement of Mob1-like proteins in the progression of the mitotic process, exit from it and cytokinesis, dynamics and domains of Mob1-like protein localization and accumulation during sporogenesis and gametogenesis account for a key role of the gene in either the meiotic process and the formation of embryo sacs. A large number of the analyzed ovules displayed aberrant phenotypes emerging at multiple time points of the ovule developmental pattern. The morphological alterations found in the *Mob1*-like RNAi lines can be divided in two main groups: i) alterations related to an

altered regulation of the cytokinetic machinery; ii) modifications of the programmed cell death regulation pathway. The post-transcriptional silencing of the gene seems to interfere with the normal progression of both female meiosis and megagametogenesis, leading to multinucleated megaspores and embryo sacs carrying cellularization defects. The post-transcriptional silencing of the gene is also responsible for alterations of the onset of PCD in micropylar megaspores next to the functional one and ovular cells surrounding the embryo sac. Considering the involvement of *Mob1*-like genes in different pathways controlling the cell cycle coordination with cytokinesis and cellular proliferation, it is not surprising that the silencing of the gene results in multiple phenotypes evocative of the biological role that Mob1-like proteins play in the MEN and HIPPO networks. The most dramatic phenotype observed as a consequence of the *Mob1*-like post-transcriptional gene silencing is the lack of embryo sac development, due to the degeneration of megaspores or gametophytes at different developmental time points. It is likely that correct progression of the embryo sac development is interrupted by severe mis-regulation of fundamental processes, such as exit from the meiotic or mitotic program and its coordination with unconventional cytokinesis. Moreover, meiotic alterations caused by the silencing of *Mob1*-like gene were attributable to cytokinesis abnormalities finally resulting in the formation of unreduced dyads. Most importantly, unreduced megaspores produced by the silenced lines morphologically and genetically resemble the SDR mechanism found in the alfalfa apomeiotic mutant where the *Mob1*-like gene was firstly identified as differentially expressed with the wild-types. Similarly to the silencing of the *Mob1*-like gene, it was recently reported that mutation of *swi1*, a gene involved in chromatid cohesion and centromere organization, causes a single equational division in place of normal female meiosis, followed by arrest in further progression (Mtamayor *et al*., 2000, Siddiqui *et al*., 2000, Ravi *et al*., 2008). Further, these defects lead to the production of two diploid cells in place of four haploid megaspores, and failure to form a female gametophyte. It is particularly interesting that the dyad allele of SWI1 specifically causes female sterility, without affecting the pollen developmental pathway. In the other side, different mutation as: *tardy asynchronous meiosis* (Magnard *et al*., 2001), *tetraspore* (Spielman *et al*., 1997), and *sidecar pollen* (Chen and McCormick, 1996) are known to specifically affect cytokinesis during pollen development. Recent studies on *S. cerevisiae* and *Arabidopsis*

enabled the identification of *spo12-1*, *spo13-1*, *cdc5-1*, *cdc14-3*, and *slk19* mutant lines, characterized by single meiotic division instead of normal meiosis, leading to unreduced spore formation (Klapholz and Esposito, 1980; Marston *et al*., 2003 Sharon and Simchen, 1990a, 1990b; Kamieniecki *et al*., 2000). Authors reported that cells carrying any of this mutation undergo a single meiotic division with a "mixed" chromosome segregation pattern, in which some chromosomes segregate predominantly in a reductional manner (meiosis I-like; homologs are separated) and others preferentially segregate equationally (mitosis-like; sister chromatids are separated; Sharon and Simchen, 1990a, 1990b; Kamieniecki *et al*., 2000). Spo12-1, spo13-1, cdc5-1, cdc14-3, and slk19 are now known to be active component of the FEAR (cdc-Forteen Early Anaphase Release) network. It is likely that FEAR is a major regulator of early anaphase entry by targeting the same protein phosphatase (cdc14p) that is object of the MEN activity involving interaction with Mob1p. Marston *et al*. (2003) suggested that SpCDK1 might interact with FEAR network to act as a binary molecular switch by dropping to low levels so as to allow exit from MI but sufficient enough to prevent a S-phase between MI and MII, whereas both FEAR and MEN interact with CDK1 in mitosis (Stern *et al*., 2003). Several *Arabidopsis* hortologues of the yeast MEN/SIN networks such as spg1p, cdc7p and sid1p were recently identified by Bedhomme *et al*. (2008). Interestingly plant proteins seem to possess new motives, such as perfect consensus sites for phosphorylation by CDK (AtSGP2, AtMAP3Kepsilon1) or putative nuclear localization signal (AtMAP4Kalpha1). Moreover, Bedhomme *et al*. (2008) demonstrated the presence of two *Arabidopsis* paralogues for each *S. pombe* sequence. These features suggest that the plant SIN-related proteins might perform additional functions compared to their yeast counterparts. This hypothesis is reinforced by the identification of partners of plant proteins that act as signalling elements AtSGP1 and AtMAP3Kepsilon1 and that do not possess homology with SIN elements. Interestingly Vitulo *et al*. (2008) recently reported that all plant MOB-domain containing sequences likely developed from a single ancestor sequence, followed by single gene and whole genome duplication (Vitulo *et al*., 2008; Bedhomme *et al*., 2008). Similarly to what observed for the swi1/dyad mutant, FCSS analysis of seeds isolated from all the RNAi lines confirmed the possibility for some of the binucleated megaspores to precede throughout gametogenesis, leading to the formation of unreduced functional egg cells. As

a matter of fact, polyploidy (*i.e*. tetraploidy) was shown to occur in 1% plants of the progeny originated by self pollination of both 2F and 6M lines, characterized by silencing of the gene *Mob1*-like in Arabidopsis.

References

Agashe B, Prasad CK, and Siddiqi I (2002) Identification and analysis of DYAD: a gene required for meiotic chromosome organisation and female meiotic progression in *Arabidopsis*. Development, 129: 3935–3943

Barcaccia G, Tavoletti S, Falcinelli M and Veronesi F (1997a) Environmental influence on the frequency and viability of meiotic and apomeiotic cells in a diploid mutant of alfalfa. Crop Sci., 37: 70–76.

Barcaccia G, Tavoletti S, Falcinelli M and Veronesi F (1997b) Verification of the parthenogenetic capability of unreduced eggs in an alfalfa mutant by a progeny test based on morphological and molecular markers. Plant Breed., 116: 475–479.

Barcaccia G, Albertini E, Rosellini D, Tavoletti S and Veronesi F (2000) Inheritance and mapping of 2n egg production in diploid alfalfa. Genome, 43: 528–537.

Barcaccia G, Varotto S, Meneghetti S, Albertini E, Porceddu A, Parrini P and Lucchin M (2001) Analysis of gene expression during flowering in apomeiotic mutants of Medicago spp.: cloning of ESTs and candidate genes for 2n eggs. Sex Plant Reprod., 14: 233–238.

Barcaccia G, Tavoletti S, Mariani A and Veronesi F (2003) Occurrence, inheritance and use of reproductive mutants of alfalfa (*Medicago* spp). Euphytica, 133: 37-56.

Brukhin V, Curtis MD, Grossniklaus U (2005) The angiosperm female gametophyte: No longer the forgotten generation. Curr. Sci., 89:1844-1852

Chen YC, and McCormick S (1996) sidecar pollen, an *Arabidopsis* thaliana male gametophytic mutant with aberrant cell divisions during pollen development. Development, 122: 3243-3253.

Christensen C A, King EJ, Jordan JR and Drews GN (1997) Megagametogenesis in *Arabidopsis* wild type and the *Gf* mutant. Sex. Plant Reprod., 10: 49–64.

Christensen CA, Subramanian S and Drews GN (1998) Identification of gametophytic mutations affecting female gametophyte development in *Arabidopsis.* Dev. Biol., 202: 136-151.

Christensen CA, Gorsich S W, Brown RH, Jones LG, Brown J, Shaw JM and Drews GN (2002) Mitochondrial GFA2 is required for synergid cell death in *Arabidopsis.* Plant Cell, 14: 2215–2232.

Citterio S, Varotto S, Albertini E, Feltrin E, Soattin M, Marconi G, Sgorbati S, Lucchin M and Barcaccia G (2005) Alfalfa Mob1-like proteins are expressed in reproductive organs during meiosis and gametogenesis. Plant Mol. Biol., 58: 789-808.

Citterio S, Piatti S, Albertini E, Aina R, Varotto S and Barcaccia G (2006) Alfalfa Mob1-like proteins are involved in cell proliferation and localize in the cell division midplane during cytokinesis. Exp. Cell Res., 312: 1050-1064.

Clough SJ and Bent AF (1998) Floral dip: a simplified method for *Agrobacterium*-mediated transformation of *Arabidopsis thaliana*. The Plant Journal, 16: 735-743.

Devroe E, Erdjument-Bromage H, Tempst P and Silver PA (2004) Human Mob proteins regulate the NDR1 and NDR2 serine-threonine kinases. J. Biol. Chem., 279: 24444-24451.

Drews GN, Lee D and Christensen CA (1998) Genetic analysis of female gametophyte development and function. Plant Cell, 10: 5–18.

Drews GN, Yadegari R (2002) Development and function of the angiosperm female gametophyte. Annu. Rev. Genet., 36: 99-124.

Feldmann KA, Coury DA and Christianson ML (1997) Exceptional segregation of a selectable marker (KanR) in *Arabidopsis* identifies genes important for gametophytic growth and development. Genetics, 147: 1411–1422.

Gifford EM and Foster AS (1989) Morphology and Evolution of Vascular Plants (New York: W.H. Freeman)

Grini PE, Schnittger A, Schwarz H, Zimmermann I, Schwab B, Jürgens G and Hülskamp M (1999) Isolation of ethyl methanesulfonate- induced gametophytic mutants in

Arabidopsis thaliana by a segregation distortion assay using the multimarker chromosome 1. Genetics, 151: 849–863.

Grini PE, Jürgens G and Hülskamp M (2002) Embryo and endosperm development is disrupted in the female gametophytic *capulet* mutants of *Arabidopsis*. Genetics, 162: 1911–1925.

Grossniklaus U and Schneitz K (1998) The molecula and genetic basis of ovule and megagametophyte development. Semin. Cell Dev. Biol., 9: 227-238

Haig D (1990) New perspectives on the angiosperm female gametophyte. Bot. Rev., 56: 236–275

Hauser BA, He JQ, Park SO, Gasser CS (2000) TSO1 is a novel protein that modulates cytokinesis and cell expansion in *Arabidopsis*. Development, 127: 2219-2226.

Huang B-Q and Russell SD (1992) Female germ unit: Organization, isolation, and function. Int. Rev. Cytol., 140: 233–292.

Huck N, Moore JM, Federer M and Grossniklaus U (2003) The female gametophytic control of pollen tube reception is disrupted in the *Arabidopsis* mutant *feronia*. Development, 130: 2149-2159.

Hülskamp M, Parekh NS, Grini P, Schneitz K, Zimmermann I, Lolle S, Pruitt R (1997) The *STUD* gene is required for male-specific cytokinesis after telophase II of meiosis in *Arabidopsis thaliana*. Dev Biol., 187: 114-124.

Johnston AJ, Meier P, Gheyselinck J, Wuest SEJ, Federer M, Schlagenhauf E, Becker JD and Grossniklaus U (2007) Genetic subtraction profiling identifies genes essential for *Arabidopsis* reproduction and reveals interaction between the female gametophyte and the maternal sporophyte. Genome Biology, 8: R204

Kagi C and Gross-Hardt R (2007) How female become complex: cell differentiation in the phenotype. Current Opinion in Plant Biology, 10: 633-638

Karimi M, De Meyer B and Hilson P (2002) Modular cloning and expression of tagged fluorescent protein in plant cells. Trends Plant Sci., 10: 103–105.

Kwee HS and Sundaresan V (2003) The NOMEGA gene required for female gametophyte development encodes the putative APC6/CDC16 component of the Anaphase Promoting Complex in *Arabidopsis*. Plant J., 36: 853–866.

Lauber MH, Waizenegger I, Steinmann T, Schwarz H, Mayer U, Hwang I, Lukowitz W and Jürgens G (1997) The *Arabidopsis* KNOLLE protein is a cytokinesis-specific syntaxin. J. Cell Biol., 139: 1485-1493

Liu J and Qu L-J (2008) Meiotic and mitotic cell cycle mutants involved in gametophyte development in *Arabidopsis*. Mol. Plant, 1(4): 564-574

Luca FC and Winey M (1998) MOB1, an essential yeast gene required for completion of mitosis and maintenance of ploidy. Mol. Biol. Cell., 9: 29-46.

Luca FC, Mody M, Kurischko C, Roof DM, Giddings TH and Winey M (2001) *Saccharomyces cerevisiae* Mob1p is required for cytokinesis and mitotic exit. Mol. Cell Biol., 21: 6972-6983.

Magnard JL, Yang M, Chen YC, Leary M and McCormick S (2001) The *Arabidopsis* gene tardy asynchronous meiosis is required for the normal pace and synchrony of cell division during male meiosis. Plant Physiol., 127: 1157–1166.

Maheshwari P (1950) An Introduction to the Embryology of Angiosperms, McGraw-Hill, New York., pp. 453.

Mansfield SG, Briarty LG and Erni S (1991) Early embryogenesis in *Arabidopsis thaliana*. I. The mature embryo sac. *Can. J. Bot*., 69: 447–460.

McCormick S (1993) Male gametophyte development. Plant Cell, 5: 1265-1275

Mercier R, Vezon D, Bullier E, Motamayor JC, Sellier A, Lefevre F, Pelletier G and Horlow C (2001) SWITCH1 (SWI1): a novel protein required for the establishment of sister chromatid cohesion and for bivalent formation at meiosis. Genes Dev., 15: 1859–1871.

Murashige T and Skoog F (1962) A revised medium for rapid growth and bioassay with tobacco tissue culture. Physiol. Plant, 15: 473–497.

Otegui M and Staehelin LA (2000) Cytokinesis in flowering plants: more than one way to divide a cell Current Opinion in Plant Biology, 3: 493–502

Pagnussat GC, Yu HJ, Ngo QA, Rajani S, Mayalagu S, Johnson CS, Capron A, Xie LF, Ye D and Sundaresan V (2005) Genetic and molecular identification of genes required for female gametophyte development and function in *Arabidopsis*. Development, 132: 603-614.

Pfaffl MW (2001) A new mathematical model for relative quantification in real-time RT-PCR. Nucleic Acid Research, 29 (9): 2002-2007

Ponchon L, Dumas C, Kajava AV, Fesquet D and Padilla A (2004) NMR solution structure of Mob1, a mitotic exit network protein and its interaction with an NDR kinase peptide. J. Mol. Biol., 337: 167–182

Ramakers C, Ruijter JM, Lekanne Deprez RH and Moorman AFM (2003) Assumption-free analysis of quantitative real-time polymerase chain reaction (PCR) data. Neurosci. Lett., 339: 62-66

Raven PH, Evert RF and Eichhorn SE (1992) Biology of Plants (New York: Worth Publishers)

Ravi M, Marimuthu MPA and Siddiqi I (2008) Gamete formation without meiosis in *Arabidopsis*. Nature, 451: 1121-1124

Reiser L and Fischer RL (1993) The ovule and the embryo sac. Plant Cell, 5: 1291–1301

Robinson-Beers K, Pruitt RE and Gasser CS (1992) Ovule development in wild-type *Arabidopsis* and two female-sterile mutants. Plant Cell, 4: 1237-1249.

Schiefthaler U, Balasubramanian S, Sieber P, Chevalier D, Wisman E and Schneitz K (1999) Molecular analysis of *NOZZLE*, a gene involved in pattern formation and early sporogenesis during sex organ development in *Arabidopsis thaliana.* Proc. Natl. Acad. Sci. USA, 96: 11664-11669

Schneitz K, Hülskamp M and Pruitt RE (1995) Wild-type ovule development in *Arabidopsis thaliana*: A light microscope study of cleared whole-mount tissue. Plant J., 7: 731–749.

Sheridan WF *et al.* (1999) The *mac1* mutation alters the developmental fate of the hypodermal cells and their cellular progeny in the maize anther. Genetics, 153: 933–941

Siddiqi I, Ganesh G, Grossniklaus U and Subbiah V (2000) The dyad gene is required for progression through female meiosis in *Arabidopsis*. Development, 127: 197–207.

Smyth DR, Bowman JL, Meyerowitz EM (1990) Early flower development in *Arabidopsis*. Plant Cell, 2: 755-767.

Söllner RS, Glässer G, Wanner G, Somerville CR, Jürgens G, and Assaad FF (2002) Cytokinesis-Defective Mutants of *Arabidopsis.* Plant Physiology, 129: 678–690

Song J-Y, Leung T, Ehler LK, Wang C, Liu Z (2000) Regulation of meristem organization and cell division by *TSO1*, an *Arabidopsis* gene with cystein-rich repeats. Development, 127: 2207-2217.

Spielman M, Preuss D, Li F-L, Browne WE, Scott RJ (1997) *TETRASPORE* is required for male meiotic cytokinesis in *Arabidopsis thaliana.* Development, 124: 2645-2657.

St John, M.A., Tao, W., Fei, X., Fukumoto, R., Carcangiu, M.L., Brownstein, D.G., Parlow AF, McGrath J, and Xu T (1999). Mice deficient of *Lats1* develop soft-tissue sarcomas, ovarian tumours and pituitary dysfunction. Nature Genet., 21: 182-186.

Stavridi ES, Harris KG, Huyen Y, Bothos J, Verwoerd PM, Stayrook SE, Pavletich NP, Jeffrey PD and Luca FC (2003) Crystal structure of a human Mob1 protein: toward understanding Mob-regulated cell cycle pathways. Structure, 11: 1163-1170.

Stegmeier F, Visintin R and Amon A (2002) Separase, polo kinase, the kinetochore protein Slk19, and Spo12 function in a network that controls Cdc14 localization during early anaphase. Cell, 108: 207-220.

Stegmeier F and Amon A (2004) Closing mitosis: The functions of the cdcd14 phosphatase and its regulation. Annu. Rev. Genet., 38: 203-232

Stelly DM, Peloquin SJ, Palmer RG and Crane CF (1984) Mayer's hemalum-methyl salicylate: A stain clearing technique for observations within whole ovules. Stain Technol., 59: 155-161.

Tavoletti S, Mariani A and Veronesi F (1991). Cytological analysis of macro- and microsporogenesis of a diploid alfalfa clone producing male and female 2n gametes. Crop Sci., 31: 1258–1263.

Van Damme D, Bouget FY, Poucke K van, Inzé D, and Geelen D (2004) Molecular dissection of plant cytokinesis and phragmoplast structure: a survey of GFP-tagged proteins. Plant J., 40: 386-398.

Vitulo N, Vezzi A, Galla G, Citterio S, Marino G, Ruperti B, Zermiani M, Albertini E, Valle G and Barcaccia G (2007) Characterization and evolution of the cell cycle-

associated Mob domain-containing proteins in Eukaryotes. Evolutionary Bioinformatics, 3: 121-158

Willemse MTM, Went JL van (1984) The female gametophyte. In: Johri BM (ed) Embryology of angiosperms. Springer, Berlin Heidelberg New York, 159-196

Webb MC, Gunning BES (1990) Embryo sac development in *Arabidopsis thaliana*. I. Megasporogenesis, including the microtubular cytoskeleton. Sex. Plant Reprod., 3: 244–256

Webb MC, Gunning BES (1994) Embryo sac development in *Arabidopsis* thaliana. II. The cytoskeleton during megagametogenesis. Sex. Plant Reprod., 7: 153-163

Yang M, Hu Y, Lodhi M, McCombie WR, and Ma H (1999) The *Arabidopsis* SKP1-LIKE1 gene is essential for male meiosis and may control homologue separation. Proc. Natl Acad. Sci. *U S A*., 96: 11416-11421.

Yang W-C and Sundaresan V (2000) Genetics of gametophyte biogenesis in *Arabidopsis*. Curr. Opin. Plant Biol., 3: 53-57

Yang W-C, Ye D, Xu J, and Sundaresan V (1999) The SPOROCYTELESS gene of *Arabidopsis* is required for initiation of sporogenesis and encodes a novel nuclear protein. Genes Dev., 13: 2108-2117.

Yadegari R and Drews GN (2004) Female gametophyte development. Plant Cell, 16: S133-141.

Yu HJ, Hogan P and Sundaresan V (2005) Analysis of the female gametophyte transcriptome of *Arabidopsis* by comparative expression profiling. Plant Physiol., 139: 1853 1869.

Capitolo III

St. Jonh's wort (*Hypericum peroratum*) as a model species for studying apomixis: a review

Summary

St. John's wort (*Hypericum perforatum* L., 2*n*=4*x*=32) is a medicinal plant that produces pharmaceutically important metabolites with antidepressive, anticancer and antiviral activities. It is also regarded as a serious weed in many countries. Wild populations are composed of diploid sexual or polyploid (mostly tetraploid) pseudogamous facultative apomicts. Recent research has shown that *H. perforatum* is an attractive model system for the study of apomixis, as it is characterized by a relatively small genome size, a versatile mode of reproduction ranging from complete sexuality to nearly obligate apomixis, and a relatively short generation time. A better understanding of its reproductive and inheritance patterns is required to facilitate the identification of factors associated with apomixis, if these traits are to ever benefit agriculture. This paper reviews the cyto-embryological, molecular and ecological data which have been collected to elucidate apomixis in St. John's wort, and includes an overview of the main tools which have been and are being used to investigate apospory, parthenogenesis and apomixis within this system.

Introduction

Among the numerous medicinal herbs used throughout the history of Occidental culture, St. John's wort (*Hypericum perforatum* L.) has been, and remains of great interest. From the time of the ancient Greeks through to the middle Ages, the plant was considered to be imbued with magical powers which were used to ward off evil and to protect against disease (Hobbs, 1998). Extensive clinical and laboratory testing has led to the recognition of St. John's wort as a medicinal species that produces pharmaceutically important metabolites with possible antidepressant, anticancer, antiviral, antifungal and antimicrobial activities (Di Carlo *et al*., 2001; Agostinis *et al*., 2002; Miskovsky, 2002; Schempp *et al*., 2002; Dulger *et al*., 2005; Fenner *et al*., 2005; Ferraz *et al*., 2005; Francis, 2005; Malaty, 2005). It is additionally regarded as a serious weed in many countries (Holm *et al*., 1979; Mayo and Roush, 1997; Buckley *et al*., 2003).

Wild populations of St. John's wort are composed of diploid sexual and polyploid (mostly tetraploid) pseudogamous facultative apomicts, and hence this species represents a potentially interesting model system for apomixis research (see Matzk *et al*., 2001). The purpose of this paper is to review what is known regarding apomixis in the genus *Hypericum*, with a focus on *Hypericum perforatum*.

Taxonomy, Hybridization and Polyploidy

Hypericum perforatum belongs to the family Clusiaceae (alternative name Guttiferae), and four intergrading subspecies have been identified based upon variable morphology and geographic distribution: subsp. *perforatum*, subsp. *songaricum*, subsp. *veronense* and subsp. *chinense* (Robson, 2002). All subspecies reproduce through seed (mature capsules contain about 50-100 seeds and plants produce an average of 15-33 thousand seeds) in addition to vegetative propagation through rhizomes. Mature seeds (less than 1 mm in length and 0.5 mm in width) are hard-coated and typically require no post-ripening period for germination; they can remain viable for several years in the soil, and when consumed by animals remain intact and viable (Robson, 2002).

The species *H. perforatum* is characterized by a relatively small genome size (1*C*=0.650 pg, *http://www.rbgkew.org.uk/cval*) which corresponds to about 630 Mbp (Bennett, 1976). It has a basic chromosome number equal to 8, and its populations are composed mainly of tetraploids (2*n*=4*x*=32), although diploid and hexaploid chromosome numbers have also been reported (Matzk *et al*., 2001; Robson, 2002). In over 113 accessions characterized by Matzk *et al*. (2001) for the mode of reproduction, the basic ploidy level was for the most part tetraploid, although diploid and hexaploid plants were also identified. Neither triploid nor pentaploid plants were detected, whereas two pure diploid accessions were found. Interestingly, the diploid and tetraploid plants of *H. perforatum* were not morphologically distinguishable at either the juvenile or adult stages of development (Matzk *et al*., 2001). This variable ploidy is likely due to a dynamic reproductive system, as haploidization and polyploidization are mediated by parthenogenesis of meiotic egg cells and fertilization of aposporous egg cells, respectively.

It is unclear whether *H. perforatum* is allotetraploid or autotetraploid, although an ancient interspecific hybridization event between the diploids *H. attenuatum* and *H. maculatum* with subsequent chromosome doubling has been hypothesized on the basis of their morphological traits and geographical distribution areas (Campbell and Delfosse, 1984; Robson, 2002). In contrast, recent cytogenetic characterizations of different *Hypericum* species have demonstrated that *H. perforatum* may have originated through autopolyploidization from an ancestor closely related to the diploid *H. maculatum* (Brutovská *et al*., 2000). Interestingly *H. maculatum obtusiusculum,* a tetraploid subspecies of *H. maculatum* (Robson, 1981), has been demonstrated to be facultatively apomictic (Matzk *et al.,* 2003), and hence it is unknown whether this taxon has also played a role in the evolution of *H. perforatum.*

H. perforatum is morphologically intermediate between *H. maculatum* and *H. attenuatum*, two diploid species which have sessile herbaceous leaves and overlapping ranges in western Siberia (Robson, 2002). However, the most closely related subspecies of *H. maculatum* to *H. perforatum* is not one that occurs in Siberia today (subsp. *maculatum*) but instead subsp. *immaculatum* which is now confined to the Balkan region. One possibility is that subsp. *immaculatum* was at some time present in Siberia where it hybridized with *H. attenuatum*. Chromosome doubling in the resultant interspecific

diploid hybrid would then have given rise to an allotetraploid species, which through genetic isolation from the parental taxa and stabilization by apomixis (see below), may have spread from Asia to occupy its current native distribution across Europe, Asia to Northwest China, Asia Minor, Northwest India and North Africa (Mártonfi *et al*., 1996). *H. perforatum* has furthermore been successively introduced into North and South America, South Africa and Australia (Campbell and Delfosse, 1984; Crompton *et al*., 1988), where the species often behaves as an invasive weed.

H. perforatum is characterized by a number of traits reflective of hybridity, including: variability in morphology and chemical compound production, meiotic abnormalities (*e.g*., lagging chromosomes), elevated pollen grain sterility, parthenogenetic development of unreduced egg cells and pseudogamy. Male sterility is usually about 30%, but can be up to 70% (Nielsen, 1924; Hoar and Hartl, 1932) or higher (Matzk, pers. comm.), while apospory can vary from about 0 to 100% for unreduced egg cells (Matzk *et al*., 2001). When crossed with diploids, the reduced pollen grains of tetraploid *H. perforatum* lead to the production of triploid ($2n=3x=24$) hybrids, while the fertilization of aposporous egg cells by a reduced sperm nucleus from a diploid gives rise to pentaploid ($2n=5x=40$) offspring. In experimental hybrids involving *H. perforatum* and diploid species, Noack (1939) found that the triploid progeny were morphologically intermediate between the parents whereas pentaploid progeny could not be distinguished from the parental species. However, in the pentaploid progeny obtained from a cross between *H. maculatum* subsp. *maculatum* and *H. perforatum*, Mártonfi *et al*. (1996a) identified some intermediate characters and demonstrated additive patterns of the secondary metabolites from both parents. The hybrids involving *H. perforatum* can also be hexaploid ($2n=6x=48$), presumably resulting from the fertilization of aposporous egg cells by a normally reduced sperm nucleus from a tetraploid. The diploids ($2n=2x=16$) reported in this species should be referred as dihaploids or amphihaploids resulting from the parthenogenetic development of meiotic, normally reduced egg cells (Robson, 2002).

Allotetraploids (amphidiploids) are characterized by fixed (*i.e*. non-segregating) heterozygosity, the result of divergent parental genomes which undergo homoeologous bivalent formation at meiosis to yield disomic inheritance at each locus. In contrast, autotetraploids usually exhibit multivalent formation at meiosis and are characterized by

polysomic inheritance when more than two alleles occur at each locus. The relative genetic divergence of the parental taxa in allotetraploids is directly correlated with the potential for multiple chromosomes pairing, and thus amphihaploids are often sterile because they can form only univalents (Soltis and Soltis, 2000). This does not hold true for autotetraploids since their dihaploids are usually characterized by bivalent chromosome pairing and fertile gamete production. On the basis of the available data, *H. performatum* plants with a diploid chromosome number ($2n=2x=16$) are able to regularly set viable seeds. If this holds true as more populations are analyzed, this may indicate that the *H. perforatum* genome is allo- rather than autotetraploid in nature, or alternatively the segregation patterns may reflect genome homogenization via segmental allopolyploidy followed by diploidization (Gaut and Doebley, 1997).

Recently, molecular tools have helped elucidate the genome organization of tetraploid *H. perforatum*. Brutovská *et al*. (2000a) cytogenetically analyzed *H. perforatum* and its putative diploid ancestor parents, *H. maculatum* and *H. attenuatum*, by means of fluorescent *in situ* hybridization (FISH) with 5S/25S rRNA probes. The tetraploid nature of *H. perforatum* was confirmed by the observation of a doubled number of all loci compared to *H. maculatum*. Furthermore, *H. perforatum* and *H. maculatum* were characterized by identical chromosomal gene positions irrespective of their ploidy differences, supporting the hypothesis that *H. perforatum* may have arisen via autopolyploidization of *H. maculatum* or a closely related ancestor. A number of positional differences in genes were nonetheless identified in comparisons between *H. perforatum* and both *H. maculatum* and *H. attenuatum*, thus providing evidence against the hypothesis of allopolyploidization. Reciprocal genomic *in situ* hybridization (GISH) using genomic DNAs from *H. perforatum* and *H. maculatum* has demonstrated that even the repetitive sequence distribution of both species are very similar, and that those repeats derived from *H. maculatum* could not be distinguished from *H. perforatum*-like repeats, although these data are inconclusive due to the absence of *H. attenuatum* for comparison. The multiplied basic chromosome set reconstructed by karyogram analysis using selected metaphase plates from tetraploid plants provides further evidence supporting the autotetraploid nature of *H. perforatum* (Brutovská *et al*., 2000b). Firstly, it is worth noting that natural hybridization between *H. perforatum* and an autotetraploid form of *H.*

maculatum, subsp. *obtusiusculum,* gives rise to fertile interspecific apomictic hybrids (Robson, 1981). Taken together, the close relationship between *H. perforatum* and *H. maculatum* suggests that *H. perforatum* could have evolved from *H. maculatum* or, alternatively, from a common ancestor of both species (Lihova *et al*., 2000).

It is unclear what cytological mechanism has led to the origin of autotetraploid *H. maculatum*, although a restitutional mechanism leading to the formation and fusion of unreduced gametes (*i.e*., meiotic polyploidization; Harlan and deWet, 1975) is possible, as has been hypothesized for other autotetraploid species (*e.g*., *Solanum tuberosum*, Hermsen, 1984; *Paspalum rufum*, Quarin *et al*., 1998; *Medicago sativa*; see Barcaccia *et al*., 2003). Although karyological analyses of chromosomal pairing behaviour could help elucidate the genomic constitution of *H. perforatum* tetraploids, cytological observations at meiosis are difficult due to the morphologically indistinguishable chromosomes combined with their very small size. *Hypericum perforatum* has one of the smallest chromosomes of all *Hypericum* species for which chromosomes have been measured, with estimated lengths ranging from 0.78 to 1.52 μm (Reynaud,1986; Brutovská *et al*., 2000b). Karyotype analyses of *H. perforatum* have revealed that only the largest metacentric chromosome pairs are distinguishable in uniformly stained preparations, whereas the rest of chromosome complement can be recognized on the basis of the measured total length, centromeric index and arm ratio (Brutovská *et al*., 2000b). For example, the chromosomes of the genus *Hypericum* have been characterized to include 5 median and 3 submedian centromeres (Robson and Adams, 1968; Kogi, 1984), with arm ratios within the ranges of 1.0-1.7 and 1.8-3.0 respectively (Figure 1). Recently, *in situ* hybridization analysis with rRNA-specific probes have provided the necessary landmarks to discriminate 6 of the *H. perforatum* chromosomes (Brutovská *et al*., 2000a), and thus crucial information for the correlation of linkage groups with specific chromosome pairs.

Reproductive biology: apomictic and sexual pathways

Apomixis in this species was first described in the pioneering work of Noack (1939), but only recently characterized in great detail by Matzk *et al.* (2001). While *H. perforatum* reproduces mainly through facultative aposporous parthenogenesis, it has an extremely versatile mode of reproduction which ranges from nearly obligate apomixis to complete

sexuality. Embryo sacs may be either reduced (meiotic) or unreduced (aposporous) and both types of egg cells may be either fertilized (gamic) or develop partenogenetically (agamic), resulting in six possible categories of progeny (Figure 2). Pollination timing may influence the fate of aposporous and meiotic embryo sacs and hence the relative proportions of apomictically and sexually derived offspring from a single individual. It has been suggested that the earlier maturity of aposporous relative to meiotic embryo sacs means that the former are likely to have passed the stage of receptivity by the time of pollen tube penetration (Savidan, 2000). For example, artificially-induced earlier pollination produces a higher proportion of triploid hybrids, while delayed pollination may induce parthenogenesis originating so amphihaploids (reviewed by Savidan, 2000; Espinoza *et al*., 2002). Additional factors, such as photoperiod, temperature, nutrition, competition and pollen donor are thought to affect the balance between apomixis and sexuality in facultative apomicts (Grimanelli *et al*., 2001).

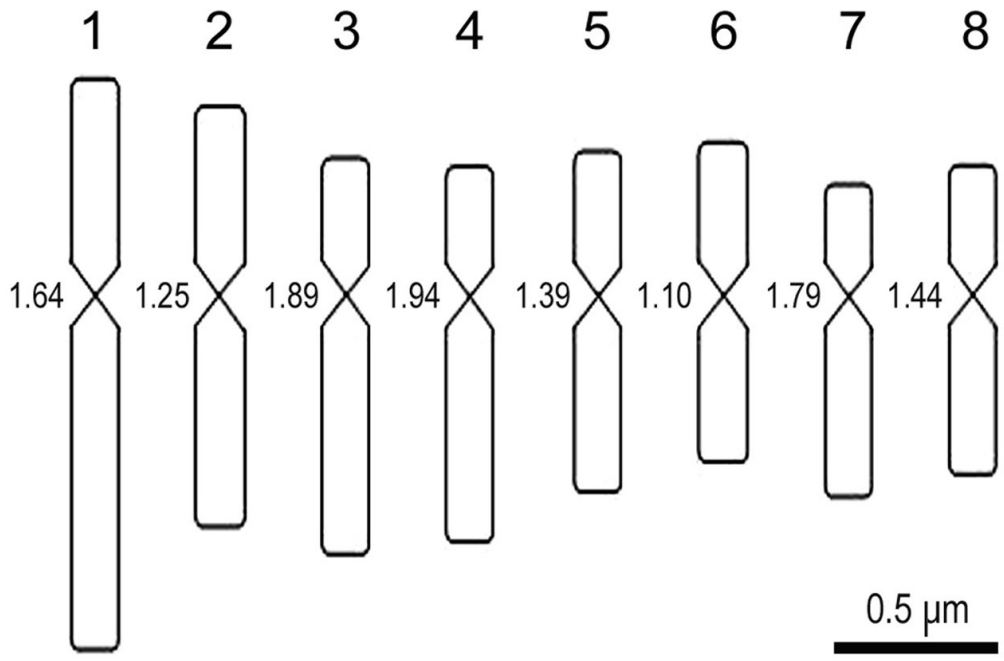

Figure 1. Karyogram of the basic chromosome complements (n=8) of *H. perforatum* reconstructed using mesurements by Brutovská *et al*. (2000b) with indications of arm ratios.

The flowers of *H. perforatum* are yellow, profuse, arranged in branched cymes and bisexual (Figure 3). Flowers are characterized by many anthers arranged in bundles of threes, with filaments basally united, bisporangiate and producing two-celled pollen grains at maturity. *H. perforatum* is characterized by elevated levels of degenerated pollen (Robson, 2002) which appears to be influenced in part by ploidy, as pollen tests have demonstrated 86% and 38% germination rates in diploids and tetraploids, respectively (Mártonfi *et al*., 1996b). As with many other gametophytic apomicts, abnormalities in pollen meiosis are common in *H. perforatum*, and may be due to the occurrence of lagging chromosomes (Nogler, 1984; Hoar and Haertl, 1932). In addition to partial male-sterility, another reproductive barrier to sexuality may be self-incompatibility, a mechanism apparently widespread in the genus *Hypericum* (Robson, 1977; 1981) but of which little information is available for *H. perforatum*.

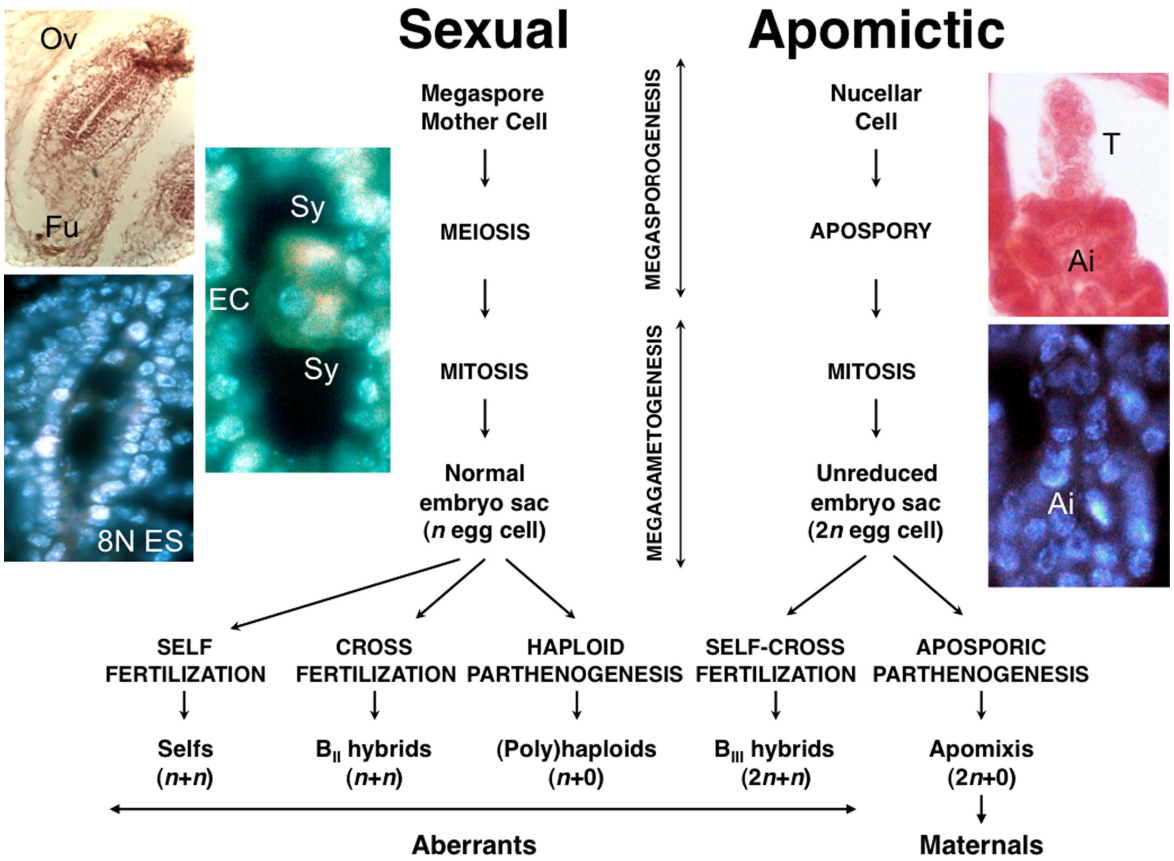

Figure 2. Reproductive routes in *H. perforatum*: embryo sacs may be either reduced (meiotic) or unreduced (aposporous) and both types of egg cells may be either fertilized (gamic) or develop partenogenetically (agamic), resulting in six possible categories of progenies.

The pistil is three-carpellar, while the ovary is superior, capsicular, with completely or almost completely axile placentae. It includes many ovules, and presents three styles diverging from discrete bases with a narrowly capitate stigma. The ovules themselves are anatropous and tenuinucellar. Megasporogenesis proceeds by an archesporial cell differentiating into a primary sporogenic cell which functions directly as the megaspore mother cell to meiotically generate a linear tetrad. At this point, *H. perforatum* can go through either a sexual (amphimictic) or asexual (apomictic) reproductive pathway. In the sexual pathway, the three micropylar megaspores degenerate while the chalazal one is functional and develops into a seven-celled *Polygonum*-type embryo sac. In contrast, the more ubiquitous apomictic pathway is typically characterized by the megaspore mother cell entering meiosis, followed by embryo sac degeneration.

In its vicinity, in the basal part of the nucellus or, more frequently, in the deeper part of the chalaza, a somatic cell becomes an aposporous initial and divides mitotically to form an *Hieracium*-type unreduced embryo sac (Noack, 1941; Barcaccia *et al*., 2006). Interestingly, mature aposporous embryo sacs show the same structure as the meiotic ones.

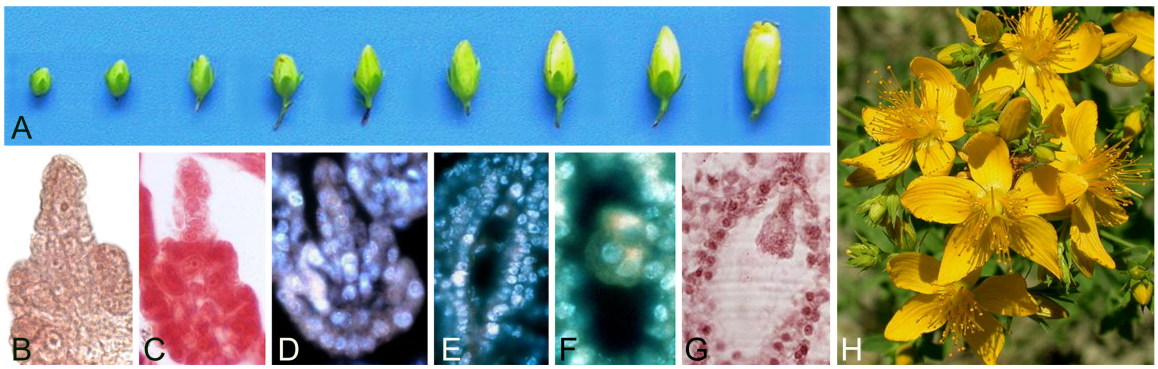

Figure 3. A, Flower buds of *H. perforatum* of different sizes spanning the stages from sporogenesis (ovules with primary sporogenic cells) to early embryogenesis; H, *H. perforatum* inflorescence; B, megaspore mother cell; C, D, ovules showing a tetrad of linear meiotic megaspores and aposporous initials in the chalazal part; E, multi-nucleated embryo sac containing the egg cell, synergids, and unfused polar nuclei and antipodals; F, detail of the egg cell flanked by the synergids; G, heart-shaped embryo with the suspensor. (Bar = 25 μm).

The facultativeness of the species indicates that sexual and aposporous embryo sacs can initially coexist, although it is unclear in *H. perforatum* (and other apomictic taxa) whether the degeneration of the sexual embryo sac has a genetic basis or results from competition with the aposporous initial or embryo sac. The trigger for sexual embryo development is the initiation of the endosperm, which requires polar nuclei fertilization. While pseudogamous apomixis is the rule, the endosperm can develop autonomously in rare cases (Matzk *et al*., 2001; Barcaccia *et al*., 2006). As the apomictic egg cell is in an active metabolic state before pollination, the parthenogenetic activation of embryogenesis can likely occur before fertilization and endosperm initiation (Barcaccia *et al*., 2006). Embryogenesis in *Hypericum* is Solanad, *i.e*. the terminal cell divides by a transverse wall during the second cell generation and the basal cell forms a several-celled suspensor (Robson, 1981).

Compared with sexual reproduction, the relative contribution of maternal and paternal genomes to endosperm formation is disturbed when apomictic seed formation occurs in eight-nucleated embryo sacs. In tetraploids, although the embryo maintains the maternal ploidy irrespective of its amphimictic or apomictic origin, sexual reproduction leads to a balanced 2:1 (*i.e*. 4:2) maternal to paternal genome ratio in the hexaploid endosperm, whereas apomictic reproduction typically leads to decaploid endosperm with an unbalanced 8:2 genome contribution. In the rare case of autonomous seed development, the maternal to paternal ratio in the octoploid endosperm is 8:0. This likely reflects relaxation of natural selection pressure, as in most sexual species, the alteration of the normal 2:1 genome dosage usually results in embryo abortion due to the disturbed endosperm formation (Johnston *et al*., 1980). Triploid offspring can be generated through interploidy mating (*i.e*. 4*x*-2*x* and reciprocals), although they may suffer from endosperm imbalance and irregular chromosome segregation.

In addition to regular apomictic and amphimictic pathways, combinations of apomictic (apospory and parthenogenesis) and sexual components (meiosis and fertilization) can take place in *H. perforatum* (Matzk *et al*., 2001), giving rise to non-maternal progeny often referred as aberrant (Figure 2). A convenient nomenclature used to define progenies of aberrant origin is B_{II} for *n*+*n* diploid hybrids and B_{III} for 2*n*+*n* triploid hybrids (*i.e*. fertilization of reduced and unreduced egg cells, respectively). For example, meiotic egg

cells may occasionally develop through parthenogenesis to generate amphihaploids. The dynamic reproductive system of *H. perforatum* is related to the apparent dissociation of ploidy (from 4*x* to 6*x* and from 4*x* to 2*x*) and seed viability.

Expression and inheritance of apomixis

Noack (1939) performed controlled crosses between different diploid *Hypericum* species with tetraploid *H. perforatum* and concluded from the proportion of triploid seedlings that normally reduced embryo sacs occurred in approximately 3% of ovules. He thus hypothesized that the vast majority of ovules (97%) contained functional aposporous embryo sacs, and for many years, this estimate was the only available estimate of apomixis expression levels in *H. perforatum*.

The reconstruction of the reproductive diversity in *H. perforatum* was more recently investigated by Matzk *et al*. (2001) using the innovative flow cytometric seed screen (FCSS), a method which allows the discrimination of apomixis from sexual processes of reproduction based on the seed DNA contents of embryo and endosperm (Matzk *et al*. 2000).

Table 1 - Available data on the expression of apomixis in *H. perforatum*.

Degree of apomixis	Sources of sexuality	Method of analysis	References
97%	B_{II} and B_{III} hybrids	Triploid frequency in interploidy crosses	Noack (1939)
20-90%	(Poly)haploids, B_{II} and B_{III} hybrids	Flow cytometric screen of single seeds	Matzk *et al*. (2001)
94%	B_{III} hybrids and one aneuploid	Molecular fingerprints and chromosome counts	Mayo and Langridge (2003)
23-82%	(Poly)haploids, B_{II} and B_{III} hybrids	Flow cytometric screen of bulked and single seeds	Barcaccia *et al*. (2006)
69-89%	(Poly)haploids, B_{II} and B_{III} hybrids	Flow cytometric screen of single seeds	Galla *et al*. (in press)

With rare exceptions, seeds of tetraploid taxa can demonstrate four distinct (embryo : endosperm) ploidy ratios: reduced, double-fertilized (sexually produced) balanced B_{II} or selfed plants (4*C* embryo : 6*C* endosperm); unreduced, pseudogamous (apomictically produced) maternal types (4*C* : 10*C*); reduced, parthenogenetic amphihaploid types (2*C* : 6*C*); or unreduced, double-fertilized (poly)triploid B_{III} plants (6*C* : 10*C*). The authors clearly demonstrated that most of the accessions were facultative apomictics characterized by 4*C* embryo : 10*C* or 6*C* endosperm (Figure 4). The mode of reproduction ranged from almost complete sexuality to obligate apomixis, with the proportion of seeds originating via the pseudogamous pathway varying from 20% to 90% in facultative apomicts (Table 1). Interestingly, one genotype with full (100%) capacity for apospory but only about 25% parthenogenesis was identified. These data demonstrate the extreme plasticity of the reproductive system in *H. perforatum*. Quantification of apomixis and sexuality in *H. perforatum* ecotypes was also attempted by using the FCSS of bulked samples of 30 seeds (Barcaccia *et al*., 2006). The ratio between the 10*C* peak and the sum of the 10*C* and the 6*C* peaks was used to estimate of the degree of apomixis, and showed that most plants were facultative with the relative frequency of apomictically-derived seeds ranging from 0 to 40% and having an average of 23% (Figure 4). The occurrence of haploid parthenogenesis was 7%, on average, and sexual seed production ranged from 49% to 88%. However, the estimation of apomixis expression based on relative flow cytometric peak heights is not straightforward with bulked samples. For example, the proportion of sexual seed production may have been overestimated since the 6*C* peak may represent both endosperm nuclei from sexual reproduction (balanced B_{II} hybrids and selfed progenies) and embryo nuclei from the fertilization of unreduced egg cells (B_{III} hybrids), while the 10*C* peak represents endosperm only. Furthermore, *H. perforatum* embryos contain more nuclei than do endosperm residuals, and hence the occurrence of B_{III} hybrids in a population can bias the value of 10*C* and 6*C* peaks in the sample of pooled seeds. The analysis of single seeds was additionally performed in two ecotypes that showed the most contrasting mode of reproduction, one of which exhibited a reduced level of parthenogenesis in aposporous embryo sacs as indicated by the high frequency of B_{III} hybrids (Barcaccia *et al*., 2006). Overall, the frequency of events reflective of sexual reproduction (meiosis and/or fertilization) leading to genetically off-type seeds was 45.5%.

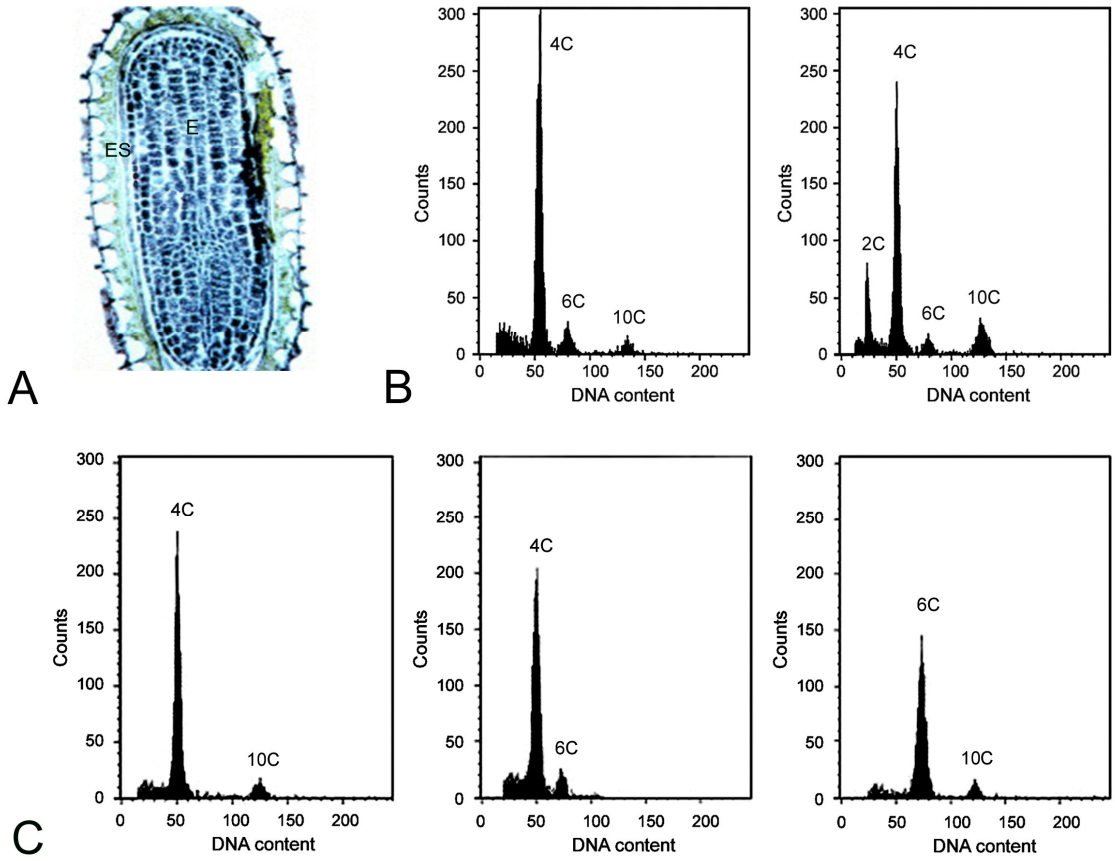

Figure 4. A, Longitudinal section of a mature seed of *H. perforatum* (source: Matzk *et al*., 2001; E, embryo; ES, endosperm). Estimation of the seed DNA contents of embryo and endosperm by flow cytometry: (B, C) flow cytometric (FCM) analysis of bulked seeds produced by pseudogamous apomixis and amphimixis (6*C* : 10*C* and 4*C* : 6*C* peaks, respectively) and by haploid parthenogenesis (2*C* : 6*C* peaks); (D–F) flow cytometric seed screen (FCSS) peaks of single seeds produced by apomixis (4*C* : 10*C* peaks) and sexuality (meiotic double fertilization, 4*C* : 6*C* peaks, e.g., BII hybrid, and aposporous double fertilization, 6*C* : 10*C* peaks, i.e., BIII hybrid) (for additional details see text).

The second ecotype was characterized by a high potential for asexual reproduction, as 82.4% of its seeds were derived from pseudogamous apomixis (Barcaccia *et al*., 2006). In seeds of maternal origin, the endosperm arose mostly from fertilization of the unreduced polar nuclei, thus demonstrating the prominence of pseudogamy, although autonomous endosperm development was occasionally observed. Both ecotypes revealed comparable frequencies of balanced B_{II} hybrids (8.8% and 9.1%), and in addition amphihaploids resulting from meiotic parthenogenesis as well as twins were identified (Table 1).

Several independent experiments have similarly revealed the dynamic reproductive system of *H. perforatum*. On the basis of cytological observations, Noack (1939) reported that selfing of tetraploid *H. perforatum* resulted in 73% maternal and 27% hexaploid plants, and that crossing tetraploid *H. perforatum* with diploid *H. maculatum* produced only 32% maternals and as high as 68% pentaploid hybrids. Diploids have never been reported for any *H. perforatum* experimental progeny produced by controlled pollination, whereas triploids were recovered by Matzk (pers. comm.) by performing interploidy crosses between sexual diploid and apomictic tetraploid *H. perforatum* used as pollinator.

The distinction between selfed and hybrid genotypes within sexually generated plants can be achieved by performing progeny tests using morphological traits and/or molecular markers. Progenies are classified as *maternal* when their DNA fingerprints are identical with those of the seed parent and as *aberrant* when bands of paternal origin or new bands are present, or when maternal bands are lacking in at least one fingerprint (Barcaccia *et al*., 1997; 1998). Within the aberrant progenies, three putative classes can be scored: (*B_{II} hybrids*) when the fingerprint shows maternal and paternal markers, in which at least one maternal marker segregates; (*B_{III} hybrids*) when all maternal markers are conserved and one or more paternal markers are present; and (*non-hybrids*) when paternal markers are absent and one or more maternal markers are lacking (which could include plants from selfing or from haploid parthenogenesis).

Molecular markers have proven to be an efficient tool for the identification of maternal and aberrant individuals in different progenies of *H. perforatum* (Halušková and Čellárová, 1997; Arnholdt-Schmitt, 2000; Halušková and Košuth, 2003; Koperdáková *et al*., 2004; Barcaccia *et al*., 2006). DNA fingerprinting techniques combined with chromosome counting have additionally been exploited to determine the extent of offtypes in progeny sets, and the level of normally reduced embryo sacs in mother plants (Mayo and Langridge, 2003). For example, 94% of the progeny from four crosses likely originated by apomixis, as their genetic fingerprints and ploidy were identical to the maternal parent (Table 1). Karyological analysis additionally identified recombinants composed of B_{II} and B_{III} hybrids, and one aneuploid ($2n$-1=31) (see Mayo and Langridge, 2003).

Most of the *H. perforatum* plants so far investigated by different genetic screening methods have been shown to be almost exclusively tetraploid and facultatively apomictic/sexual (Matzk *et al*., 2001; Mayo and Langdrige, 2003; Barcaccia *et al*., 2006). However, hexaploid and diploid plants have also been identified, demonstrating that parthenogenesis without apospory and, *vice versa*, apospory without parthenogenesis is possible under natural conditions (Matzk *et al*., 2001; Mayo and Langdrige, 2003; barcaccia *et al*., 2006). These data show that (1) unreduced egg cells of aposporous embryo sacs are frequently fertilized and (2) that reduced egg cells of meiotic embryo sacs may develop autonomously, and it is unclear to what extent these traits may be influenced by genetic, epigenetic and environmental factors. The identification of genotypes able to produce embryos either from aposporous fertilized egg cells or meiotic parthenogenesis at a high frequency suggests that two distinct genetic factors control apospory and parthenogenesis, and that apospory and parthenogenesis may be developmentally uncoupled, and idea previously hypothesized by Noack (1939). Of particular interest is the identification of *H. perforatum* genotypes which almost exclusively express only one component of apomixis or suppress the other (Matzk *et al*., 2001). The analysis of DNA content ratios of embryo to endosperm nuclei (Matzk *et al*., 2001) and the cyto-histological investigations of ovules and ovaries (Barcaccia *et al*., 2006) suggest that sexual and aposporous embryo sacs may cooperate and have demonstrated that the developmental timing of embryo and endosperm may be different. The possibility that the absence of endosperm in an aposporous embryo sac could be compensated by the endosperm signal of a meiotic embryo sac, or *vice versa,* was proven by Matzk *et al*. (2001). If true, this is likely a rare phenomenon in *H. perforatum* since the coexistence of sexual and aposporous embryo sacs within a given ovule has rarely been observed (Noack, 1939; Barcaccia *et al*., 2006).

Although pollination is usually required to set seed, the parthenogenetic activation of the egg cell to form an embryo may occur before polar nuclei fertilization and/or endosperm initiation (Barcaccia *et al*., 2006). Heterochronic development change could thus represent a mechanism which prevents fertilization of an unreduced egg cell in *H. perforatum*. Precocious embryonic development has also been observed in aposporous species, including *Panicum maximum* (Naumova and Willemse, 1995), *Brachiaria brizantha*

(Alves *et al.*, 2001) and the diplosporic apomict *Tripsacum dactyloides* (Grimanelli *et al.*, 2003). Alternatively, the cell wall might impede fusion of the second sperm cell with the unreduced egg cell (Asker and Jerling, 1992) to thus prevent egg cell fertilization, as has been demonstrated in *Pennisetum ciliare* (Vielle-Calzada *et al.*, 1995). Hence, the apomictic egg cell, unlike the sexual one, can initiate embryogenesis before pollination and fertilization of the embryo sac central cell, and as a consequence, autonomous embryo initiation and development may not be necessarily dependent on endosperm cues (Grossniklaus, 2001; Chaudhury *et al.*, 2001).

While facultative apomixis is the rule in *H. perforatum*, the discovery of low numbers of diploid obligate sexuals and tetraploid obligate apomicts, showing either pseudogamous or autonomous endosperm development, presents a potentially interesting model for testing hypotheses concerning the rarity of diploid apomixis in plants and animals (parthenogenesis).

Population genetics

In *H. perforatum*, the relative occurrence of apomictic and sexual events is apparently under genetic control, although both modifying genes and environmental factors likely influence the expressivity of agamic reproduction as in other facultative aposporous apomicts (*i.e. Poa pratensis*; Barcaccia *et al.*, 1998; Matzk *et al.*, 2005). More research is thus required to differentiate between the relative contributions of environmental and genetic factors to the reproductive variation inherent to *H. perforatum*.

A population of asexually-reproducing individuals is expected to be characterized by low levels of genetic variability compared to an outcrossing sexual population. Population level genetic variability in apomictic taxa may nonetheless be high, the result of multiple origins of different clonal lineages, backcrossing with conspecific sexuals, interspecific hybridization, and/or recombination (automixis). Clonal diversity within a population is reflective of the sexual genetic pool from which the clones originated and the frequency of clonal origin, in addition to somatic mutations which subsequently accumulate in established clones (see Meirmans and Van Tienderen, 2004). The former source of diversity (clonal origin) is directly dependent upon reproductive mode, and hence varying degrees of apomixis between *H. perforatum* genotypes likely has a significant impact

upon the diversity of local populations. The diversity and high levels of heterozygosity characteristic of many apomictic taxa are concordant with the idea that occasional recombination with meiosis and fertilization influence population structure. The low but detectable levels of sexuality in *H. perforatum* suggests that ecologically important quantitative traits, such as secondary metabolite content, herbicide tolerance and disease resistance should be relatively uniform within populations and not correlated among populations (Burdon and Marshall, 1981). This idea nonetheless requires empirical testing since so little is known about gene flow between apomictic populations.

An insight into the reproduction dynamics and the developmental events of apomixis in *H. perforatum* was recently gained by Barcaccia *et al*. (2006), who used DNA fingerprinting techniques to determine the levels of genetic diversity among and within populations of *H. perforatum* (Figure 5). The results showed all studied populations to be polyclonal, although each population was characterized by different levels of genetic variability. Flow cytometric analyses of both bulk and single seeds furthermore indicated that all populations were facultatively apomictic and characterized by variable proportions of apomixis and sexuality (Barcaccia *et al*., 2006). Analyses of diversity among *H. perforatum* populations showed high levels of genetic differentiation and low estimates of genetic similarity, and no correlation between geographic and genetic distance among collection sites (Barcaccia *et al*., 2006). For example, the Polish cultivar *Topas* (Seidler-Lozykowska and Dabrowska, 1996) was used as reference standard, and was found clustered with Italian ecotypes in a multifactorial analysis (Figure 5). Three clusters of genetically similar populations were identified, with clear genetic differentiation between clusters and high similarity within the same clusters, suggesting that each represented a different subspecies or variety of *H. perforatum*. This conclusion is not without scientific basis, as Robson (2002) used morphological characters to identify four *H. perforatum* subspecies, of which the subsp. *perforatum* and subsp. *veronense* and several varieties are found in Italy. Furthermore, it is possible that the distinct *H. perforatum* groups identified in this analysis have originated through multiple hybridization events. Of course other factors (*e.g*., post-glacial dynamics, genetic drift, etc.) may have also influenced the genetic diversity and distribution of Italian *H. perforatum* populations. The analysis of genetic diversity within the Italian populations additionally showed identical multilocus

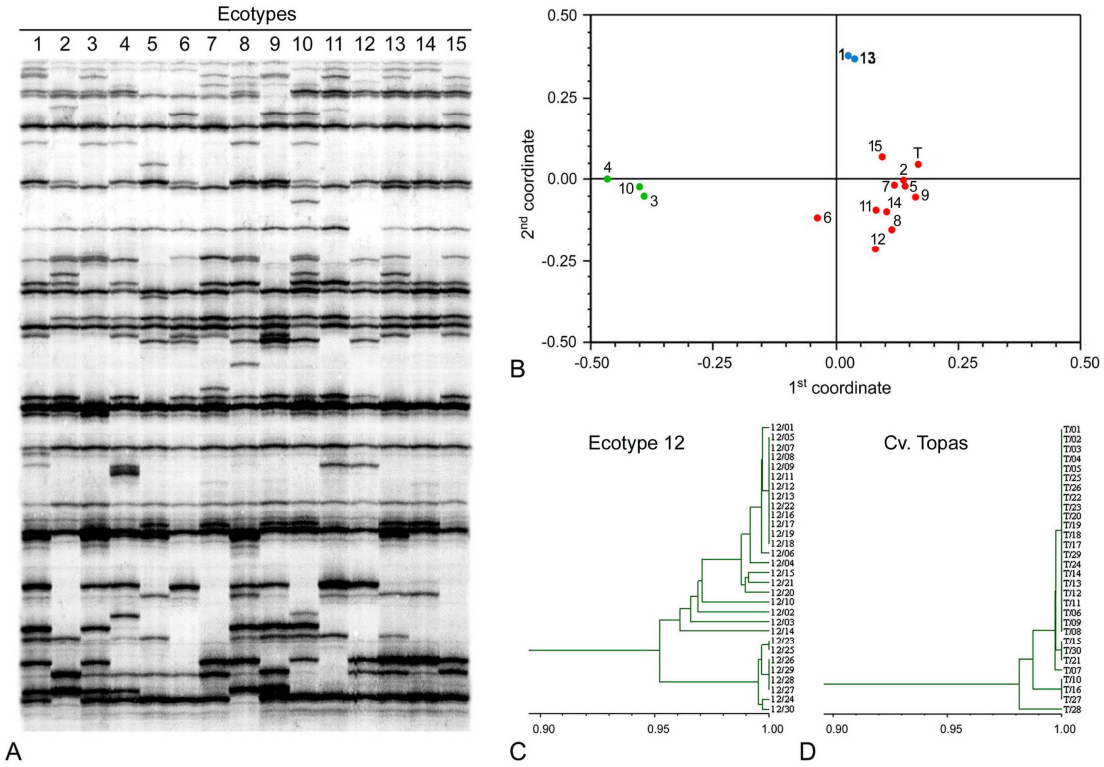

Figure 5. A, AFLP fingerprints of *H. perforatum* ecotypes (each lane includes all markers detectable in a given population by using a bulked DNA sample of 12 plants as template), generated with a *Pst*I/*Mse*I primer combination, which show several polymorphic markers (details in Barcaccia et al., 2006); B, centroids based on principal coordinates analysis showing relationships among fifteen ecotypes of *H. perforatum* and the cultivar Topas; C, D, UPGMA dendrograms constructed according to the genetic similarity matrix depicting the level of polymorphism detectable within a local population (ecotype 12) and the cultivar *Topas* (T) (source: Barcaccia et al., 2006).

genotypes to be shared by multiple individuals in a number of populations, thus giving evidence for agamic reproduction as has been shown in *Taraxacum* (Van Der Hulst *et al.*, 2000). Considering the total number of different genotypes observed in the analyzed populations, 37 were represented by more than one individual (from 2 to 16 plants per single genotype), a result inconsistent with what would be expected from a purely sexually reproducing population (Figure 5). All populations but one were dominated by a single genotype or composed of several (>2) genotypes with the same frequency. Only one population was characterized by equal frequencies of two distinct genotypes, suggesting that sexually-derived genetic variation has become fixed through apomixis.

In the short term apomixis can be advantageous since it preserves locally adapted gene combinations, although this may be disadvantageous in the long run since apomictic clones cannot adapt well to changing environments and are expected to accumulate deleterious mutation. While apomixis ensures the spread of high fitness genotypes, the retained sexual behaviour of facultative apomicts ensures the production of recombinant genotypes upon which natural selection can act. Thus, facultative apomicts not only follow the strategy adopted by strict selfers since they can also maintain high levels of heterozygosity and polyploidy. Such an hypothesis has been put forward for the two apomictic genera *Taraxacum* and *Chondrilla*, as it is thought that gene flow between apomicts and their sexual relatives has enabled apomixis to be maintained for longer evolutionary periods than originally predicted (van Dijk, 2003).

Molecular approaches to study the inheritance of and cloning candidate genes for apomixis

A detailed understanding of the inheritance of apomixis in *H. perforatum* is required for the isolation of candidate genes and eventual transfer of this valuable trait to species that naturally propagate through sexuality. Detailed genetic mapping analysis is extremely difficult due to the association of facultative apomixis with polyploidy and variable but elevated levels of heterozygosity. The chromosomal regions associated apomixis factors have nonetheless been identified in several species, and DNA markers tightly linked to presumed apomeiosis and parthenogenesis loci have been isolated. With the exception of *Taraxacum* (see van Dijk *et al*., 2001), strong suppression of recombination around the loci linked to apomeiosis has been found in all documented cases. DNA markers linked with parthenogenesis have been isolated in *Poa pratensis* (Barcaccia *et al*., 1998) and *Erigeron annuus* (Noyes and Rieseberg, 2000), although no evidence for recombinational suppression was found.

To gain an insight into the molecular basis of apomixis in *H. perforatum*, a molecular analysis at the genomic and transcriptome levels has been attempted. Amplified fragment length polymorphism (AFLP) analysis was performed on several apomictic and sexual genotypes from unrelated ecotypes, in addition to a hybrid population created by crossing

diploid sexual and tetraploid apomictic plants which demonstrated segregation for apospory (Matzk *et al*., unpublished data).

A set of *Pst*I/*Mse*I primer combinations were identified that yielded putative reproduction-specific polymorphic AFLP markers between unrelated apomicitic and sexual ecotypes. In order to verify the specificity of association between the DNA markers and reproductive mode, the same AFLP primer combinations were analyzed in the segregating triploid population, and a single 254 bp AFLP fragment was identified which showed strict co-segregation with apospory. This AFLP band was isolated and cloned, and analysis revealed that the genomic DNA sequence was highly similar to genes encoding ARIADNE proteins, a class of RING-finger proteins that putatively function as ubiquitin-protein ligases (Mladek *et al*., 2003). PCR primers were developed to amplify the specific band from genomic DNA, and amplifications yielded two bands (a strong and faint band) rather than a single product. Both PCR products were cloned and sequenced and the alignment of the two sequences revealed 5 single nucleotide polymorphisms which were responsible for amino acid changes between the two fragments.

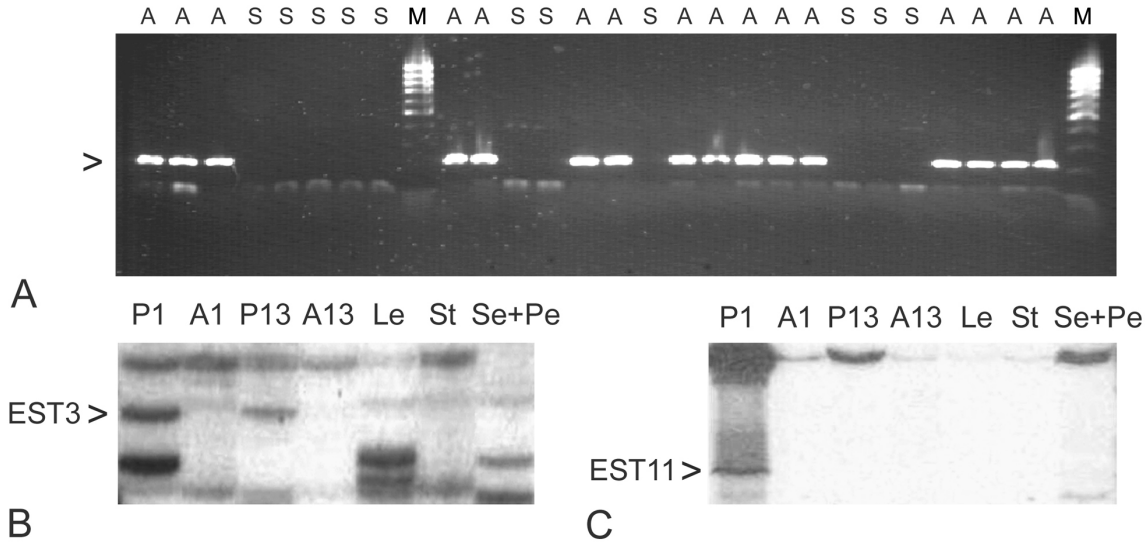

Figure 6. A, Controlled crosses between a completely sexual diploid plant and an obligate apomictic tetraploid plant result in a F1 population cosegregating for apospory and the presence of a CAPS marker. M = weight markers, A = aposporous and S = sexual plants as determined by Flow Cytometric Seed Screen (F. Arzenton, F. Matzk and H. Bäumlein, unpubl.; see Arzenton, 2004). B, expression patterns of two transcript-derived fragments, EST3 and EST11, with similarity to an RNA helicase and a zinc-finger protein (F. Arzenton et G. Barcaccia, unpubl.; see Arzenton, 2004) (P1, pistils of the apomictic ecotype 1; P13, pistils of the sexual ecotype 13; A1, anthers of the apomictic ecotype 1; A13, anthers of the sexual ecotype 13; Le, leaves; St, stems; Se+Pe, sepal and petals).

The sequence of the faint band contained an *Eco*RI restriction site not found in the stronger band sequence, and thus the presence of the two bands could be confirmed by cleaved amplified polymorphic sequence (CAPS) analysis (Figure 6). The segregation patterns of the single-dose AFLP and the derived CAPS markers proved to match perfectly with apospory in the triploid progeny set (Barcaccia *et al*., 2006), and the segregation ratio of 26 presences to 14 absences was skewed but not significantly distorted from the expected 1 to 1 ($X^2 = 3.6$). The correlation between these markers and apospory segregation is presently being tested in other *H. perforatum* populations with the hope that they may provide a path towards finding more closely linked markers and eventually candidate loci.

In a second experiment, the transcription profiles of sporogenesis and gametogenesis were analyzed from unripened anthers and unpollinated pistils sampled from *H. perforatum* ecotypes characterized by contrasting degrees of apomixis/sexuality. This differential display method led to the isolation of several mRNAs specifically expressed in the pistils of the highly apomictic ecotype, including a particular 169 bp EST (*EST3*) showing partial homology to a putative RNA helicase as well as the cdc28 gene identified in fission yeast (Table 2). Interestingly, cdc28 is involved with mitosis initiation, and encodes a member of the DEAH-box family of putative RNA-dependent ATPases and helicases involved in the splicing of mRNA precursors and regulation of the cell cycle (Lundgren *et al*., 1996).

Table 2 - Information on the genomic DNA marker cosegregating with apospory and list of the three mRNA sequences found in the pistils of an apomictic ecotype.

Sequence	**Size (bp)**	**Gene product**	**Identity***	**E-value***
AFLP254	254	RING-finger protein (ARIADNE)	91	$5e^{-20}$
EST3	169	RNA helicase or ATPase (DEAH box)	93	$2e^{-20}$
EST7	250	Beta-3 tubulin protein (TUB3 type B)	92	$2e^{-16}$
EST11	264	Zinc-finger protein (C2H2 type)	65	$3e^{-10}$

*Identity and E-value are referred to the homologues *Arabidopsis thaliana* accessions.

A second 264 bp fragment (*EST11*) was found to be highly similar to a C2H2 type zinc-finger protein of *Arabidopsis* (Table 2), a potentially interesting discovery since a number of zinc-finger proteins have been implicated in the developmental regulation of various flower organs, embryogenesis and seeds. For example, mutation of the *Arabidopsis* FIS2 gene, which encodes a protein containing a C2H2 zinc-finger motif, leads to fertilization-independent initiation of endosperm development (Luo *et al*., 1999).

The recovery of DNA markers and cDNA clones linked to the mode of reproduction and related to the expression of apomictic determinants, respectively, is a preliminary step towards the understanding of the genetic control and molecular regulation of apomixis in *H. perforatum*. These data support *H. perforatum* as an appropriate model system for the molecular comparison of sexual and apomictic genotypes, a conclusion that has led a number of laboratories to adopt this system for more systematic studies of apomixis.

Ongoing research and future perspectives

One of the first major milestones to be completed in the short-term is the construction of a first genetic linkage map for sexual *Hypericum perforatum* using a two-way pseudo-testcross strategy and multiple PCR-based marker systems. Mapping populations have already been constructed at the IPK Gatersleben, including 4 families of crosses between 4 unrelated diploid sexual *H. perforatum* accessions. Following the completion of the genetic map derived from the diploid sexual crosses, a linkage mapping project will be carried out using crosses between sexual and apomictic accessions. Two series of sexual-apomictic *H. perforatum* crosses have already been established at the IPK. The first is a diploid sexual cross with tetraploid facultative apomictic accession characterized by high expression of the apomictic trait, as measured using the FCSS (Matzk, unpublished data). The progeny of this first cross are for the most part triploid, and thus a relatively low number of offspring suitable for phenotypic (FCSS) analysis was obtained, likely the result of meiotic imbalance (Matzk, unpublished data). Accurate quantification of reproduction of these offspring was therefore impossible due to the loss of some reproductive classes. A second cross was thus completed using colchicine-induced tetraploid sexual individuals and tetraploid apomicts in the hopes of decreasing the influence of meiotic disturbances. Fertility of these crosses is higher than the previous

diploid-tetraploid crosses, and FCSS characterization of the F_1 generation is presently underway.

As firstly reported by Matzk *et al*. (2001), we believe *H. perforatum* is a suitable model species for apomixis research due to a number of important and facilitating traits, including: i) small genome size; ii) the availability of a large number of morphologically distinct ecotypes; iii) the high degree of molecular polymorphism among ecotypes; iv) the versatile and dynamic mode of reproduction; v) the relatively short generation time; vi) the self-compatibility and easy crossability; vii) the high number of seeds produced per flower pollinated (seed set); and viii) last but not least, its use as medicinal plant with increasing demand from the pharmaceutical industry. It will be interesting to follow the development of this system as more laboratories join forces with the common goal of elucidating the apomictic pathway.

References

Agostinis P, Vantieghem A, Merlevede W and de Witte PA (2002) Hypericin in cancer treatment: more light on the way. Int J Biochem Cell Biol, 34: 221-41.

Albertini E, Marconi G, Barcaccia G, Raggi L and Falcinelli M (2004) Isolation of candidate genes for apomixis in *Poa pratensis* L. Plant Mol Biol, 56: 879-894.

Albertini E, Marconi G, Barcaccia G, Raggi L and Falcinelli M (2005) *APOSTART* and *SERK*: candidate genes for apomixis in *Poa pratensis* L. Plant Phys, 138: 2185-2199.

Arzenton F (2004) Apomixis in *Hypericum perforatum* L.: a survey of the genetic diversity and multidisciplinary approaches to understand the reproductive biology of the species. Ph.D. thesis, University of Padova, Italy. pp. 73.

Arnholdt-Schmitt B (2000) RAPD analysis: a method to investigate aspects of the reproductive biology of *Hypericum perforatum*. Theor Appl Genet, 100: 906-911.

Asker SE and Jerling L (1992) Apomixis in Plants. CRC Press, London.

Barcaccia G, Mazzucato A, Belardinelli A, Pezzotti M, Lucretti S and Falcinelli M (1997) Inheritance of parental genomes in progenies of *Poa pratensis* L. from sexual and apomictic genotypes as assessed by RAPD markers and flow cytometry. Theor Appl Genet, 95: 516-524.

Barcaccia G, Mazzucato A, Albertini E, Zethof J, Pezzotti M, Gerats M and Falcinelli M (1998) Inheritance of parthenogenesis in *Poa pratensis* L.: auxin test and AFLP linkage analyses support monogenic control. Theor Appl Genet 97:74-82.

Barcaccia G, Arzenton F, Sharbel T, Varotto S, Lucchin M and Parrini P (2006) Genetic diversity and reproductive biology in ecotypes of the facultative apomict *Hypericum perforatum* L. Heredity, 96: 322-334.

Brutovská R, Čellárová E and Doležel J (1998) Cytogenetic variability of *in vitro* regenerated *Hypericum perforatum* L. plants and their seed progenies. Plant Sci, 133: 221-229.

Brutovská R, Kušniriková P, Bogyiová E and Čellárová E (2000a) Karyoptype analysis of *Hypericum perforatum* L. Biologia Plant 43: 133-136.

Brutovská R, Čellárová E and Schubert I (2000b) Cytogenetic characterization of three *Hypericum* L. species by *in situ* hybridization. Theor. Appl. Genet. 101: 46-50.

Buckley YM, Briese DT and Rees M (2003) Demography and management of the invasive plant species *Hypericum perforatum* L. using multi-level mixed-effects models for characterizing growth, survival and fecundity in a long-term data set. J Appl Ecol, 40: 481-493.

Burdon JJ and Marshall DR (1981) Biological control and the reproductive mode of weeds. J Appl Ecol, 18: 649-658.

Campbell MH and Delfosse ES (1984) The biology of Australian weeds. 13. *Hypericum perforatum* L. J Aust Inst Agric Sci, 50: 63-37.

Carino DA and Daehler CC (1999) Genetic variation in an apomictic grass, *Heteropogon contortus*, in the Hawaiian Islands. Molecular Ecology, 8: 2127–2132.

Chapman HM, Parh D and Oraguzie N (2000) Genetic structure and colonizing success of a clonal, weedy species, *Pilosella officinarum* (Asteraceae). Heredity, 84: 401-409.

Chaudhury AM, Koltunow A, Payne T, Luo M, Tucker MR, Dennis ES and Peacock WJ (2001) Control of early seed development. Annu Rev Cell Dev Biol, 17: 677-699.

Citterio S, Varotto S, Albertini E, Feltrin E, Soattin M, Marconi G, Sgorbati S, Lucchin M and Barcaccia G (2005) Alfalfa Mob1-like proteins are expressed in reproductive organs during meiosis and gametogenesis. Plant Mol. Biol., 58: 789-808

Crompton CW, Hall IV, Jensen KIN and Hildebrand PD (1988) The biology of Canadian weeds. 83. *Hypericum perforatum* L. Canad J Pl Sci 68: 149-162.

Di Carlo G, Borrelli F, Ernst E and Izzo AA (2001) St John's wort: Prozac from the plant kingdom. Trends Pharmacol Sci, 22: 292-297.

Dulger B and Gonuz A (2005) Antibacterial activity of the endemic Hypericum kazdaghensis. Fitoterapia. 76(2): 237-9.

Ellstrand NC and Roose ML (1987) Patterns of genotypic diversity in clonal plant species. Amer J Bot, 74: 123-131.

Espinoza F, Pessino SC, Quarin CL and Valle EM (2002) Effect of pollination timing on the rate of apomictic reproduction revealed by RAPD markers in *Paspalum notatum*. Ann. Bot (Lond.) 89(2): 165-170.

Fenner R, Sortino M, Rates SM, Dall'Agnol R, Ferraz A, Bernardi AP, Albring D, Nor C, von Poser G, Schapoval E and Zacchino S (2005) Antifungal activity of some Brazilian *Hypericum* species. Phytomedicine, 12(3): 236-40.

Ferraz AB, Grivicich I, von Poser GL, Faria DH, Kayser GB, Schwartsmann G, Henriques AT and da Rocha AB (2005) Antitumor activity of three benzopyrans isolated from *Hypericum polyanthemum*. Fitoterapia, 76(2): 210-5.

Francis AJ (2005) Antidepressant action of St. John's Wort, *Hypericum perforatum*: a test of the circadian hypotheses. Phytomedicine, 12(3): 167-172.

Galla G, Barcaccia G, Shallau A, Puente Molins M, Bäumlein H, and TF Sharbel (in press) The cytohistological basis of apospory in *Hypericum perforatum*

Gaut BS and Doebley JF (1997) DNA sequence evidence for the segmental allotetraploid origin of maize. Proc Natl Acad Sci USA, 94(13): 6809-6814.

Grossniklaus U (2001) From sexuality to apomixis: Molecular and genetic approaches. In: Savidan Y, Carman JG and Dresselhaus T (eds.) (2001) The flowering of

apomixis: from mechanisms to genetic engineering. Mexico, D.F.: CYMMIT, IRD, European Commission DG VI (FAIR) 168-211.

Grimanelli D, Garcia M, Kaszas E, Perotti E and Leblanc O (2003) Heterochronic expression of sexual reproductive programs during apomictic development in *Tripsacum*. Genetics, 165: 1521-1531.

Halušková J and Čellárová E (1997) RFLP analysis of *Hypericum perforatum* L. somaclones and their progenies. Euphytica, 95: 229-235.

Halušková J and Košuth J (2003) RAPD analysis of somaclonal and natural DNA variation in *Hypericum perforatum*. Acta Biologica Cracoviensia, 45: 101-104.

Harlan JR and deWet JMJ (1975) On: Ö Winge and a prayer: The origins of polyploids. Bot Rev, 41: 361-390.

Hermsen JG (1984) The potential of meiotic polyploidization in breeding allogamous crops. Iowa State J Res 58: 421-435.

Hoar CA and Hartl EJ (1932) Meiosis in the genus *Hypericum*. Bot Gaz, 93: 197-204.

Hobbs C (1998) St. John's wort (*Hypericum perforatum* L.): A review. Available on the web.

Holm K, Pancho JV, Herberger JP and Plucknett DL (1979) A geografical atlas of world weeds. John Wiley and Sons, Inc. New York, NY.

Hosseinzadeh H, Karimi GR, Rakhshanizadeh M. (2005) Anticonvulsant effect of *Hypericum perforatum*: role of nitric oxide. J Ethnopharmacol, 98(1-2): 207-8.

Johnston SA, den Nijs TPM, Peloquin SJ and Hanneman RE (1980) The significance of genetic balance to endosperm development in interspecific crosses. Theor Appl Genet 57: 5-9.

Kogi M (1984) A karyomorphological study of the genus *Hypericum* (*Hypericaeae*) in Japan. Bot Mag 97: 333-343.

Koperdáková J, Brutovská R and Čellárová E (2004) Reproduction pathway analysis of several *Hypericum perforatum* L. somaclonal families. Hereditas, 140: 34-41.

Lihova J, Martonfi P and Martonfiova L (2000) Experimental study on reproduction of *Hypericum* X *desetangsii* nothosubsp. *carinthiacum* (A. Frohl(.)) N. Robson (Hypericaceae). Caryologia, 2(53): 127-132.

Luo M, Bilodeau P, Koltunow A, Dennis ES, Peacock WJ and Chaudhury AM (1999) Genes controlling fertilization-independent seed development in *Arabidopsis thaliana*. Proc Natl Acad Sci USA, 97: 10637-10642.

Lundgren K, Allan S, Urushiyama S, Tani T, Oshima Y, Frendewey D and Beach D (1996) A connection between pre-mRNA splicing and the cell cycle in fission yeast: *cdc28+* is allelic with *prp8+* and encodes an RNA-dependent ATPase/helicase. Mol Biol Cell, 7: 1083-1094.

Malaty W (2005) St. John's wort for depression. Am Fam Physician, 71(7): 1375-1376.

Mártonfi P, Repčák M and Mihoková (1996a) *Hypericum maculatum* subsp. *Maculatum* x *H. perforatum* (*Hypericaceae*): corroboration of natural hybridization in Hypericum by secondary metabolite analysis. Folia Geobot Phytotax, 31: 245-250.

Mártonfi P, Brutovská R, Čellárová E and Repčák M (1996b) Apomixis and hybridity in *Hypericum perforatum*. Folia Geobot Phytotax, 31: 389-396.

Matzk F, Meister A and Schubert I (2000) An efficient screen for reproductive pathways using mature seeds of monocots and dicots. Plant J, 21(1): 97-108.

Matzk F, Meister A, Brutovská R and Schubert I (2001) Reconstruction of reproductive diversity in *Hypericum perforatum* L. opens novel strategies to manage apomixis. Plant J, 26: 275-282.

Matzk F, Hammer K and Schubert I (2003) Coevolution of apomixis and genome size within the genus *Hypericum*. Sex Plant Reprod, 16: 51-58.

Mayo GM and Roush RT (1997) Genetic variability of *Hypericum perforatum* L. (Clusiaceae) and the detection of resistance to the biological control agent *Aculus hyperici* Liro (Eriophyidae). Plant Prot Q, 12: 70-72.

Mayo GM and Langridge P (2003) Modes of reproduction in Australian populations of *Hypericum perforatum* L. (St. John's wort) revealed by DNA fingerprinting and cytological methods. Genome, 46: 573-579.

Miskovsky P (2002) Hypericin - a new antiviral and antitumor photosensitizer: mechanism of action and interaction with biological macromolecules. Curr Drug Targets, 3: 55-84.

Mladek C, Guger K and Hauser MT (2003) Identification and characterization of the ARIADNE gene family in *Arabidopsis*. A group of putative E3 ligases. Plant Phys, 131: 27-40.

Nielsen N (1924) Chromosome numbers in the genus *Hypericum*. Hereditas, 5: 378-382.

Noack KL (1939) Über *Hypericum* - Kreuzungen VI: Fortpflanzungsverhältnisse und bastarde von *Hypericum perforatum* L. Z Indukt Abstamm Vererbungsl, 76: 569-601.

Noack KL (1941) Geschlechtsverlust und bastardierung beim Johanniskraut. Forsch Fortschr, 17: 13-15.

Nogler GA (1984) Gametophytic apomixis. In: Johri BM (ed.) Embryology of Angiosperms. Springer-Verlag, Berlin. pp 475-518.

Novak SJ and Mack RN (2000) Clonal diversity within and among introduced populations of the apomictic vine *Bryonia alba* (Cucurbitaceae). Can J Bot, 78: 1469-1481.

Noyes RD and Soltis DE (1996) Genotypic variation in agamospermous *Erigeron compositus* (*Asteraceae*). Amer J Bot, 83: 1292-1303.

Noyes and Rieseberg (2000) Two independent loci control agamospermy (apomixis) in the triploid flowering plant *Erigeron annuus*. Genetics, 155: 379-390.

Quarin CL, Normann GA and Espinoza (1998) Evidence for autotetraploidy in apomictic *Paspalum rufum*. Hereditas, 129: 119-124.

Reynaud MC (1986) Étude cytotaxonomique des Millepertuis du Bassin méditerranéen et des Iles Canaries. Bull Soc Bot France Lett Bot, 133: 167-177.

Robson NKB and Adams P (1968) Chromosome number in *Hypericum* and related genera. Brittonia 20: 95-106.

Robson NKB (1977) Studies in the genus *Hypericum* L. (Guttiferae) 1. Infrageneric classification. Bull Brit Mus Nat His (Bot), 5: 291-355.

Robson NKB (1981) Studies in the genus *Hypericum* L. (Guttiferae) 2. Characters of the genus. Bull Brit Mus Nat His (Bot), 8: 55-226.

Robson NKB (2002) Studies in the genus *Hypericum* L. (Guttiferae) 4(2). Section 9. *Hypericum sensu latu* (part 2): subsection 1. *Hypericum* series 1. *Hypericum*. Bull Nat Hist Mus Lond (Bot), 32: 61-123.

Robson NKB (2003) *Hypericum* botany. In: Ernst E (ed.) *Hypericum*. The genus *Hypericum*. London, Taylor and Francis, pp 1-22.

Savidan Y (2000) Apomixis: genetics and breeding. In: Janick J (ed) Plant Breeding Reviews. John Wiley and Sons, New York, NY. Vol. 18, pp 13-76.

Schempp CM, Kirkin V, Simon-Haarhaus B, Kersten A, Kiss J, Termeer CC, Gilb B, Kaufmann T, Borner C, Sleeman JP and Simon JC (2002) Inhibition of tumour cell growth by hyperforin, a novel anticancer drug from St. John's wort that acts by induction of apoptosis. Oncogene, 21: 1242-1250.

Seidler-Lozykowska K and Dabrowska J (1996) Topas - the Polish variety of St. John's wort (*Hypericum perforatum* L.). Herba Polonica, 42: 140-143.

Soltis PM and Soltis DE (2000) The role of genetic and genomic attributes in the success of polyploids. Proc Natl Acad Sci USA, 57: 7051-7057.

Steck N, Messmer M, Schaffner W and Berger Bueter K (2001) Molecular markers as a tool to verify sexual and apomictic off-spring of intraspecific crosses in *Hypericum perforatum*. Planta Med, 67: 384-385.

Van Der Hulst RGM, Mes THM and den Nijs JCM and Bachmann K (2000) Amplified fragment length polymorphism (AFLP) markers reveal that population structure of triploid dandelions (*Taraxacum officinale*) exhibits both clonality and recombination. Mol Ecol, 9: 1-8.

Van Der Hulst RGM, Mes THM, Falque M, Stam P and den Nijs JCM and Bachmann K (2003) Genetic structure of a population sample of apomictic dandelions. Heredity, 90: 326-335.

Van Dijk PJ, van Baarlen P and de Jong H (2001) The occurrence of phenotypically complementary apomixis recombinant in crosses between sexual and apomictic dandelions (*Taraxacum officinale*). Sex Plant Reprod, 16: 71-76.

Van Dijk PJ (2003) Ecological and evolutionary opportunities of apomixis: insights from *Taraxacum* and *Chondrilla*. Phil Trans R Soc Lond B, 358: 1113-1121.

Capitolo IV

A multidisciplinary approach to shed light on the cytological and molecular bases of apomixis in *Hypericum* spp.

Abstract

Recently gained information has shown that *H. perforatum* is an attractive model system for the study of apomixis. This specie is characterized by a relatively small genome size and a low basic chromosome number. Natural populations of *H. perforatum* are mostly composed of tetraploid, although diploid and hexaploid are known to occur. It has been demonstrated that while diploids individuals are sexual, polyploids are facultative apomictic and thus have the propensity to produce both sexual and apomictic seeds from the same individual. A multidisciplinary approach has been attempted to shed light on the molecular and cytological bases of apomixis in different species of *Hypericum*. The *Hypericum* embryo sac formation and seed genetic constitution have been studied by means of stain-clearing of ovules/ovaries supported by DIC microscopy and FCSS analyses of embryo and endosperm DNA contents, respectively. Our detailed analyses of female sporogenesis and gametogenesis enabled to define the major morphological traits of all structures playing a role in embryo sac formation. The major developmental features of apospory are the following: i) mis-expression of the meiotic program, ii) failure or delay of degeneration of the epidermal layer of the nucellus, iii) differentiation of aposporic initials, and iv) development into an illegitimate embryo sac. FCSS analysis provided a powerful tool to study the complex fertilization scenarios in reduced and unreduced male and female gametes, providing new insights in the production of aposporic seeds in *H. perforatum*. Furthermore, the genome organization of the three species *H. perforatum*, *H. maculatum* and *H. attenuatum* has been investigated by means of different genetic approaches. The hypothesis that *H. perforatum* arose from an ancient interspecific hybridization event between the diploids *H. attenuatum* and *H. maculatum* has been tested by the isolation of codominant SNP markers and their investigation in *H. perforatum* and its putative ancestors. Moreover, a new technology of DNA fingerprinting has been ideated and applied for the construction of linkage maps in *H. perforatum*. The expression pattern of two *APOSTART*-like genes, potentially involved in parthenogenesis, have been tested revealing new insights in the genetic control of apomixis in *H. perforatum*.

Introduction

Recent studies have proposed the adoption of St. John's worth (*Hypericum perforatum*) as a model species for the study of aposporic apomixis (Matzk *et al.*, 2001; Barcaccia *et al.*, 2007). This species is characterized by a relatively small genome size (1*C*=0.650 pg≈630 Mbp; Bennett, 1976), and the basic chromosome number is 8. Natural populations of *H. perforatum* are composed mostly of tetraploid, although diploids and hexaploids are known to occur (Matzk *et al.*, 2001; Robson, 2002). As reported by Matzk *et al.* (2001), polyploids are facultative, and thus have the propensity to produce both sexual and apomictic seeds from the same individual. Apomictic seed production is highly variable, and is characterized by complex fertilization scenarios between reduced and unreduced male and female gametes (Matzk *et al.*, 2001). It is unclear whether the polyploids are allotetraploid or autotetraploid in origin, although an ancient interspecific hybridization event between the diploids *H. attenuatum* and *H. maculatum* with subsequent chromosome doubling has been hypothesized on the basis of their morphological traits and geographical distribution areas (Campbell and Delfosse 1984; Robson 2002). Alternatively, cytogenetic characterizations of different *Hypericum* species imply that *H. perforatum* may have originated via autopolyploidization in an ancestor closely related to the diploid *H. maculatum* (Brutovská, Kušniriková *et al.* 2000). *Hypericum perforatum* is characterized by a number of traits reflective of hybridity, including: variability in morphology and chemical compound production, meiotic abnormalities (*e.g.*, lagging chromosomes), elevated pollen grain sterility, parthenogenetic development of unreduced egg cells and pseudogamy (Matzk et al 2001, Barcaccia *et al.*, 2001). Our understanding of the cytological and molecular basis of both sporogenesis and gametogenesis have been advanced by studies in different model systems including: *Arabidopsis* (Smyth *et al.*, 1990; Mansfield *et al.*, 1991; Robinson-Beers *et al.*, 1992; Schneitz *et al.*, 1995; Christensen *et al.*, 1997), maize (Huang and Sheridan, 1994) and others. This work has shown that normal embryo sac development requires the coordinated progression of several major process including meiosis, sporogenic cell specification (Sheridan *et al.*, 1999, Schiefthaler *et al.*, 1999) and mitosis. Moreover, a number of associated cellular processes are under precise control for normal development, such as cytokinesis at both meiotic and mitotic time points (Jingjing Liu and Lia-Jia Qu, 2008), and nuclear migration

and fusion (Christensen *et al.*, 2002). The *Arabidopsis* type of embryo sac development, the monosporic *Polygonum*-type, is the most well known and documented (Maheshwari, 1950; Willemse and Van Went, 1984; Haig, 1990; Huang and Russell, 1992; Reiser and Fischer, 1993). The isolation and characterization of a number of mutants along with hybridization approaches allowed a better understanding of genes and pathways involved in embryo sac and embryo development (Gasser *et al.*, 1998; Schneitz 1999; Yang and Sundaresan, 2000; Sieber *et al.*, 2004). A number of genes are now considered to play a role in the apomictic molecular machinery such as *NZZ* (Yang *et al.*, 1999), *SPL* (Schiefthaler *et al.*, 1999), SWY1/DYAD (Siddiqi *et al.*, 2000; Agashe *et al.*, 2002), LOA1 (Okada *et al.*, 2007), MAC1 (biblio), MOB (Galla *et al.*, in press), *FIS1* (or *MEA*), *FIS2* and *FIS3* (or *FIE*) (Ohad *et al.*, 1996; Grossniklaus and Schneitz, 1998; Kiyosue *et al.*, 1999; Luo *et al.*, 1999; Vielle-Calzada *et al.*, 1999).

Recently, extensive analyses conduced in sexual, aposporic and recombinant genotypes of *Poa pratensis* led Albertini *et al.* (2005) to propose that also two genes of the family *APOSTART* are involved in the formation of embryo sacs and embryos. Along with candidate gene identification and characterization, the fine mapping of the chromosomal regions controlling the expression of apomixis has been reported in a number of apomictic biological systems. The identification of molecular markers closely associated with the main fearures of apomixis and the study of their pattern of inheritance have been described for several species such as *Pennisetum squamulatum* (Dujardin and Hanna, 1983; Ozias-Akins *et al.*, 1998); *Cenchrus ciliaris* syn. *Pennisetum ciliare* (Jessup *et al.*, 2002; Sherwood *et al.*, 1994), *Panicum maximum* (summarized in Savidan, 2000) (Ebina *et al.*, 2005), *Brachiaria* spp. (do Valle *et al.*, 1993; Miles and Escandon, 1996), *Paspalum notatum* (Martinez *et al.*, 2001), *Ranunculus* spp. (Nogler, 1984b), *Poa pratensis* (Albertini *et al.*, 2001b), *Taraxacum* spp. (Tas and van Dijk, 1999), *Erigeron* spp. (Noyes and Rieseberg, 2000) and *Tripsacum dactyloides* (Grimanelli *et al.*, 1998; Leblanc *et al.*, 1995).

Since the introduction of the AFLP technology (Vos *et al.*, 1995), a number of AFLP-based protocols have been developed for genome fingerprinting and gene mapping in plants. Multigene family domain polymorphism (MFDP) is an alternative AFLP-derived molecular marker system we ideated and exploited for displaying functional polymorphic

markers and constructing genetic linkage maps in *Hypericum perforatum*. In particular, MFDP was developed with the aim of identifying and displaying molecular markers associated to expressed genomic regions in groups of structurally and functionally similar sequences characterized by the presence of common highly conserved protein domains.

This chapter deals with the development of a new molecular marker display and the assessment of the molecular system utility for constructing functional linkage maps of sexually and apomictically reproducing plants of *Hypericum* spp. Moreover, the results obtained by means of two different approaches aimed at testing the nature of apomixis in *H. perforatum* are also presented. Being *Hypericum* wild populations largely composed by polyploids and considering the role that hybridization might have had in apomixis (Carman *et al.*, 2005) the polyploid origin of *H. perforatum* has been investigated to shed light on genome organization of tetraploids. This was achieved by the isolation and characterization about 1.5 Kb of the *APOSTART* genomic region by using *H. perforatum*, along with its putative ancestors *H. maculatum* and *H. attenuatum*, as biological materials. At the same time, the hypothesis that apomixis might take place as a consequence of an expression shift of specific genes during the ovule development have been tested and the role of different *Hp APOSTART* genes/alleles with respect to the reproductive behaviour better elucidated. Despite our increasing understanding of processes related to sexual reproduction, relatively little is known regarding the molecular and cytological basis of apomixis. With the ultimate goal of elucidating the molecular genetic mechanisms leading to apomictic seed production in *H. perforatum*, we also present a detailed description of female sporogenesis and gametogenesis in both sexual and aposporic *H. perforatum* accessions of different geographical origin.

Materials and methods

Biological material

Tetraploid (2*n*=4*x*=32) *Hypericum perforatum* L. plants of known reproductive behaviour along with diploid *Hypericum maculatum* (2*n*=2*x*=16) and *Hypericum attenuatum* (2*n*=2*x*=16) were used in the phylogenetic approach. By contrast, two genetically unrelated diploid plants isolated by Fritz Matzk (IPK, Gatersleben, Germany) within

German ecotypes were chosen for antagonist morphological traits and crossed to originate the hybrid segregating population suitable for the mapping purpose. The construction of genetic linkage maps for sexual *H. perforatum* parental genotypes was based on a two-way pseudo-testcross strategy. The originated F1 population consisting of 68 individuals was analyzed by means of AFLP and MFDP markers for the presence and segregation of molecular markers selected a spolymorphic between seed and pollen parents.

Flow cytometric screening of *H. perforatum* seeds

We used the flow cytometric seed screen (FCSS; Matzk *et al.*, 2001) to measure the reproductive mode of 4 *H. perforatum* accessions (Table 1), using a high-throughput method developed in our laboratory. Single seeds were ground in a 96 deep well plate with 80µl of grinding buffer (Citric acid monohydrate 0.1 M, Tween 20, 0.5 %, pH adjusted to 2-3 and mercaptomethanol) and 3 ball bearins in a 2000 Geno/Grinder homogenizer (Spex Certiprep) (50 strokes/2 minutes). After grinding, 250 µl of staining buffer were added to each sample and the obtained suspensions (160 µl out of the total) filtered through a 30 µm mesh width nylon tissue. 80 µl of the filtrated was then transferred in to a new 96 well plate and 80 µl of a staining buffer (Na2HPO4. 12 H2O, 0.4 M, 2 ml of DAPI solution, pH adjusted to 8.5) was added to each sample. The fluorescence intensity of DAPI-stained nuclei was determined using the a Ploidy Analyser PA II hooked up to a Robby-Well autoloader (Partec GmbH, Münster, Germany), and the flow cytometric profile of each seed sample was evaluated for embryo and endosperm DNA quantification by using the Flomax software (Partec GmbH).

Cytohistological investigations of female sporogenesis and gametogenesis

Flower buds were sampled at different developmental stages, according to the length (Figure 10). Pistils were dissected from the outer carpels under a Zeiss Discovery.V20 (Carl Zeiss MicroImaging, Germany) stereomicroscope prior to subsequent staining procedures. Dissected pistils were cleared and stained following the protocol reported by

Stelly *et al.* (1984) with some minor modifications. Briefly, the tissues were fixed in FAA (3.7% formalin, 5% acetic acid, 50% ethanol) overnight at 4°C, and then progressively rehydrated for the following staining steps. Samples were stained with pure Mayer's hemalum for 48 hours, placed in 2% acetic acid for 24 hours, and then dehydrated in 25%, 50%, 70%, 95% and 100% progressive ethanol solutions for 40 min each. After dehydration, samples were cleared with absolute ethanol:methyl salicylate solutions (2:1 and 1:2) and twice with pure methyl salicylate (10 min per step). Ovules were dissected on a slide under a Zeiss Discovery.V20 (Carl Zeiss MicroImaging, Germany) stereomicroscope, and then mounted with one drop of pure methyl salicylate and coverslipped. Cytohistological observations were made using a Zeiss Axioplan (Carl Zeiss MicroImaging, Germany) microscope under DIC optics, using a 100X objective (immersion Decolorized aniline blue (DAB; 0.005% w/v) was used to detect the presence of callose as described by Worrall *et al.* (1992). Ovules were dissected from fresh pistils directly in DAB:glycerol (1:1, w/v) under a Zeiss Discovery.V20 (Carl Zeiss MicroImaging, Germany) stereomicroscope. After ovule isolation, samples were coverslipped and observed under UV light using a Zeiss Axioplan (Carl Zeiss MicroImaging, Germany) microscope with a 365-400 λ filter set.

DNA and RNA extraction

For genomic DNA extraction, young leaves were sampled and immediately flash frozen in liquid nitrogen. For RNA extraction, pistil at different developmental stages were dissected from the flowers and immediately frozen in liquid nitrogen. RNA extraction was also performed in leaves and roots. For RNA extractions, the selections of pistil stages were done with respect to the pistil length in which the maximum frequencies of aposporic initials (AI) development have been reported. Therefore, all expression analyses were carried on Pre-AI, AI and aposporic gametogenesis developmental stages (Galla *et al.*, in press). Along with pistils, leaves and roots were sampled and immediately flash frozen in liquid nitrogen.

DNA extractions were carried by using the DAeasy Plant Mini Kit (QIAGEN) following the recommendation of the supplier. Total RNA was extracted and purified using the SIGMA-Aldrich RTN70 Mammalian RNA extraction Kit, following the manufacturer's

instructions. Reverse transcription was performed with the SuperScript® VILO™ cDNA Synthesis Kit (Invitrogen) according to the manufacturer's instructions.

MFDP primer design

The detection of multigene family domain polymorphism markers relies on the specific annealing of primers to target sequences highly conserved among different members belonging to the same multigene family. A set of 8 primer pairs was designed to specifically amplify sequences encoding protein domains characteristic of eight selected multigene families (Table 1). For MFDP primer design and multiple sequence alignments were performed using the *Arabidopsis* and rice genome sequences available in the NCBI database (http://www.ncbi.nlm.nih.gov) as input datasets. For each specific domain, a forward and reverse degenerated MFDP primer was designed in the most conserved upstream and downstream gene coding region, respectively, using two to three different primer combinations (Table 1).

Primer design and PCR amplification of the genomic sequence of *APOSTART* in *Hypericum*

Heterologous degenerated primers were designed by using the PriFi (http://cgi-www.daimi.au.dk/cgi-chili/PriFi/main) software with default parameters to amplify the selected sequences of *APOSTART*. To ensure high specificity of the amplification reaction, the genomic region was PCR assayed by using the Pfu DNA Polymerase (Fermentas life sciences). The final volume of 20 µl PCR reaction consisted of 15 ng of DNA, 1.5 µl forward and reverse primers (6 pmol/µl), 2 µl of 10× PCR buffer, 4 mM dNTPs and 0.5 U *Pfu* DNA polymerase. The temperature profile adopted for PCR reactions consisted of an initial denaturation step of 3 min at 95°C, followed by 35 cycles of 2 min at 95°C, 30 s at 62°C and 2 min at 72°C, and a final step of 5 min at 72°C. Obtained PCR products were cloned into a GeneJet-BLUNT PCR Cloning Kit (Fermentas Life Sciences) according to the recommendations of the suppliers prior to sequencing reactions.

Semi-quantitative Real-Time RT-PCR

Semi-quantitative real-time RT-PCRs were performed using Mx3000P QPCR (Stratagene, La Jolla, CA) with SYBR Green JumpStart Taq ReadyMix (Sigma-Alricht). All the experiments were performed in three technical replicates with two independent sets of RNA samples. To test the expression of different alleles for the genes *HpAPOSTART*1 and *HpAPOSTART*2, eight different primer combinations were designed to specifically discriminate between haplotypes of the same gene. For each primer combination, the amplification of a single product was assayed by sequencing of the obtained amplicons. Quantitative RT-PCR was performed in a final volume of 25 µL containing 1 µL of cDNA, 0.2 µM of each primer, and 12.5 µL of 2XSYBR Green PCR Master Mix according to the manufacturer's instructions. The following thermal cycling profile was used for all PCRs: 95°C for 10 min, 40 cycles of 95°C for 30 s, 60°C for 30 s, 72°C for 30 s. All quantifications were normalized to *Hp*TIP41-like and *Hp*PPA subunit PDF2 (Czechowski *et al.*, 2005) cDNA fragments, amplified in the same conditions. Each real-time assay was tested by a dissociation protocol to ensure that each amplicon was a single product. Negative template controls were run in these experiments, and no signal was observed (data not shown). The relative expression ratio value was calculated relative to the first developmental stage of flowers according to the Pfaffl equation (Pfaffl, 2001).

MFDP procedure

MFDP marker analysis was performed according to the AFLP procedure reported by Barcaccia *et al.* (1999) modified to adapt it to *Hypericum* DNA templates and degenerated 22-24 *mer* primers. For restriction and ligation of adapters, genomic DNA (500 ng) was digested and ligated at 37°C for 4 h using 5 U *Eco*RI (or *Pst*I), 5 U *Mse*I (New England Biolabs, Inc.), 1× Restriction-Ligation buffer (20 mM Tris-acetate, 20 mM magnesium acetate, 100 mM potassium acetate, 5 mM DTT and 2.5 µg BSA), 50 pmol of *Mse*I adapter, 5 pmol of *Eco*RI (or *Pst*I) adapter, 10 mM ATP and 1 U T4 DNA ligase (GE Healthcare). Pre-amplications were performed by mixing 5 µl of the digested and ligated DNA with 75 ng of AFLP primer (*i.e.*, restriction-site anchored primers: *Eco*RI: 5′–GACTGCGTACCAATTC+C–3′; *Pst*I: 5′–GACTGCGTACATGCAG+C–3′; or *Mse*I:

5′−GATGAGTCCTGAGTAA+A−3′) having one selective nucleotide, 75 ng of domain-specific primer, 1× PCR buffer (50 mM MgCl, 1.5 mM $MgCl_2$, 10 mM Tris-HCl), 10 mM dNTPs and 1 U *Taq* DNA polymerase (GE Healthcare). The following cycling conditions ensured optimal primer selectivity: 1 cycle of 45 s at 94°C, 30 s at 65°C, 1 min at 72°C followed by 13 cycles of 0.7°C lower annealing temperature each cycle and 18 cycles of 30 s at 94°C, 30 s at 55.9°C, 1 min at 72°C and a final step of 5 min at 72°C. End labelling sufficient for 45 selective amplications was performed by combining 4.5 µCi γ-[^{33}P] ATP, 225 ng of MFDP primer, 1× T4 buffer (10 mM Tris-acetate, 10 mM magnesium acetate, 50 mM potassium acetate), 5 U T4 DNA kinase (GE Healthcare) and distilled water up to 30 µl. Samples were incubated at 37°C for 1 h then heated to 70°C for 15 min to stop the reaction. Selective gene domain-specific restriction fragment amplification was performed with the labeled MFDP primer and an unlabeled AFLP primer. Each 20 µl PCR reaction consisted of 5 µl pre-amplified DNA, 5 ng labeled primer, 30 ng unlabeled primer, 2 µl of 1× PCR buffer, 4 mM dNTPs and 0.4 U *Taq* DNA polymerase. The temperature profile adopted for hot-PCR reactions was 1 cycle of 45 s at 94°C, 30 s at Annealing temperature, 1 min at 72°C followed by 13 cycles of 0.7°C lower annealing temperature each cycle and 18 cycles of 30 s at 94°C, 30 s at 55.9°C, 1 min at 72°C and a final step of 5 min at 72°C. Optimal Annealing temperature was sated for each primer combination to ensure optimal primer selectivity. For gel electrophoresis, each completed PCR amplification product was mixed with 20 µl formamide labelling buffer (98% formamide, 10 mM EDTA, 0.005% each of xylene-cyanol and bromo-phenol-blue) and denaturated for 5 min at 98°C. Electrophoresis was performed using a Sequi-Gen GT Sequencing Cell (BIO-RAD) apparatus. After a pre-run step of 30 min, 5 µl of the mixture was loaded on to a 4.75% denaturing polyacrylamide gel (Sequagel-4, National Diagnostic) and run with a 1× Maxam buffer (125 mM Tris-HCl, 125 mM ortoboric acid and 2 mM EDTA) at 95 W for 3 h. Gels were blotted on Whatmann 3 MM paper, dried at 75°C for 50 min and visualized by autoradiogram (BIOMAX MR-1 film, Kodak) after 18 h exposure at −80°C into hypercassette using intensifying screens (Amersham, Life Science).

Specific amplicons were excised and purified from the polyacrilamide gels, subcloned into plasmid vectors and sequenced.

Computational analyses

Nucleotide sequences were screened for vector contamination by using a home made BioPearl script prior than analyses. Since all sequences derived from non directional cloning, the complete sequence dataset were analyzed with the CAP3 software for contigs creation (http://deepc2.psi.iastate.edu/aat/cap/cap.html). Contigs information was used for correct sequence orientation in the alignment and editing processes. Alignments were performed by using the 3.6.2 version of the Geneious software for sequences analysis. The MEGA 4.1 software was used for genetic distances computation and phylogenetic analysis.

For MFDP derived sequences a different computational strategies was adopted. Retrieved nucleotide sequences were screened for vector contamination by using a home made BioPearl script. Computational analysis of the *Hypericum* datasets was performed using the Blast2GO software v1.3.3 (http://www.blast2go.org, Conesa *et al.*, 2005, Aparicio *et al.*, 2006) as described by Botton *et al.* (2008) with some minor modifications. Briefly, a sequence length threshold of 200 bp was considered for all libraries and used to split the datasets according to the length. BlastX algorithm was used for both short and long sequence datasets with different parameters. The Blast expectation value threshold was constantly set to 10, whereas the HSP length cutoff was set to 15 and 33, respectively. Basic statistical analyses of BLAST results were performed by using the same software Blast2GO software v1.3.3, with standard settings. All AFLP and MFDP marker alleles polymorphic between parental plants were preliminarily assayed to fit a 1:1 segregation ratio by the chi-square test with the Yates's correction factor. For the construction of linkage groups a minimum LOD score of 3.0 and a maximum recombination frequency of r=0.35 were applied using the JoinMap (van Oijen and Voorrips, 2001) software.

Weblogo representation of cytological data

Pistils were dissected from flower buds of different lengths, ranging from 3 to 12 millimeters (Figure 1). For each pistil, 20 randomly selected ovules were screened to define the developmental stage that were classified as pre-meiotic, megaspore mother cell (MMC), dyad, and tetrad for the sporogenesis, and 2N, 4N, 8N and mature embryo sac for

the gametogenesis. Aposporic development was defined as aposporic initial (AI), 2N, 3-4N, 6-8N and mature aposporic embryo sac. The frequency of each observed stage was calculated for each pistil and each stage was reported using arbitrarily selected acronyms. This analysis was performed using the weblogo web application (http://weblogo.berkeley.edu/, Crooks GE *et al.* 2004).

Results

Developing and testing primers for MFDP display in *Hypericum* spp.

Multi-locus PCR-based genomic fingerprints were generated by using heterologous primer sets designed on highly conserved regions of sequences belonging to the selected multigene family and used in combination with standard restriction-site related AFLP primers. The conserved sequences of eight protein domain were considered for multigene family domain polymorphism primer design (Table 1). Protein domains were selected in order to functionally enrich the genetic map with respect to the processes of cell cycle regulation, flower development or gametophyte formation. Number and distribution of genes carrying the selected motives was assayed in the heterologous genome of *Arabidopsis thaliana* by using the MapView application (http://www.ncbi.nlm.nih.gov/projects/mapview/mapsearch.cgi?taxid= 3702) available in the webpage of the National Centre of Biotechnology Information (NCBI, http://www.ncbi.nlm.nih.gov). As an example, querying the Arabidopsis genome for presence and distribution of ARF-like sequences (Auxin Response Factor-like) revealed the presence of 114 hits distributed within the genome in a range of 9 to 43 hits per chromosome. MFDP-AFLP primer combinations generated from a minimum of 10 to a maximum of 38 amplicons respectively with the primer combination for the TUB/ECO and CDK/ECO (Figure 1). As many as 64 MFDP amplicons were sequenced in order to confirm the specificity of the amplification reactions. The average length of sequenced amplified fragment was 151 bp, ranging from a minimum of 23 bp to a maximum of 315 bp. The *Hypericum* sequences was used as BlastX queries to search for structural

Table1. Conserved domains arbitrarily chosen for designing MFDP primers. The corresponding protein domain code and conserved amino acid sequence used for primer design are reported.

Conserved domain	Protein domain	Marker designation	Amino acid sequence
Auxine responding factor (ARF)	*pfam06507*	ARFfor2	(K)V(Y/F)YFPQG
		ARFrev2	LTASDTS
Cycline	*pfam00134*	CYCfor	LAAK(V/I/M)EE
		CYCrev	(I/V)(K/Q)RMELLV
Cycline Dependent Kinase (CDK)	*pfam00069*	CDKfor	EKLEK(V/I)GEG
		CDKrev	LWYRAPE
Expansin	*pfam01357*	EXPfor	NWGQNWQ
		EXPfor2	AALSTALF
		EXPrev	NWGQNWQ
MADS box	*smart00432*	MADrev	RIENKINR
		AGLfor	(M/L/V/I)KRIENK(I/T)
Mitogen associated protein Kinase (MAPK)	*pfam00069*	MAPKfor2	KICDFGLA
		MAPKrev2	ID(I/V)WS(V/I)GCI
NB-ARC	*pfam00931*	NBSfor	L(V/L)VLDDVW
		NBSfor2	MGGIGKTT
		NBSrev	L(V/L)VLDDVW
Tubulin	*cd02187*	TUBfor	DLEPGTMD
		TUBrev	MDEMEFTE

homologies and significant similarities by means of the Blast2GO software. For about two third of analyzed sequences no Blast result was recovered. The remaining 23 sequences revealed significant similarity with deposited entries, showing an average similarity estimated within the alignment of 68% and a median E-value of 2.4 E−7. Moreover, using the *Hypericum* dataset to query the non-redundant sequence database (NCBI) retrieved a number of blast hits referred to *Oryza sativa* (78) *Vitis vinifera* (67) and *Arabidopsis*

thaliana (44), while only 4 hits referred to *Populus alba*, and not hits were retrieved from the recently sequenced *Populus tricocarpa*. The extensive use of bioinformatics partially confirmed the specific domain-associated sequences of MFDP marker alleles.

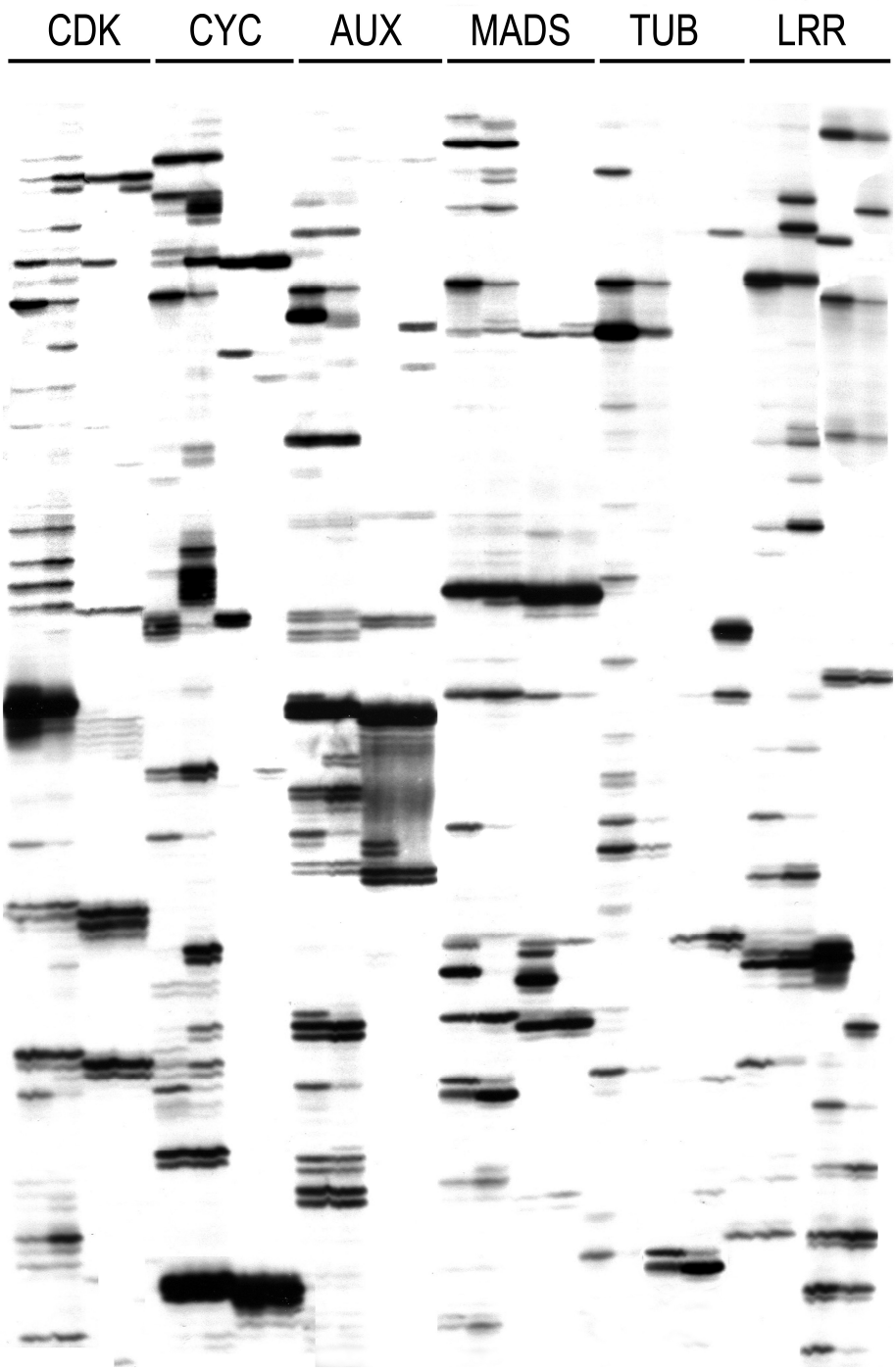

Figure 1. Example of MFDP fingerprint, originated with six different MFDP primers combinations.

MFDP display is useful for the construction of functional linkage maps in *Hypericum perforatum*

A total of 521 AFLP marker loci were investigated, yielding as many as 135 polymorphic marker alleles between the seed parent and pollen donor. Of the total polymorphic alleles, 107 marker alleles were characterized by segregation patterns significantly deviating from the expected ratios. In addition, as many as 151 MFDP marker alleles were obtained with the designed domain-specific primer combinations, yielding as many as 59 polymorphic marker alleles between the parental genotypes. As far as the MFDP marker alleles are concerned, 28 markers proved to segregate from the two parental lines with a significant distortion from the expected ratios, while 31 did not significantly deviate from the expected ratio. The best AFLP primer combination proved to be P+CCA/M+AAT, whereas of the MFDP marker system the most informative primers were the MADS and NBS domain-specific ones. From this body of information, two linkage maps were constructed for the seed parent and the pollen donor, respectively (Figures 2 and 3).

The genetic map of the seed parent was composed by 37 marker loci (28 AFLP and 9 MFDP derived markers alleles) distributed in 10 linkage groups, for a total length of about 370 cM (Figure 2). The average length of the linkage group was 37.1 cM, ranging from a minimum value of 12 cM to a maximum value of 108 cM, respectively for the linkage group number 2 and 1. The average distance between marker loci was 10 cM, ranging from a minimum loci distance of 1cM (loci pairs: ECCA/ACA/311 - ECAA/ACA/276) to a maximum distance of 27 cM (linkage groups 7 and 8). On the whole the number of loci identified for each linkage group ranged from 2 to 11, with an average number of loci per linkage group equal to 3.7. It worth nothing to mention that the number of mapped markers were 27.2% of total markers segregating within the F1 population and 55.2% of markers segregating from the seed parent genotype. Noticeably, 71.4% of markers loci (23 out of 37) were mapped in the three linkage groups 1, 4 and 5, while the remaining 14 markers were distributed in 7 distinct linkage groups each composed by 2 loci.

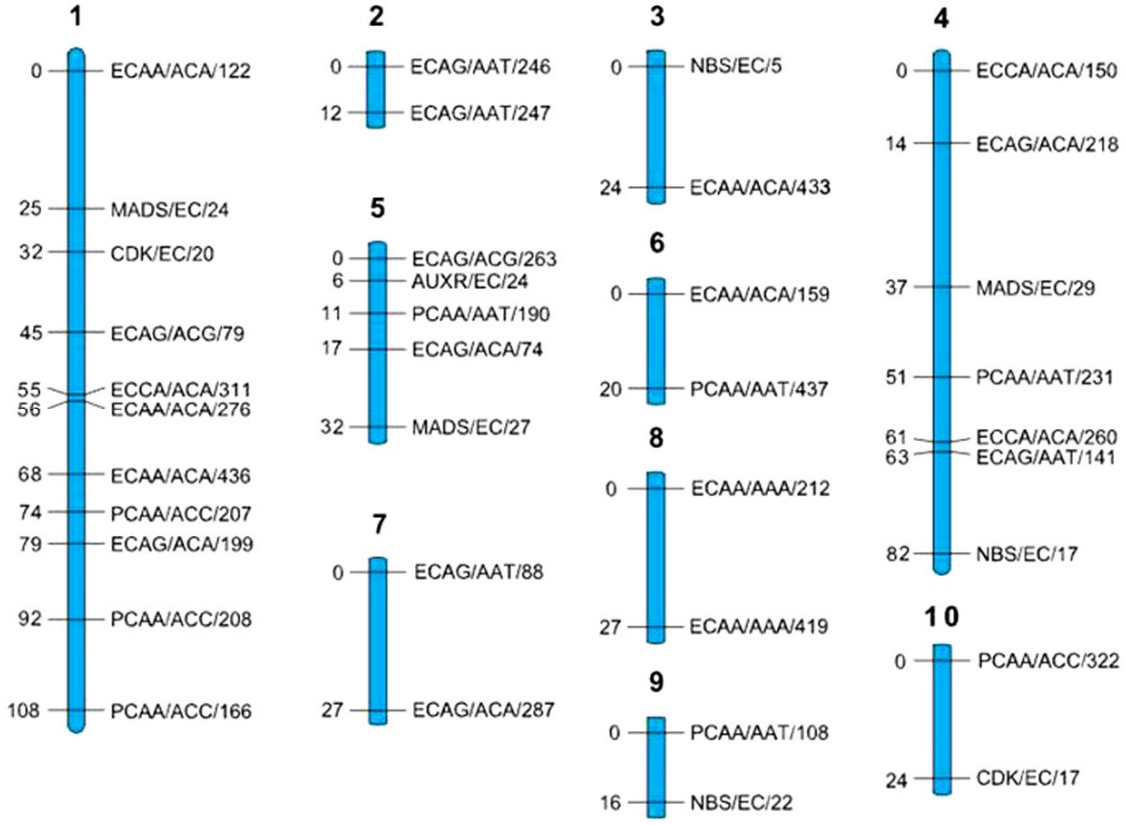

Figure 2. Genetic linkage map of the pollen donor genotype (names and distances for each marker loci are reported).

The same approach was applied for the construction of the linkage map relative to the pollen donor (Figure 3). As far as the pollen donor linkage map is concerned, a total of 27 marker loci derived from both AFLP (20 marker loci, 74% of mapped loci) and MFDP (7 marker loci, 26% of mapped loci) were mapped. Marker alleles were distributed through 7 linkage groups for a total coverage of 250 cM. The number of mapped loci in each linkage group varied from a minimum of 2, for the linkage group 3, 5, 7, to the maximum values of 12, recorded in the linkage group 1, with an average of was 3.9 marker loci each linkage group (Figure 3). Consequently, the average distance between marker loci was estimated in 9.25 cM, ranging from a minimum of 1 (loci pairs: PCAA/ACA/110 / PCAA/ATC/340) to a maximum values of 37, this latter observed in the linkage group 3 (loci pairs: CDK/EC/13b / PCAA/ACC/307). The number of mapped markers alleles was estimated as equal to 19.8%, for the seed parent, and to 65.8%, for the pollen donor, of the total number of marker alleles segregating in the F1 population.

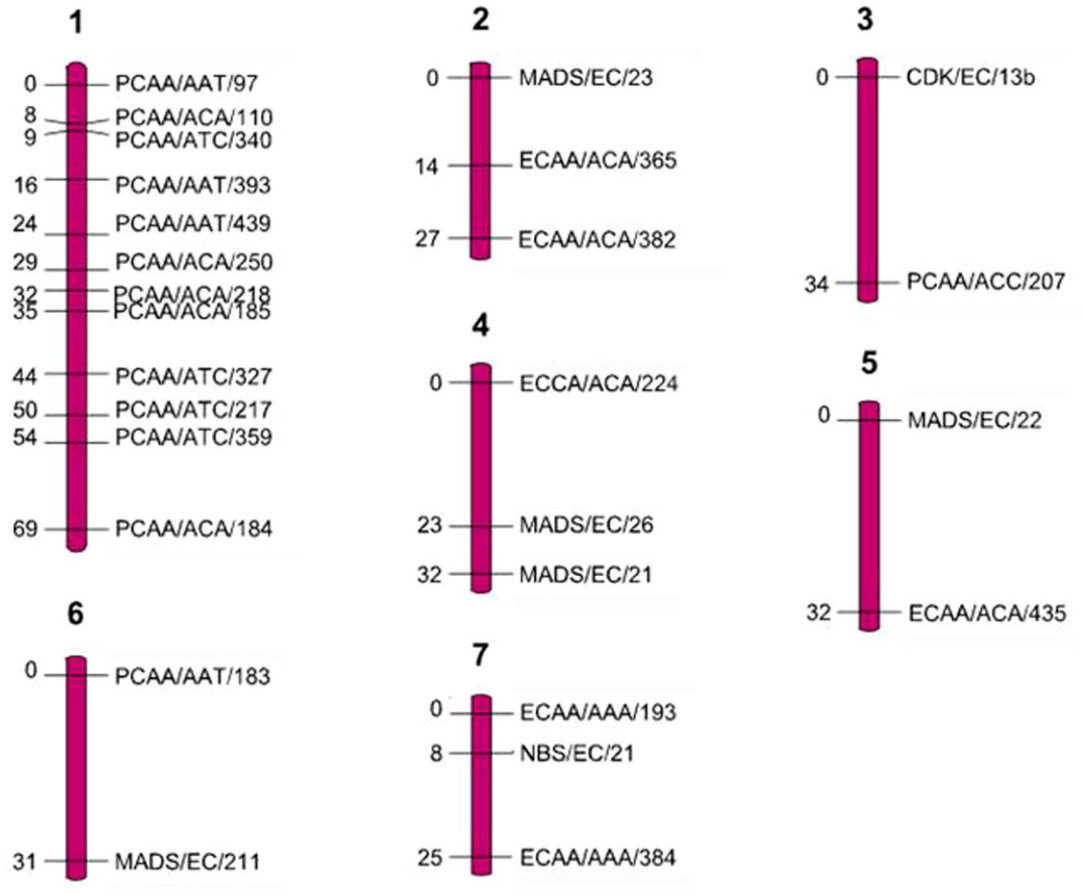

Figure 3. Genetic linkage map of the pollen donor genotype (names and distances for each marker loci are reported).

Isolation and characterisation of *HpAPOSTART*1 and *HpAPOSTART*2

A 1.7 kb long *APOSTART* genomic sequence was amplified and sequenced by using *H. perforatum*, *H. attenuatum* and *H. maculatum* as biological materials. Moreover, heterologous primers were used to isolate the partial CDS of *APOSTART1* and *APOSTART2* genes from mRNA isolated from pistils of both aposporic and sexual reproducing individuals. Sequence analyses in *Hypericum* spp. revealed the presence of two major clusters of sequences, named *HpAPOSTART1* and *HpAPOSTART2* (Figure 6). Coherently with this result, two genes have been reported in the *A. thaliana* and *O. sativa* genomes (Albertini *et al.*, 2005). Noticeably, no match with poplar was retrieved by using the *Hypericum* sequences as query (Figure 4). For each clone, the identification of the

intronic regions was done by aligning the genomic sequence to the corresponding CDS. The use of *Hypericum* genomic sequence dataset to query the GENscan web tool (http://genes.mit.edu/GENSCAN.html, Burge and Karlin, 1997) did not result in the prediction of most splicing sites within the *Hypericum* sequences. Alignment of the *Hypericum* sequences to the horthologs of *P. pratensis* confirmed the isolation of a partial trascribed region, corresponding to the exons 9 to 13 (out of 23 total exons) in *Poa pratensis*. Similarly, all partial clones isolated were composed of 5 exons, partially encoding the STAR protein domain (STeroidogenic Acute Regulatory (STAR) related lipid Transfer protein, protein domain: pfam01852) and 4 introns. On the whole, the CDSs were as long as 500 bp, while the remaining intronic regions ranged from a minimum of 993 bp to a maximum of 1266bp in the two different genes of both species. We found the length of introns to be slightly different between species, being as much as 1,215 bp, 1,266 bp, and 1,255 bp with respect to the *APOSTART1* sequence amplified from *H. maculatum*, *H. attenuatum* and *H. perforatum*, respectively. By contrast, the amplified intronic region of *APOSTART2* resulted more conserved in length, being as long as 1,204 bp, 1,218 bp and 1,219 bp in the same three species. An additional sequence identified in *H. perforatum* was apparently characterized by a deletion of 263 bp localized in the first intron. Alignment of the identified clones allowed the determination of consensus sequences of the two genes for each species.

Computational back translation of the transcribed sequences in the three species (http://www.expasy.org/tools/) resulted in a 167 residues long protein sequence. The pairwise percentage similarity calculated for over three APOSTART*1* and APOSTART*2* sequences were as high as 99.2% and 99.6%, with 165 and 166 identical sites, respectively. Moreover, the similarity of the *Hypericum* sequences with other START-domain containing proteins previously isolated from *Arabidopsis*, *Vitis vinifera*, *Oryza sativa*, *Zea mays* and *Poa pratensis* was as high as 84.9% (along with 58.1% of identity) (Figure 4).

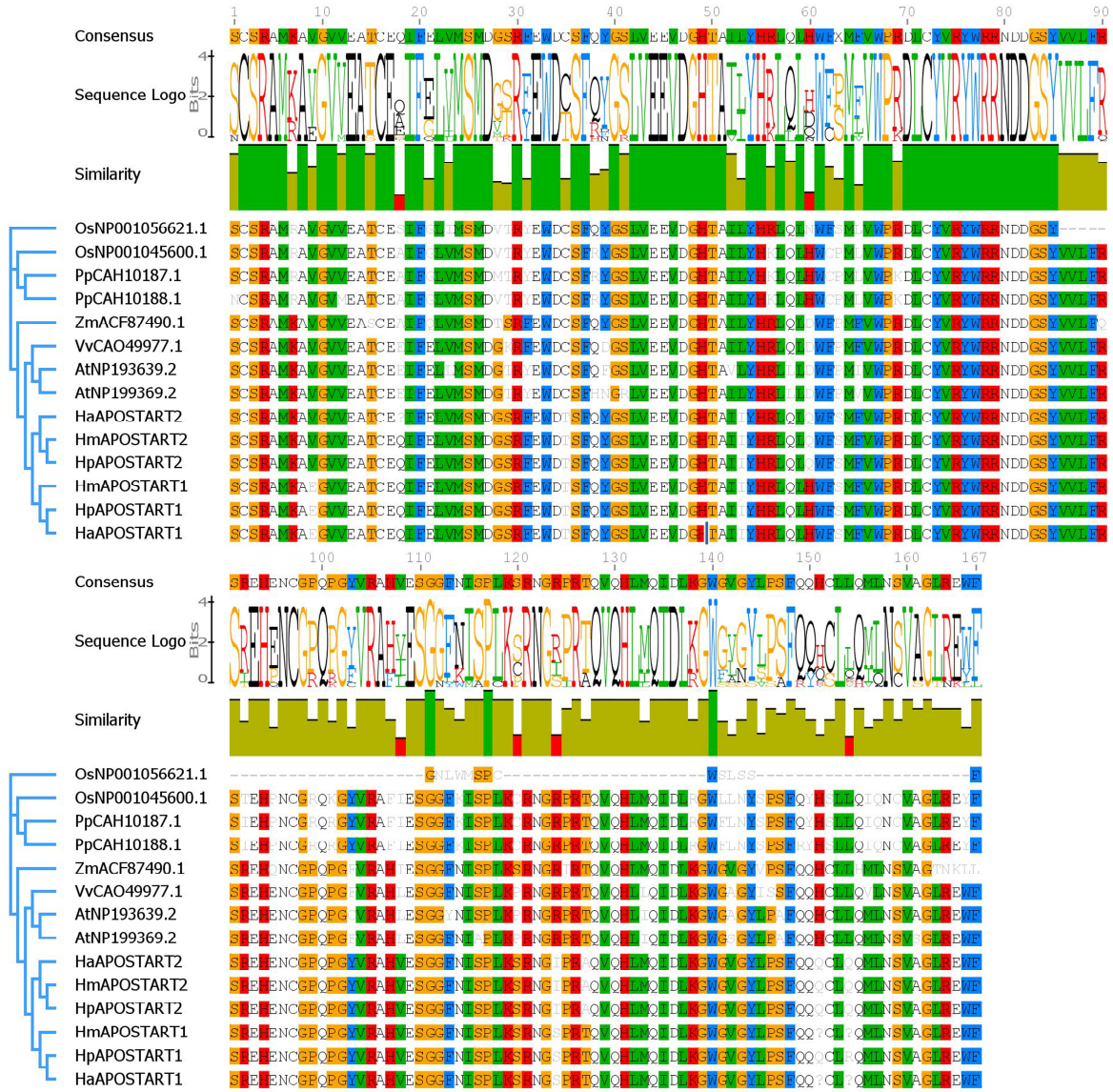

Figure 4. Alignment of *Hypercum* spp. sequences of APOSTART1 and APOSTART2 to the putative horthologs of *Oryza sativa* (Os), *Poa pratensis* (Pp), *Zea mays* (Zm) *Vitis vinifera* (Vv) and *Arabidopsis thaliana* (At). The consensus sequence of the alignment is presented as text and graphical layout. A WebLogo was originated to better describe the amino acid frequencies at each position.

Phylogenetic analysis

As many as 25 sequences were isolated from 4 tetraploid *H. perforatum* accessions along with 2 diploid *H. maculatum* and *H. attenuatum* ecotypes. Both sexual and aposporic *H. perforatum* accessions were considered for the phylogenetic analyses. Expressed and intronic regions of the two selected genes were screened for the presence of single nucleotide polymorphisms (SNPs) and their distribution throughout the amplified sequences. Sequence analyses were carried separately on intronic and esonic regions. This was possible by splitting the intronic regions from the complete sequences, followed by the generation of sequence contigs with non-overlapping regions. Merging the four non-coding regions of the clones in a single hit allowed a faster and comprehensive analysis of the sequence datasets. As far as *APOSTART1* is concerned, the CDS of the three species were characterized by a rate of SNPs equal to 4.2 SNPs/100 bp (21 SNPs out of 500 bp), whereas the intronic regions were characterized by a frequency of 7.2 SNPs/100 bp (96 out of 1,336 bp). By contrast, the rate of SNPs per 100 bp with respect to *APOSTART2* was 5.6 SNPs/100 bp (28 SNPs out of 500 bp) and 3.4 SNPs/100bp (45 SNPs out of 1,336 bp), respectively, for the CDS and intronic regions (Table 2). Coding sequences of *APOSTART1* and *APOSTART2* were characterized by 95.6% and 94.4% of identity between species, respectively. By contrast, the same parameters calculated for the intronic regions of the two genes were as low as 68.6% and 87.6% (Table 2). Intra-specific genetic divergences were estimated by computing the average genetic divergence over pairs

Table 2. SNP numbers and frequencies within coding and non-coding sequences of *APOSTART1* and *APOSTART2* over the three species *H. attenuatum*, *H. perforatum* and *H. maculatum*.

Gene	Genomic region	SNP	Length (bp)	SNP/100pb	Identity
APOSTART1	CDS	21	500	4.2	95.6 (%)
	Introns	96	1336	7.2	69.6 (%)
APOSTART2	CDS	28	500	5.6	94.4 (%)
	Introns	45	1336	3.4	87.6 (%)

of sequences belonging to the same specie (Table 3). Moreover, the inter-specific genetic divergences were computed by pairwise comparisons of sequences belonging to different species (Table 3). Since the *APOSTART* genes are putatively encoded by the nuclear genome, the estimation of the intra-specific genetic divergence reflected the estimated divergence between alleles of the same gene and between the different genotypes considered for each species. As reported in Table 3, the average genetic divergences within species were estimated over intronic and esonic regions in 0.01813 and 0.00374, for the *APOSTART1*, and as low as 0.00661 and 0.00682, respectively, for *APOSTART2*. More in detail, intra-specific genetic divergences calculated on the basis of the *APOSTART1* intronic regions were as high as 0.02642, 0.02251 and 0.00546 for the three specie *H. attenuatum*, *H. maculatum* and *H. perforatum*, respectively.

Table 3. Genetic distances computed over all retrived coding and non coding sequences belonging to the species *H. attenuatum*, *H. perforatum* and *H. maculatum*. Genetic distances between species are also reported.

	Rif.	Species	Introns		Exons	
			Genetic Distances	S.E.	Genetic distance	S.E.
APOSTART1	1	*H. attenuatum*	0.02642	0.00389	0.00407	0.00219
	2	*H. perforatum*	0.00546	0.00128	0.00444	0.00143
	3	*H. maculatum*	0.02251	0.00363	0.00271	0.00191
	4	*H. perforatum / attenuatum*	0.03305	0.00424	0.00512	0.00197
	5	*H. perforatum / maculatum*	0.01778	0.00253	0.00350	0.00117
	6	*H. attenuatum / maculatum*	0.03175	0.00380	0.00430	0.00208
APOSTART2	7	*H. attenuatum*	n/c	n/c	n/c	n/c
	8	*H. perforatum*	0.00896	0.0017	0.00327	0.00127
	9	*H. maculatum*	0.00426	0.00189	0.01037	0.00443
	10	*H. perforatum / attenuatum*	0.01998	0.00378	0.00384	0.00222
	11	*H. perforatum / maculatum*	0.01245	0.00256	0.00614	0.00220
	12	*H. attenuatum / maculatum*	0.01205	0.00284	0.00725	0.00299

The same parameters calculated with respect to the intronic regions of *APOSTART2* were equal to 0.00896 and 0.00426 for, respectively, *H. maculatum* and *H. perforatum* (Table 3). Since only one *HaAPOSTART2* sequences were retrieved, no intra-specific genetic distances were calculated. It is worthy to mention that, with the only exception of *HmAPOSTART2*, the genetic divergence estimated within species over the non coding sequences were up to 8-fold higher than the same parameters estimated on the basis of expressed sequences (Table 3, Figure 5). Moreover, the average genetic distances were calculated for all sequence pairs between the species *H. perforatum* and the hypothesized ancestors *H. maculatum* and *H. attenuatum* (Table 3, Figure 5). On the whole, all genetic distances estimated by pair-wise sequence comparisons between different species were higher than genetic distances calculated among sequences within the correspondent species. The only exception to this was the genetic distance calculated over all *H. perforatum* and *H. maculatum* sequence pairs, which resulted lower than the same parameters calculated within *H. maculatum* (Table 3).

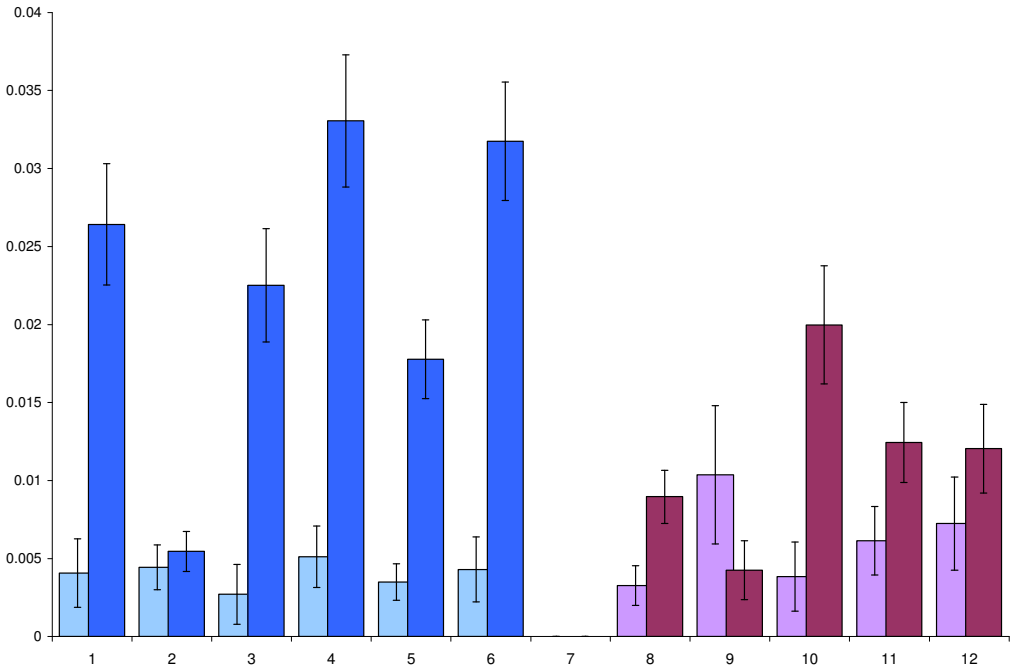

Figure 5. Genetic distances computed by pair-wise comparisons of sequences belonging to the same species (1, 2, 3 - 7, 8, 9) and sequences belonging to different species (4, 5, 6 - 10, 11, 12). For each histogram the corresponding specie is reported in Table 2.

The interspecific genetic distances computed in the comparisons between *H. attenuatum* - *H. perforatum, H. attenuatum* - *H. maculatum* and *H. maculatum* - *H. perforatum* were as high as 0.03305, 0.03175 and 0.01778, respectively for *APOSTART1*, and 0.01998, 0.01245 and 0.01205 for *APOSTART2*. It is particularly interesting that the average distances calculated between *H. attenuatum* and *H. perforatum* were significantly higher than those calculated over the combination *H. perforatum* and *H. maculatum* (Figure 5). This was true for all intonic and CDS sequence comparison with the exception of the *APOSTART2* exons. Genetic distances calculated over all intronic sequences were used to infer a Neighbour-Joining phylogenetic tree (Saitou N and Nei M, 1987) (Figure 6). To construct the tree, the evolutionary distances were computed using the Kimura 2-parameter method (Kimura, 1980) and are presented in the tree in the units of the number of base substitutions per site. Being the intronic sequences frequently interrupted by conserved gaps within the same gene, all positions containing alignment gaps and missing data were eliminated only in pair-wise sequence comparisons. For the phylogenetic tree construction, a bootstrap analysis with 1,000 replicates was performed and the percentage of replicated trees in which the associated taxa clustered together were shown above the branches (Felsenstein J, 1985). Phylogenetic graphical representation of *Hypericum* sequences clearly underlined the presence of two main groups, thus supporting the presence of the two distinct genes previously defined as *HpAPOSTART1* (Figure 6, top) and *HpAPOSTART2* (Figure 6, bottom). This was further confirmed by the observation that isolated sequences belonging to the three species were distributed within the two major branches, thus indicating that intergenic differences were higher than differences between species. For each major branch, the graphical representation of genetic distances between sequence pairs revealed the presence of different minor clusters of sequences each composed by clones belonging to different species and individuals. Coherently to the ploidy levels, up to four sequences/alleles were identified from individuals belonging to the *H. perforatum* species, while a maximum of two sequences/alleles was retrieved for both diploid *H. attenuatum* and *H. maculatum* individuals.

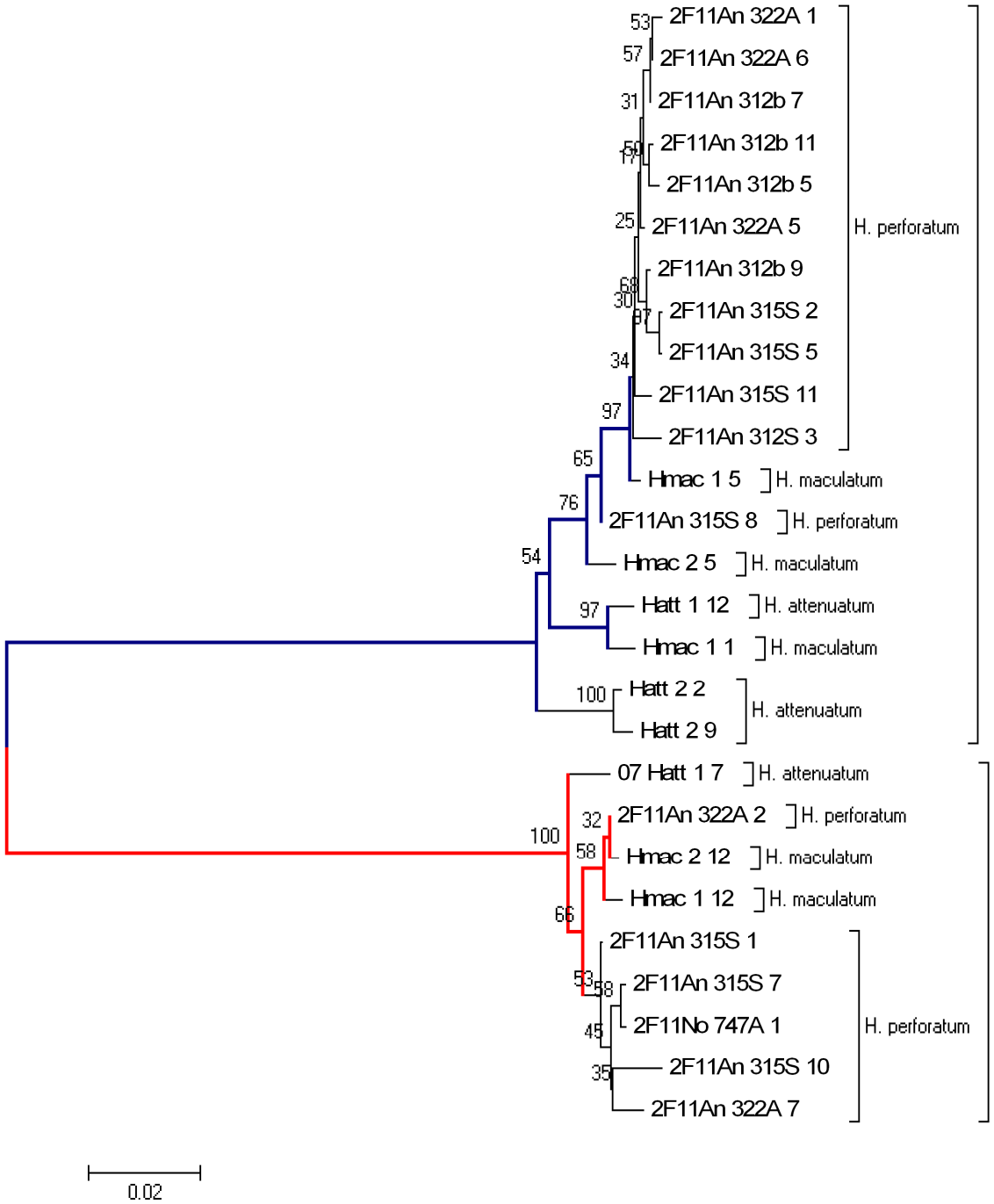

Figure 6. NJ phylogenetic tree on K2P distances computed over all intronic sequences of *H. attenuatum*, *H. perforatum* and *H. maculatum*. Two main clusters corresponding to the *APOSTART1* (blue branch) and *APOSTART2* (red branch) genes are clearly recognizable. Bootstrap values corresponding to number of trees for which the same branch were originated (number of replicates : 1000) are reported for each node.

The close relationship between the two *H. perforatum* and *H. maculatum* species, emerged by estimation of inter-specific genetic distances over all species, was further evidenced by plotting all sequence distances in a phylogenetic tree. Figure 5 shows that *HmAPOSTART1* sequences tightly group with the *H. perforatum* entries, while the *H. attenuatum* horthologs are preferentially localized in a separate group, supported by a bootstrap value equal to 66%. The low evolutionary distance estimated for *H. perforatum* and *H. maculatum* species was further confirmed by the analyses conduced with the *APOSTART2* sequences (Figure 6, bottom).

FCSS analyses

The reproductive behavior of 4 different tetraploid (4C) accessions collected from different geographical regions was measured by the flow cytometric seed screen of 50 single seed per ecotype. The most frequent reproductive mode recorded in aposporic individuals was the parthenogenic and pseudogamous development of the unreduced embryo sac, as 65.5% to 89.2% of the analyzed seed per accession were characterized by an embryo:endosperm ratio of 4:10. This ratio reflects pathenogenetic development of the unreduced egg cell (4C) and fertilization of the unreduced central cell (8C) with a 2C sperm nucleus (Table 6). Moreover, all analyzed apomictic individuals exhibited low levels of a 4:6 embryo:endosperm ratio, which likely demonstrate double fertilization of reduced embryo sacs (Table 5). Sexual seed production (amphimixy) ranged from 2.5% to

Table 4. Geographic origins and flow cytometric characterizations of *H. peforatum* used in embryological analyses

Plant	Locality	Ploidy	Degree of apomixis	Method of analysis
H06_1915	Iron Mountain MI US	4*x*	89%	FCS of single seeds
H06_2751	Bolzano, Italy	4*x*	69%	FCS of single seeds
H06_2849	Badia Polesine, Italy	4*x*	82%	FCS of single seeds
H06_2974	Cerbere, France	4*x*	75%	FCS of single seeds

10.3% (Table 5). Double fertilization of the unreduced embryo sac, as demonstrated by a 6:10 embryo:endosperm ratio, was also present in 8.1% to 22.5% of the analyzed seeds (Table 5). Beside these main patterns of embryo and endosperm formation, a number of low frequency phenotypes were also observed, and demonstrated more complex pathways of gametophyte formation and fertilization strategies. For example, low frequencies of 4:8 (parthenogenesis and autonomous endosperm formation from an unreduced embryo sac) and 2:6 (parthenogenesis and pseudogamous development of a reduced embryo sac) embryo: endosperm ratios were identified (Table 5). Furthermore, low frequencies of 2:8, 4:12 and 4:14 ratios were observed (Table 6), which could reflect either the formation of trinucleated central cells or the production of functional unreduced pollen grains. If trinucleated central cell formation was the case, the maternal:paternal genome balance within the endosperm would equal 6C:2C, 12C:0C and 12C:2C (Table 6) respectively for the three embryo:endosperm above-mentioned ratios. Alternatively, unreduced tetraploid and hexaploid pollen grain formation, could also explain the observed genome ratios. Double fertilization of either reduced or unreduced embryo sacs by unreduced pollen grains was never observed.

Table 5. Frequencies of C values ratios observed in different aposporic individuals of the *H. perforatum*. embro and endosperm. DNA contents were estimated by single seed FCSSanalyses. The total number of seed for which C values was estimated with no ambiguities is reported in the table (Total). For each C value ratios, the percentage (top, left) and absolute number (bottom, right) of seeds is reported.

Accession	Embryo/endosperm ratios								Total
	2 : 6	2 : 8	4 : 6	4 : 8	4 : 10	4 : 12	4 : 14	6 : 10	
H06_1915	-	-	**3%** (1)	-	**90%** (33)	-	-	**8%** (3)	37
H06_2751	-	3% (1)	**10%** (3)	10% (3)	**65%** (19)	-	-	**17%** (5)	29
H06_2849	2.6% (1)	-	**8%** (3)	-	**77%** (30)	3% (1)	-	**10%** (4)	39
H06_2974	-	-	**2%** (1)	-	**72%** (29)	-	2% (1)	**22%** (9)	40

Table 6. Expected C-values in seeds originated through sexual and apomictic reproduction. Haploid genotypes content (*x*) are reported for both maternal and paternal gametes and accessory cells. C values expected observed ratios for double fertilization, parthenogenesis (Partenog.) and pseudogamy are in bold characters.

			Double fertilization	**Fertilization** Autonomous Endosperm formation	**Parthenog.** Autonomous Endosperm formation	**Pseudogamy**
			Sperm nuclei (2*x* - 2*x*)	Sperm nuclei (2*x* - 0)	Sperm nuclei (0 - 0)	Sperm nuclei (0 - 2*x*)
Meiosis	Egg Cell	Central cell				
	2x	4*x* (2*x*+2*x*)	**4*C* : 6*C***	4*C* : 4*C*	2*C* : 4*C*	2*C* : 6*C*
	2x	2*x* (2*x*+0)	4*C* : 4*C*	4*C* : 2*C*	2*C* : 2*C*	2*C* : 4*C*
	2x	6*x* (2*x*+2*x*+2*x*)	4*C* : 8*C*	4*C* : 6*C*	2*C* : 6*C*	2*C* : 8*C*
Apospory	Egg Cell	Central cell				
	4x	8*x* (4*x*+4*x*)	6*C* : 10C	6*C* : 8*C*	**4*C* : 8*C***	**4*C* : 10*C***
	4x	4*x* (4*x*+0)	6*C* : 6*C*	6*C* : 4*C*	4*C* : 4*C*	4*C* : 6*C*
	4x	12*x*	6*C* : 14*C*	6*C* : 12*C*	4*C* : 12*C*	4*C* : 14*C*
			Sexuality		**Apomixis**	

Cytological investigation

Hypericum perforatum has a zygomorphic flower, composed of 5 sepals and petals surrounding the internal male and female whorls. The internal tricarpellate syncarpic gynoecium is inserted onto the receptacle above the points of insertion of the outer whorl and the numerous stamens. One single *H. perforatum* ovary yields from 50 to more than 100 ovules, and is connected to the sporophytic tissues by an axile placentation.

Megasporogenesis and sesual megagametogenesis

The ovule primordium develops as a conical protuberance originated by the placental tissues. At stage 1-I the protruding ovule is three to four cell rows in appearance, organized in an outer layer enclosing an internal hypodermal one (data not shown). As the ovule primordium reaches approximately 15 cells in length, the emerging integument undergoes periclinal division. Integument growth delineates the main funicular, chalazal and nucellar domains within the ovule. The *Hypericum* ovule is bigtemic as both outer and inner integuments differentiate from the middle region of the proximal - distal axis of the ovule. At this stage the nucellus is about five cells in length and is composed of one epidermal layer, enclosing one to two hypodermal columns of cells. We found the number of hypodermal cells to be variable between ovules of the same plant, with no obvious correlation with the reproductive behavior. As the internal integument starts to form, the evident archesporial cell differentiates just beneath the most apical epidermal cell. No intermediate division of the archesporial cell prior to MMC differentiation was observed (data not shown). Callose deposition patterns within sexual ovules fully resemble the pattern previously described for the monosporic *Polygonum* type of embryo sac formation (Figure 8). To begin with, fluorescence is strongly localized at both poles of the MMC, with crescent-like accumulation that finally interest the complete surface of the cell. First meiotic division and cytokinesis lead to marked callose deposition within the middle cell wall. At this time little or no callose is present within the proximal-distal apex of the dyads. Callose is furthermore clearly detectable within the young tetrad stage (Figure 8), being strongly accumulated among newly originated megaspores. Late tetrads are recognizable from younger ones by the massive accumulation of polysaccharide around all

but the functional megaspores. As in *Arabidopsis* and maize, only the most proximal megaspore survives to undergo further development (Figure 7). The complete degeneration of the most micropylar megaspores is accompanied by the onset of megagametogenesis which involves the enlargement of the functional megaspore to give rise to the one nucleate embryo sac (Figure 7). The first mitotic nuclear division of the one nucleate embryo sac leads to the two nucleated FG2 coenocyte formation (Figure 7). Positioning of the nucleus within the cell is strictly defined as the two nuclei are always detectable within the two proximal and distal most areas of the coenocyte. Prior to the second mitotic division, the embryo sac markedly increases in length, almost reaching the most micropylar side of the ovule, as stage which we referred to as FG3 (Figure 7). The second nuclear division of the proximal and distal nuclei is highly synchronized and results in the formation of a four nucleate embryo sac with two nuclei oppositely localized at each side of the cell (Figure 7). A precise and conserved pattern of nucleus positioning within the cell is observed at this stage, thus suggesting that nucleus positioning within the embryo sac is deeply controlled. More specifically, the nuclei are positioned one above the other with respect to the chalazal pole of the micropylar/chalazal axis while the nuclei generally are located side by side at the micropylar end (Figure 7). Similar nuclear localization within the embryo sac was also reported by Christensen *et al.* (1997) and Pagnussat *et al.* (2005) for the *Arabidopsis embryo sac*. The third nuclear division closely follows the second one and leads to the final count of eight nuclei within the FG5 embryo sac (Figure 7). As cytoplasm and organelle partitioning take place, two antipodals and synergids originate from the most external localized nucleus while all other constituents of the mature embryo sac are derived from the more centrally localized nuclei (Figure 7). The fully cellularized embryo sac, comparable to the Arabidopsis FG6 (Christensen *et al.*, 1997), is composed of the three antipodals, a bi-nucleated central cell and the egg cell positioned beneath the two most micropylar synergids. Similar to Arabidopsis, synergids and egg cell are clearly characterized by inverted localization of the large vacuole and nucleus one with respect to the other (Figure 7). Indeed, while synergids are typically characterized by a distal nucleus and a proximal vacuole, the egg cell is characterized by the presence of a distal localized vacuole and a proximal cytoplasmic area. Such organization of the egg cell results in the proximity of the large nucleus of the germ cell to

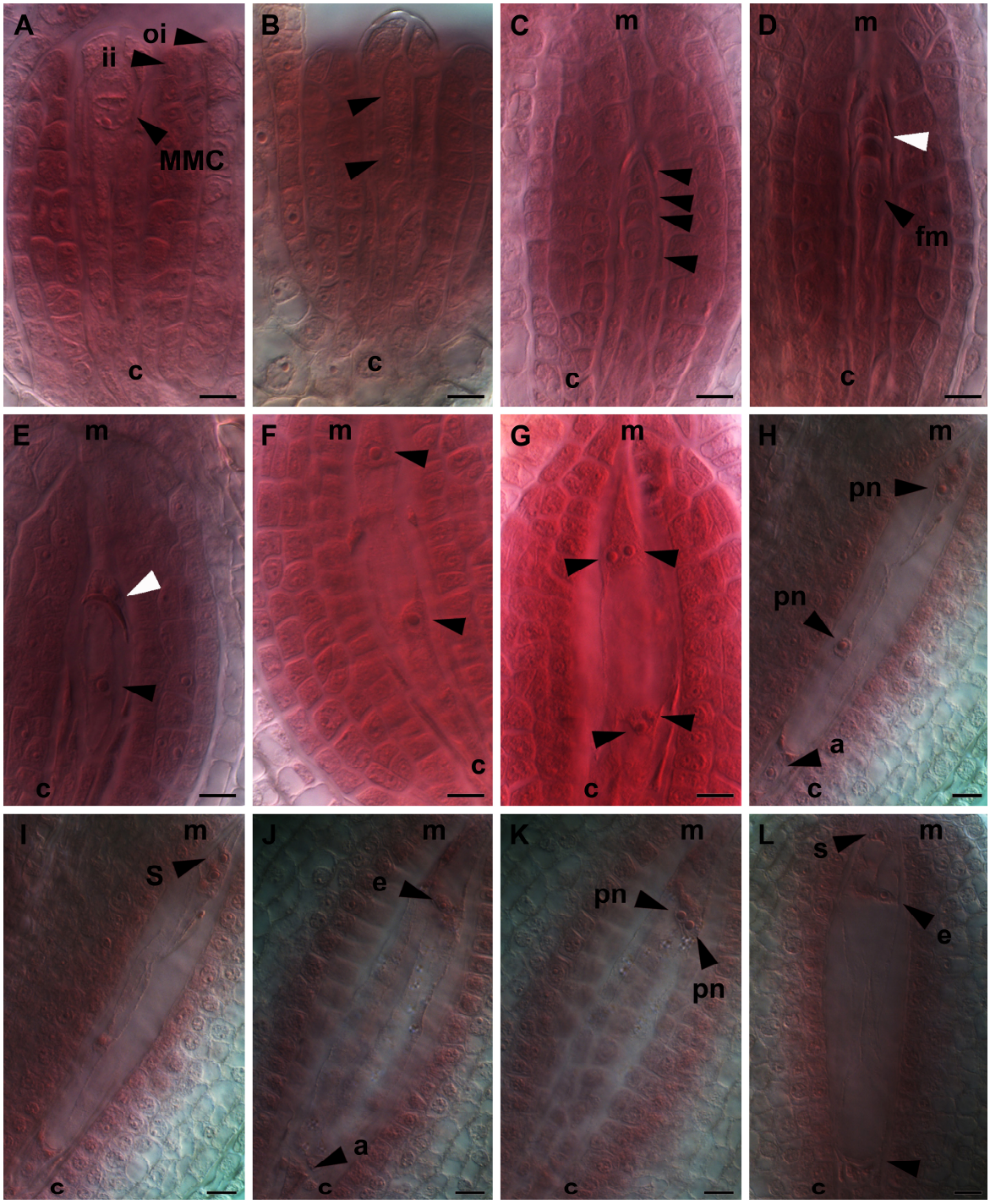

Figure 7. Megasporogenesis (A-D) and megagametogenesis (E-L) progression in sexual *H. perforatum* individuals. For each panel the micropylar (m) and chalazal (c) side of the ovules are reported. A, MMC; B, Dyad; C, Tetrad; D, Functional megaspore. E, 1N ES; F, 2N ES; G, 4N ES; H-K, 8N ES spanning the time point of antipodals degeneration. L, mature ES. Degeneration of the most micropylar megaspores is marked with the white arrow head. Nucleus within megaspores and embryo sacs are marked with black arrow heads. J, L the black arrow heads in the chalazal region (c) marks the degenerating antipodals.

the secondary nucleus of the central cell, the latter being distally localized within the large auxiliary cell. We observed that degeneration of the antipodal cells always precedes polar nuclei fusion and that secondary nucleus formation always precedes synergid cell degeneration and fertilization of the embryo sac (Figure 7).

Aposporic Initial differentiation and development

Within aposporic individuals, strong deviations from the sexual pathway were recorded. Isolated ovules from apomictic individuals are typically characterized by an archesporial cell that eventually produces a MMC which apparently mimics the developmental timing observed in sexual individuals. As shown in figure (Fig4, B-D), even if megaspore-like enlarged cells seem to be present within the hypodermic layer, meiosis frequently stops at the two to four megaspore stage. Furthermore, if distinguishable from the surrounding cells, such megaspores typically carry a small nucleus and exhibit signs of degeneration (Figure 9, C). Moreover, the ovules of aposporic individuals are characterized by novel callose deposition patterns compared to those of sexuals, and very rarely show dyads or tetrads. Furthermore, FCSS analysis confirmed that aposporic individuals retained low frequencies of sexual seed formation, and thus the possibility that our embryological observations of dyads and tetrads reflect amphimixis rather than apospory cannot be ruled out. Apomictic ovules are characterized by diffuse fluorescence signals in place of the clearly defined callose deposition normally associated with meiosis progression, and brightly-stained single cells were frequently observed in both hypodermal and epidermal areas of the nucellus, where sporogenesis is not likely to take place (Figure 8). These patterns are in strong contrast to those of the sexual individuals (Figure 8). If it is likely that callose deposition is linked to meiosis, we do not known whether this deviation is a cause or a consequence of the observed apomeiotic events. Interestingly, in addition to megasporogenesis arrest, the number of cells seems to deviate from that which is characteristic of normal development (Figure 9). These cells are clearly recognizable in the apomeiotic embryo sac, and share a number of traits: i) exclusive to apomeiotic

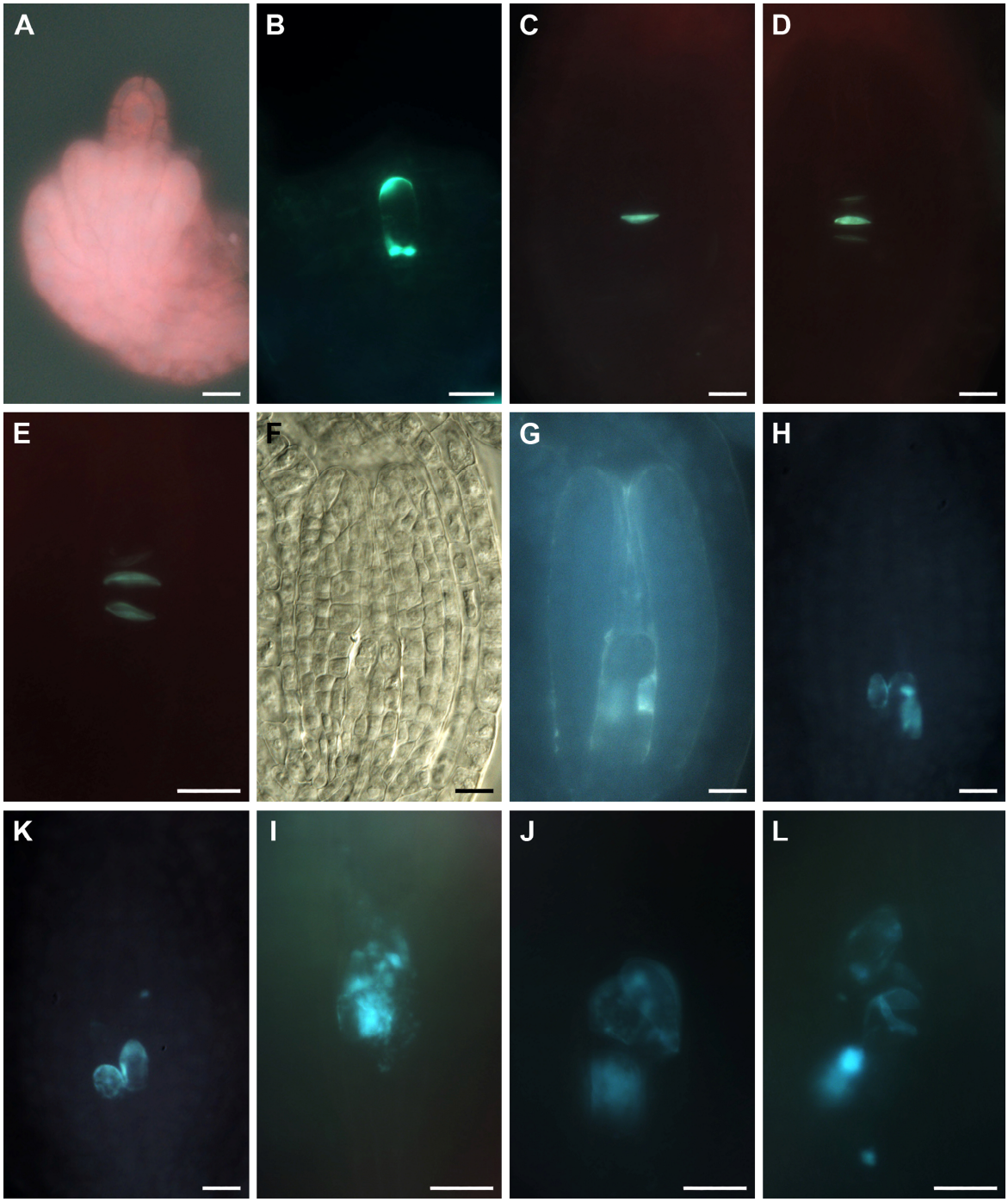

Figure 8. Callose localization recorded by DAB staining of ovules at pre-meiotic and meiotic developmental stages. A, Pre-meiotic ovule, no callose is localizable within the nucellus. Note the size of the integuments. B, MMC; C, Dyad; D-E Tetrads. The middle cell wall is the major site of callose accumulation at this developmental stage. The panels F and G show one ovule isolated from an aposporic individual, captured with normal light and UV (for callose-AB localization). Fluorescence is present out of the conventional site of deposition. H-L, callose deposition observed in dissected ovules from aposporic plants. Callose localization is frequently localized in non-conventional sites (H, K), spread or

with spotted distribution (I, J, L). J and L panels show two sexual like patterns of callose localization, but flanked by other accumulating cells (Compare E/L).

ovules; ii) differentiation from the epidermal layer of the nucellus; iii) cell size considerably increased with respect to the neighboring ones; iv) larges vacuoles frequently present along both sides of the cell and a dense cytoplasmic middle region; v) clearly defined large nucleus. It is worthy to mention that older aposporic ovules were frequently characterized by the presence of a large developing coenocyte clearly developing from the same target area of the nucellus. Considering these morphological traits and the apparent ability to escape their conventional cell fate, we defined these cellular types as Aposporic Initial (AI). Typically, AIs are elliptical in shape, frequently drop-shaped, and clearly distinguishable from the square shape neighboring epidermal cells (Figure 9). Early developmental steps of AIs are characterized by dramatic growth in length and width and the concomitant replacement of the surrounding, mostly hypodermic, tissues. Furthermore, the neighboring cells are frequently arrested in development, or appear as degenerating megaspores (Figure 9). Interestingly, the increase in size and particularly in length of the AIs was comparable to that of enlarging sexual embryo sacs (i.e. as three to four times the length of surrounding cells prior to any nuclear division is easily reached). The first nuclear division of the central localized nucleus of the AI results in the formation of a binucleate coenocyte, whose nuclei localize to the apex of the cell, in a pattern similar to the sexual FG2 embryo sac (Figure 9). After this nuclear migration, a second and third nuclear division usually takes places within the sac. Frequently the second and third division seems to be asynchronous, and lead to unconventionally-nucleated coenocytes if compared to the sexual FG4 and FG5 embryo sac morphologies reported above (Figure 7 and 9). Two main types of abnormalities were observed within aposporic coenocytes. First, aposporic embryo sacs may contain an unpaired number of nuclei, resulting in three, five and nine nucleate cells. Second, nuclear positioning within the sac frequently does not resemble the *Polygonum* type, and results, for instance, in the presence of two to six nuclei in the most micropylar pole of the cell. While these deviations in nuclear distribution are linked with asynchronous cell division, it is unclear whether this is a cause or consequence. FG4 is additionally characterized by a coenocyte

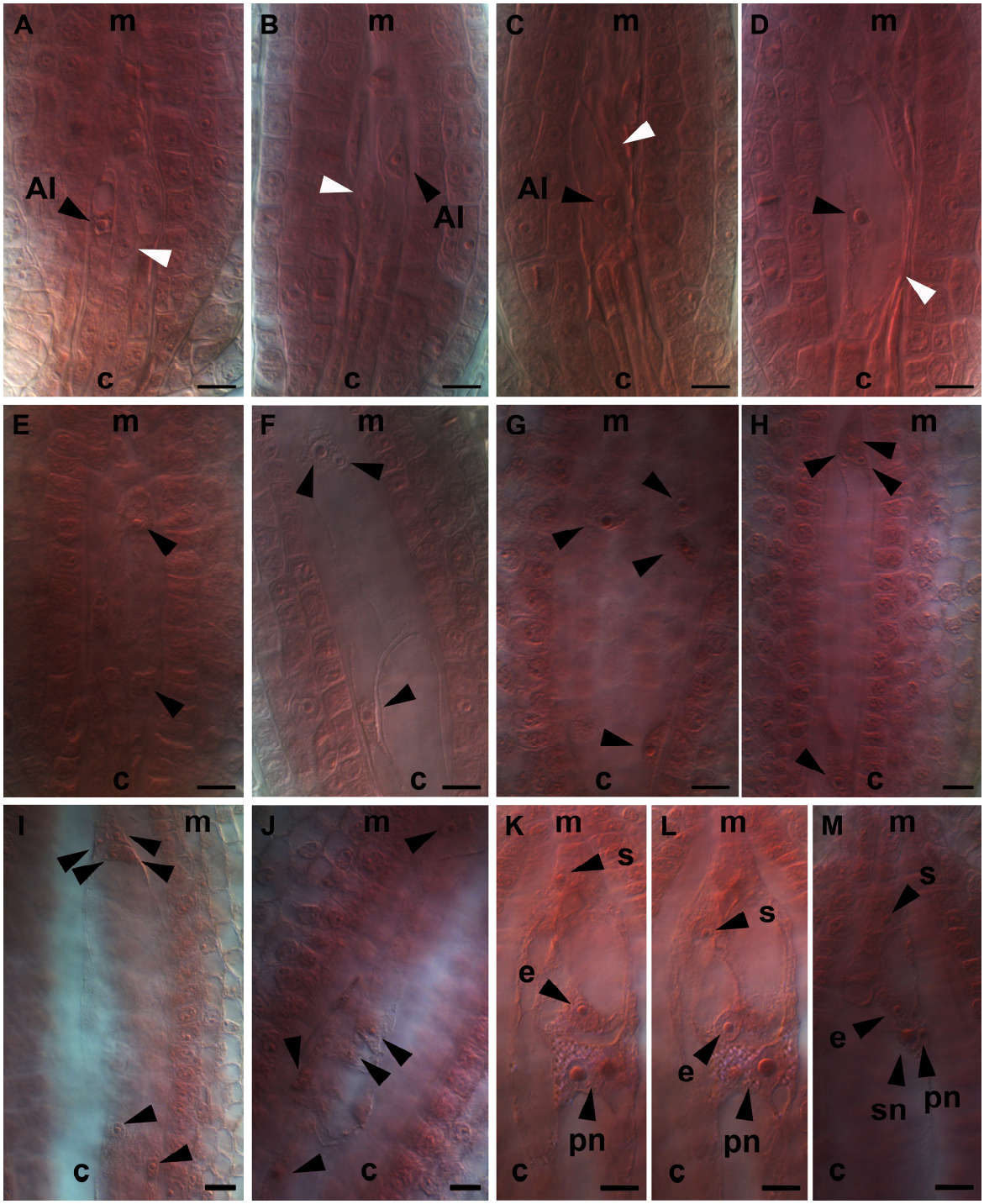

Figure 9. Embryo sac development within aposporic ovules. Micropylar (m) and chalazal (c) sides of the ovules are reported for each panel. A-C, aposporic intitials differentiation and enlargement. E-J, coenocytic growth of the aposporic intial finally giving rise to an embryo sac. K-M, egg cell apparatus in which the presence of supernumerary cells (K-L) or nucleus (M) is recognizable. From A to F, the cellular layer in which the AI differentiates is clearly detectable. White arrows heads indicates the expected site of megasporores localization. Black harrow heads marks the nucleus detectable within the coenocyte.

which frequently possessed four nuclei localized in the four corners of the cells (Figure 9). No obvious pattern of nuclei localization is typically present after the third nuclear division. In the most extreme cases the ovule contains what appear to be degenerating synergids and supernumerary nuclei (Figure 9) or cells (Figure 9). Furthermore, the nucleus and vacuole are apparently correctly positioned within multiple egg cells, if present. Therefore we cannot rule out the possibility that eventual supernumerary egg cells are functional. In contrast, synergids are frequently difficult to localize or atypically shaped and close to degeneration. Normally, one to two antipodal cells is proximally localized in the embryo sac, but they rarely resemble the characteristic triangular morphology observed in sexual embryo sac. Apomictic individuals typically had ovules bearing large degenerating cells, and in a few cases an enormously enlarged nucleus or no nucleus at all, all of which suggest embryo sac degeneration. One to four AIs were recorded within the same nucellus, which eventually led to multiple enlarged coenocytes within the same ovule. The developmental stages of multiple AIs, when present, were frequently unsynchronized. Moreover, the developmental stages of multiple aposporic embryo sacs frequently demonstrated a distal-proximal gradient distribution, with the larger coenocyte reaching the micropylar axis while the newly differentiated AIs enlarging in the chalazal proximal side. In contrast, no obvious adassial - abassial developmental gradient was observed. The formation of multiple AIs within the same ovule further enabled us to predict the target area of AI differentiation within the nucellus, which was always restricted to the epidermal cell layer of the nucellus.

Web logo-like representation of ovule stages

The *Hypericum* ovary is mainly characterized by synchronized development of the ovules within the carpels. Main synchronous development is evident in figure 10 as no more than three developmental stages each pistil were recorded, with usually one stages more numerous than the others. Some differences in stages development surely rose from the acropetal development of the ovary leading to a different timing of ovule primordial protrusion from the basal to the apical region of the placenta. Considering that the ovary development is determined, differences in ovules stages decreased with the later stages of

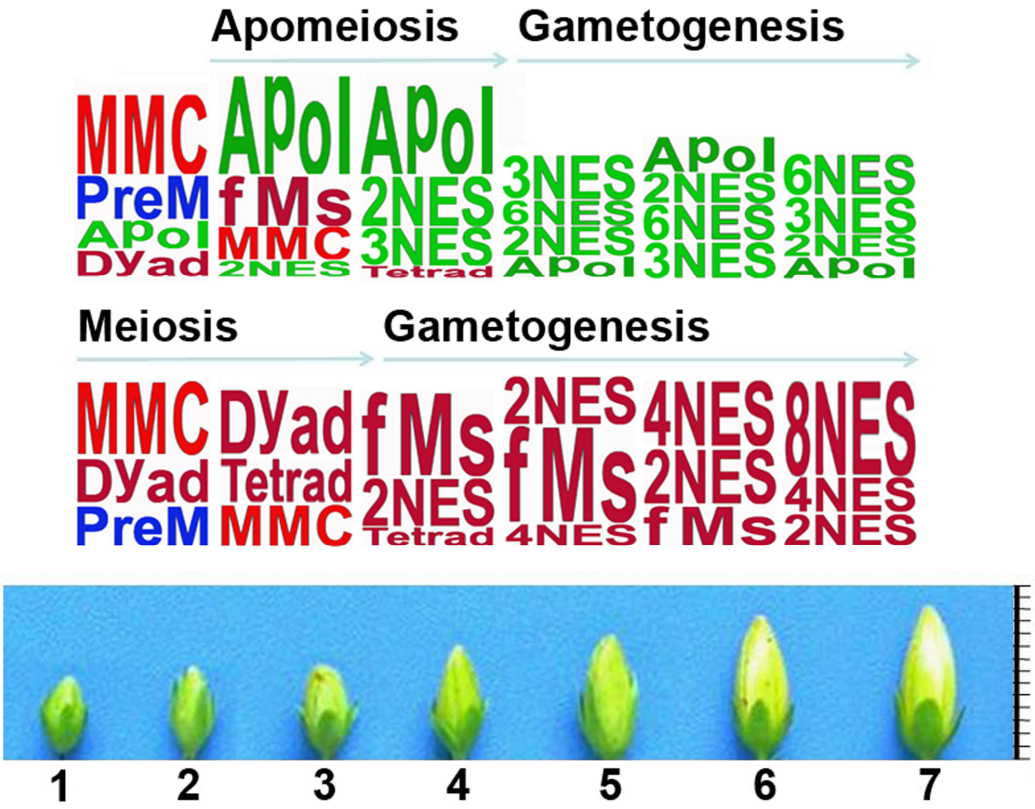

Figure 10. WebLogo representation of sporophyte (when present) and embryo sac stages in ovules of sexual (middle panel) and aposporic (top panel) individuals. Flower buds of the corresponding stages are reported in the bottom panel. For each reported cytological structures the size of the letters are proportional to the calculated frequency within the pistil. PreM: pre meiotic stage, fMs: functional megaspores, ES: embryo sac. APoI: aposporic initials.

the flower bud, ending with almost fully synchronised ovule development at bloom. Web logo like representation of ovule stages clearly evidenced the main functional synchrony within sexual reproducing individuals (Figure 10). With this respect, meiosis progression seem to be mainly focused at flower bud at stages 4 to 6, referred to the bud's length, while gametogenesis mainly proceed in flower bud at stages 6 to 10. Some differences in stages frequencies do exist, as the higher concentration of functional megaspores (P) were observed between stages 5-6 and 6-7 in the two sexual accessions considered (Figure 10). Anyway much more consistent developmental differences arises in the comparison with sexual and aposporic individuals as a consequence of the lack of sexual structures such as dyads, tetrads and functional megaspores, and their partial replacing with AIs and aposporic embryo sacs. Interestingly, multiple AIs development were detected at very

different bud stages, suggesting their partial non coordination with megasporogenesis or carpels development. Further, as direst consequence of asynchronous AIs differentiation, no obvious pattern of megagametogenesis was detected within aposporic flower bud.

Expression analysis of *HpAPOSTART1* and *HpAPOSTART2* in sexual and apomictic reproducing individuals

Transcript quantifications were carried by using primer sets properly designed in order to discriminate different genes/alleles because of the presence of SNPs throughout the CDS. A total of four and three different primer pairs were used to specifically amplify the *APOSTART1* and *APOSTART2* gene members, respectively. As shown in Figures 12 and 13, transcripts of both *APOSTART1* and *APOSTART2* were detected not only in pistils, but also in sporophytic tissues, such as leaves and roots.

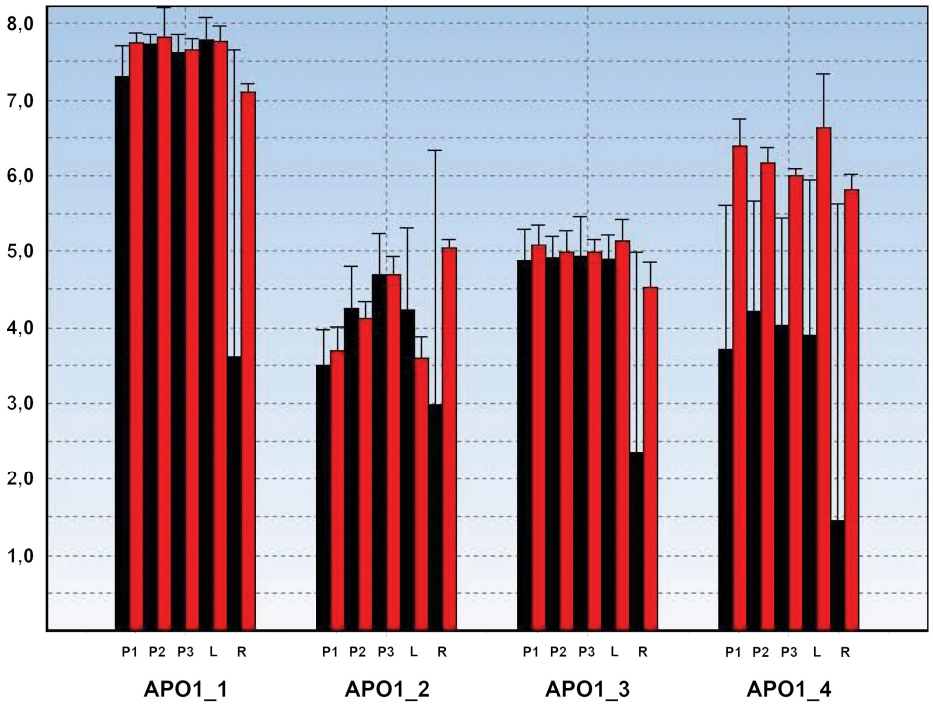

Figure 11. Expression patterns and levels of mRNAs encoded by four different *HpAPOSTART1* genes/alleles in sexual (black histograms) and apomictic (red histograms) individuals. Three different developmental stages of the pistil (P1, P2 and P3 respectively) along with leaves (L) and roots (R) were analysed. All investigations were performed in two biological replicates. Each experiment was done in three technical repetitions.

As far as the expression levels of *APOSTART1* are concerned, a similar trend was recorded for all genes/alleles whose expression was constant in all analysed stages of pistil development. The only exception in terms of expression pattern was obtained with the primer combination APO1_2, which demonstrated to be slightly modulated following pistil development. Moreover, the expression levels recorded for the APO1_1 gene/allele were higher than those of the other genes/alleles (Figure 12). Noticeably, significantly higher mRNA levels of the gene/allele APO1_4 were present in aposporic pistils if compared to the sexual ones ($p < 0.05$), while no significant differences were observed for the genes/alleles APO1_1, APO1_2 and APO1_3. By contrast to the pattern described for *APOSTART1*, the expression level of *APOSTART2* was positively modulated during the development of the pistil (Figure 13).

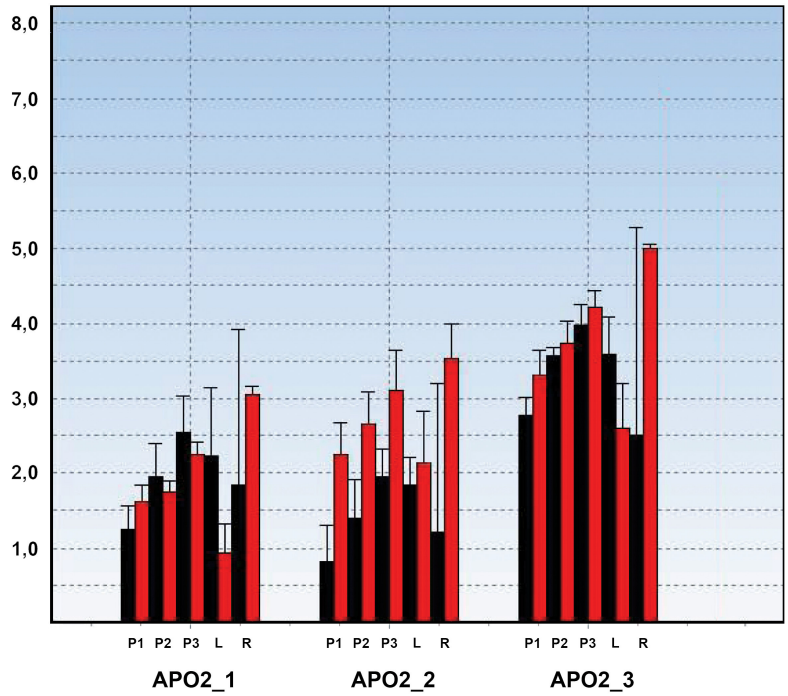

Figure 12. Expression patterns and levels of mRNAs encoded by three different *HpAPOSTART2* genes/alleles in sexual (black histograms) and aposporic (red histograms) individuals. Three different developmental stages of the pistil (P1, P2 and P3 respectively) along with leaves (L) and roots (R) were analyzed. All investigations were performed in two biological replicates. Each experiment was done in three technical replicates.

Among the three different primer combinations tested to specifically amplify *APOSTART2*-like genes/alleles, the primer combination APO2_2 allowed the identification of mRNAs differentially expressed between sexual and aposporic individuals. Indeed, even if the pattern of APO2-2 members did not differ from the pattern of *APOSTART2*-like sequences, a significant increased expression level was detected over all developmental stages of the aposporic pistil. A significant differential expression level was also recorded for the APO2_3 gene/allele, but only at the stage of meiosis.

Discussion

Construction of the first *Hypericum* linkage map based on MFDP and AFLP technologies

Combining AFLP with MFDP technology allowed the construction of the first linkage map in *Hypericum perforatum*. The combination of AFLP and MFDP primer sets allowed the amplification and mapping of as many as 64 molecular markers. MFDP primer pairs resulted highly informative for mapping purposes, allowing the identification of as many as 50 polymorphic markers between seed parent and pollen donor. As far as the linkage maps are concerned, a total of 48 marker alleles were identified by AFLP while the remaining 16 marker alleles were retrieved by means of the MFDP approach. It is worth noting that since 16 MFDP-derived marker alleles were mapped, a functional enrichment of the genetic map was achieved. Marker alleles appears to be distributed in all major linkage groups with one noticeable exception, represented by the linkage group 1 of the pollen donor, in which only AFLP markers were present. One possible explanation for the exclusive presence of AFLP marker alleles would be that the linkage group represents a heterochromatic, non- coding region. Anyway, the possibility that increasing the number of MFDP marker alleles within the map would lead to the inclusion of functional MFDP derived loci within the linkage group could not be ruled out. Specificity of amplifications due to correct heterologous primer pairing and restriction site positioning, was partially confirmed by means of BLAST analysis and sequence alignment. It is worth mentioning

that searching for structural homologies of the MFDP sequenced clones by querying the non redundant database with the *Hypericum* sequence collection retrieved significant similarities with sequences belonging to the species *O. sativa*, *V. vinifera*, and *A thaliana,* while few of no blast hits were recorded for *Populus alba* and the recently sequenced *Populut tricocarpa*. It is likely that the lack of close relative species of *H. perforatum* characterised by high research or economical impact, make the recover of BLAST hits more difficult that in other botanical families. Beside the relative phylogenic distance with other model organisms such as *Arabidopsis* and rice, the confirmation of the specificity of MFDP derived marker alleles was also probably hindered by the relative short length of originated amplicons, due to the specific enzyme combination used in our technology

As future perspectives, the development of additional informative molecular marker systems for *H. perforatum* based on arbitrarily chosen multigene family domains and their application to genetically characterize apomictically reproducing polyploid *H. perforatum* is our main future goal. A better understanding of its reproductive and inheritance patterns is required to facilitate the identification of genetic factors associated with apomixis. Moreover, the recovery of molecular markers linked to the mode of reproduction and related to the expression of apomictic determinants is a preliminary step towards the understanding of the genetic control and molecular regulation of apomixis in *H. perforatum*.

Cytohistology shed lights on the nucellar domains where AIs differentiate and develop

Our detailed analyses of female sporogenesis and gametogenesis have enabled us to define the major morphological traits of all structures playing a role in embryo sac formation. The *Hypericum* ovary bears many ovules, and is connected to the maternal tissues by an assile placentation. Sexual ovules are anatropous, bitegmic and tenuinucellate, and encloses at maturity a monosporyc, *Polygonum* type embryo sac. The aposporic ovule retains all major morphological characteristic reported herein, but fails to develop a reduced embryo sac. In place of the sexual pathway, the aposporic embryo sac develops through a series of free nuclear division from a single sporophytic cell, which belongs to the epidermal cell layer of the nucellus. Our observations show that the major

developmental features characteristic of aposporic ovule formation includes: i) mis-expression of the meiotic program, ii) failure or delay of degeneration of the epidermal layer of the nucellus, iii) AI differentiation, and iv) development into an alternative coenocyte. Furthermore, v) low frequencies of sexual developing ovules are retained within the aposporic ovary.

The importance of AI positioning with respect to the meiotic product has been reported for several apomictic model organisms. This is the case of *Hieracium*, as one to many AIs were reported to differentiate in close connection to the megaspores in *H. piloselloides* and *H. aurantiacum* (Koltunow *et al.*, 1998). Moreover, aposporic embryo sac development is influenced by AI mis-positionaling, as a result of the *loa1* mutation (Okada *et al.*, 2007). Similarly, the correct positioning of AIs in *Hypericum* ovules seems to be necessary for further development, as no AIs or embryo sacs were ever detected more distantly from the site of megasporogenesis within the nucellus. Since both sexual and aposporic initial cells share the same differentiation site in *Hypericum*, it seems likely that both processes depend on the expression of specific factors restricted to this area of the ovule. Furthermore, the fact that megasporogenesis is restricted to the hypodermal inner area and never occurs in epidermal cell layer, suggests an additional regional level of regulation within the nucellus background. In the same light, communication between different cell types and layers have been reported (Wu and Cheung 2000, Yang and Sundaresan, 2000) and are likely to be important for embryo sac formation (Koltunow *et al.*, 1998). Regulation patterns based upon relative cell positioning may be similar to what has been reported for the Arabidopsis Shoot Apical Meristem (SAM), where a population of stem cells is constantly maintained with the identity of each being further regulated based upon its relative position within the L1, L2 and L3 cellular layer (reference). Positional signals involving the functional megaspore are thought to result in the degeneration of the three non-selected megaspores, and formation of a functional megaspore might be required for nucellar degeneration (Wu and Cheung 2000; Yang and Sundaresan 2000). Plasmodesmatal connections form between the functional megaspore and adjacent nucellar cells, providing a physical, symplastic avenue for cell-to-cell communication between sporophytic and gametophytic cells during female embryo sac formation (Bajon *et al.* 1999). Further, it is generally recognized that callose deposition

during megasporogenesis progression might play a role in the isolation of megaspores from the surrounding tissues by physically limiting symplastic communication with adjacent cells. If this is true, it is particularly interesting that callose deposition within aposporic ovules is frequently lacking or follows an unconventional pattern (Figure 8). Even if we cannot rule out the possibility that the alteration in callose deposition observed in aposporic ovules is not the cause of megaspore degeneration, it is reasonable to conclude that changes in callose accumulation reflect a deregulation in normal cell-to-cell communication. Thus it is likely that developing megaspores either directly or indirectly regulate epidermal layer proliferation whereby apomeiosis leads to abnormal signalling between closely neighbouring cells.

Aposporic initials do not divide in a meiotic pattern, bur rather divide mitotically to occupy much of the area enclosed by the two integuments. Overall development of the embryo sac through unconventional free nuclear division is a common feature of the two aposporic and sexual embryo sacs. This consideration is not obvious since a somatic cell normally divides through conventional division immediately followed by cytokinesis, while the embryo sac formation always proceeds through successive free nuclear divisions and a single final cellularization event. Nonetheless, despite the high analogies between the two processes, pattern formation peculiarities in term of number and positioning of nuclei within the embryo sac do exist in aposporic ovules. Free nuclear divisions within the embryo sac were frequently asynchronous, leading to unconventional numbers of nuclei that frequently let to miss-positioning within the same coenocyte. Moreover, the degeneration of synergids, along with the presence of supernumerary nuclei within the central and additional egg-like cells within the germ cell unit was observed in fully developed aposporic embryo sacs. Our FCSS analyses clearly indicate that fully developed aposporic embryo sacs might bear both a functional egg and central cell apparatus, as the products of their fertilization were detected. Although a large number of mutants showing defects during megagametogenesis have been isolated in *Arabidopsis* (Christensen *et al.*, 1997, 1998, 2002; Moore *et al.*, 1997; Pagnussat *et al.*, 2005), the cellular and molecular basis of cell specification in the embryo sac remains largely unknown. Within the Arabidopsis embryo sac an early distinction between nuclei in the four and eight nucleate stages was reported by Webb and Gunning (1994), considering

their precise migration and positioning along the embryo sac as the third mitotic division and cellularization steps take place. In contrast, the analysis of a gametophytic mutant led Pagnussat *et al.* (2007) to report that no genetic predisposition seems to guide the fate of any embryo sac nucleus to form the egg cell. The isolation and characterization of the *eostre* gametophytic mutant (Pagnussat *et al.*, 2007) supports the possibility that a relation between cell fate and positioning of the nucleus within the embryo sac does exist, as mutation of *eostre* results in the atypical migration and positioning of nuclei within the embryo sacs, leading to a variety of morphological and functional defects including the conversion of one synergid in to a functional extra egg cell. Moreover Pagnussat *et al.* (2007) reported that the specification of cell fate within the embryo sac appeared to rely on a position-based mechanism, as the switch from synergid to egg cell is accompanied by mis-positioning of the nucleus at early developmental stages. Similarly, the auxiliary and gametic cell fates within the embryo sac of Arabidopsis were recently reported to be affected in the *lachesis* mutant (Gross-Hardt *et al.*, 2007), in which functional supernumerary egg cells differentiate from accessory cells, pointing to a mechanism that prevents accessory cells from adopting gamete cell fate. Such processes reported on ovule development, in particular with respect to nucleus positioning and cell fate, might help to explain embryo sac development in *Hypericum*, for example whether apospory involves mis-regulation of the above mentioned genes.

Hypericum perforatum is characterized by quantitative variation in reproductive mode, as demonstrated by the cytological and FCSS investigations here, in addition to previous work (Matzk *et al.*, 2001). The multiple pathways of seed formation displayed by tetraploid apomictic individuals is reflected in the variable embryo and endosperm genome ratios, which range from 2:8 (for reduced parthenogenic, pseudogamous development) to 4:14 (for unreduced parthenogenic, pseudogamous development)(Table 5). We furthermore identified significant levels of both autonomous endosperm formation (ie, 4:8) and double fertilization of both egg cell and central cell (6:10)(Table 5), as was also reported by Matzk *et al.* (2001). These deviations demonstrate relaxation from the strict endosperm balance number (EBN; Johnston *et al.*,1998) which is characteristic of sexual angiosperms. Interestingly, deviation from the strict 2m:1p endosperm ratio has been shown to exist in other apomictic taxa, including *Boechera* (Voigt *et al.*, 2007),

Tripsacum, *Paspalum* and *Hieracium* (revieved by Koltunow and Grossniklaus, 2003). *Hypericum perforatum* exhibits a wide range in embryo:endosperm C values in mature seed (Table 5), although values greater than 4:6 were observed in a very low frequence. This indicates that both embryo and endosperm with different ploidy levels might develop, but higher ploidy of the endosperm is required for the correct development of the seed.

Finally, our FCSS data demonstrate fertilization of the central cell of the illegitimate embryo sac but not the exclusive fertilization of the egg cell (Tables 5 and 6). Considering the high variability in aposporic *embryo sac* morphology (Figures 7 and 9), this observation might some predisposition of the sperm nucleus to fertilize the central cell over the egg cell. Alternatively it might be possible that exclusive fertilization of the egg cell does occur, but subsequent perturbation of embryo/endosperm ratio lead to selective abortion of specific ovules. The nutritional and physiological role of the endosperm with respect to the developing embryo might account for this latter hypothesis, since low ploidy of the former might somehow promote abortion of the seed (Scott *et al.*, 1998).

Embryo sac development in aposporic *Hypericum perforatum* frequently results in the formation of coenocyte that might not morphologically resemble the reduced sexual embryo sac. Beside differences in shape and timing, the main differences observed between sexual and aposporic embryo sacs are the number of nuclei and the organization of embryo sac following cellularization. Synergid degeneration could be interpreted as a physical barrier against fertilization, and multinucleated central cell formation might be particularly interesting with respect to autonomous endosperm formation and parthenogenesis. Unfortunately, the FCSS analysis only allows DNA quantification, while paternal vs maternal contributions to endosperm formation remain untested. Therefore, we could not rule out the possibility that supernumerary nuclei within the central cell might fuse to lead to secondary cells containing nuclei with higher ploidy levels than expected.

The elevated variation in aposporic embryo sac development (relative to sexual ones; Figures 7 and 9, Table 5) could reflect stochastic processes, for example perturbations to signalling pathways in the ovule (Okada *et al*., 2007), or mutation accumulation in independently-derived apomictic clones (Koltunow *et al*., 1993). Stochastic embryo sac development has been hypothesized in aposporic *H. aurantiacum* (Koltunow *et al.*, 1998)

where one to multiple aposporic initials were demonstrated to forms and grows without any precise developmental patterns.

Perhaps referring to the aposporic embryo sac as a female unreduced gametophyte is simply inaccurate. Although the aposporic coenocyte can be fertilized in its late developmental stages, thereby attesting to its gametophytic nature, not much is known with respect to the very early developmental stages. We hypothesize that many cells belonging to the aposporic nucellus may have the ability to develop into others structures. Thus the aposporic intial could be a somatic cell that re-enters the cell cycle and undergoes a first mitotic division, a process that could be influenced by the specific positioning of the cell within the nucellus. This could be achieved, for instance, by mis-regulation of genetic factors involved in epidermal cell identity (Sieber *et al*., 2004) although nucellus identity would have to be maintained on a more general scale. In this scenario, the degeneration of functional megaspores might somehow release surrounding cells from inhibitory regulation. This is supported by the observation that AIs were not observed together with sexual megaspores, which were still present at low frequencies within aposporic individuals. We cannot rule out the possibility that apomeiosis would induce one or more of the surrounding cells to divide, and interaction with surrounding structures is likely to be fundamental for the illegitimate coenocyte to acquire gametophytic identity as it within the integument. We would add that no known mutations affect ovule integument formation without additionally affecting the embryo sac development (Sieber *et al.*, 2004), thus pointing to the influence of sporophytic tissues on the enclosed gametophyte. Moreover, since apospory demonstrates that a gametophyte may develop from an unreduced sporophytic cell, of the importance of epigenetic mechanisms specific to the haploid functional megaspore may not be critical for gametophyte development. Further, polyploidization experiment in *Hypericum* resulted in the creation of sexual tetraploid individuals (Sharbel, unpublished data), thus supporting the idea that gene copy number or DNA quantity are not likely to be critical for gametophyte formation. Alternatively, it seems more reasonable that factors needed for both aposporic and sexual embryo sac development are somehow regulated by regulative motives active in hypoderm and epidermal areas of the nucellus.

New insights on the phylogenetic origin of *Hypericum perforatum*

Carman (1997; 2001) suggested the hypothesis that apomixis may result from the hybridization of two ecotypes or related species with differences in reproductive characters. This hypothesis is particularly interesting with respect to *Hypericum perforatum* since an allotetraploid origin of the specie have been postulated by Campbell and Delfosse (1984) and Robson (2002). In particular, the idea that *H. perforatum* arose from an ancient interspecific hybridization event between the diploids *H. attenuatum* and *H. maculatum,* with subsequent chromosome doubling, was supported by the presence in *H. perforatum* of morphological traits of the two hypothesised ancestors and by geographical distribution areas analyses.

The isolation of codominant molecular markers, such as SNPs, and their application in *H. perforatum* and its putative ancestors was useful to shed some light on the phylogenetic relationships among the three analyzed species. Genetic divergence, computed for both coding and non-coding regions of two genes that are likely involved the apomictic programs have been estimated. Genetic divergences were calculated by pirewise comparisons of sequences either belonging to the same species or different ones. Analyses were conduced by using both expressed (exons) and non-coding sequences, such as introns. As expected from a genomic region under low selective genetic pressure, a higher number of SNPs was detected within the intronic regions of the genes. The estimated genetic divergence within most species was typically lover than the genetic divergence estimated by pairwise comparisons of sequences identified in different species. The only exception was the interspecific genetic divergence calculated between the two species *H. perforatum* and *H. maculatum*, which resulted to be lower than the genetic divergence calculated considering the *H. maculatum* dataset alone. The low genetic divergence calculated between *H. perforatum* and *H. maculatum*, in particular with respect to the genetic divergence computed in the comparison *H. perforatum* - *H. attenuatum* and *H. attenuatum* - *H.maculatum*, revealed a close relationship between the two species. This finding was further supported by the analysis of the genetic distances in a Neighbor-Joining phylogenetic tree. Graphical representation of sequence similarity data revealed the phylogenetic relationship between *H. perforatum* and *H. maculatum* as all sequences belonging to this two species were tightly clustered in the same branch. By contrast, all

intronic *HpAPOSTART1* and *HpAPOSTART2* sequences isolated in the species *H. attenuatum* were grouped apart. The data here presented do not support the possibility that *H. attenuatum* participated to the hybridization events hypothesized by Campbell and Delfosse (1984) and Robson (2002) at the same levels of *H. maculatum*. Rather, the computed genetic distances between species might account for an autopolyploidization origin from an ancestor closely related to the diploid *H. maculatum*, as already hpothesized by Brutovská *et al.* (2000). However, the possibility that other species than *H. attenuatum* played a role in an eventual hybridization process in concert with *H. maculatum* might not be ruled out.

HpAPOSTART: a new candidate gene for the control of aposporic apomixis in *H. perforatum*

Sequence analysis allowed the identification of a number of SNPs among the two *APOSTART* genes. Eight haplotypes, defined by the presence of specific SNPs, were used to discriminate the two *APOSTART1* and *APOSTART2* members/alleles. The expression pattern and levels of *APOSTART1* and *APOSTART2* specific genes/alleles were analyzed focusing on different developmental stages of the pistils. Expression analyses revealed a different pattern of expression for the genes *APOSTART1* and *APOSTART2*. A similar pattern of expression was recorded by using primer combinations theoretically able to discriminate different alleles of the same gene. The only exception was the primer combination APO1_2, which was designed to specifically amplify a cluster of genes sharing higher similarity with the *APOSTART2* sequences. The two genes were characterized by a different pattern of expression in pistils at different developmental stages. Indeed, while the expression pattern of *APOSTART1* was not apparently modulated during pistil development, a positive modulation in the quantity of transcript was observed for *APOSTART2*. This pattern of expression is particularly interesting since the involvement of the *APOSTART* genes with respect to megagametogenesis was postulated in *Poa pratensis* by Albertini *et al.* (2005). Moreover, as far as the expression levels are concerned, significant variations were evidenced over the two APO1_4 and APO2_2 genes/alleles belonging to *APOSTART1* and *APOSTART2*-like genes, respectively.

Further, even if APO1_4 and APO2_2 alleles were characterized by a similar expression pattern within pistils isolated from individuals with contrasting reproductive behaviour, a significantly higher quantity of transcript was detected in aposporic individuals. Expression analyses carried on single alleles/genes allowed the identification of differences between aposporic and sexual pistils that otherwise would not be possible to detect. Since significant expression differences were detected for single alleles, which were deviating from the main gene expression levels, it is likely that single gene expression analysis would not have detected the reported differences. Overall, the positive modulation of *APOSTART2_2* expression along with its higher expression in aposporic pistils further support a major role of this gene in the apomictic pathway.

Bibliography

Albertini E, Barcaccia G, Porceddu A, Sorbolini S and Falcinelli M (2001) Mode of reproduction is detected by Parth1 and Sex1 SCAR markers in a wide range of f acultative apomictic Kentucky bluegrass varieties. Molecular Breeding 7: 293-300

Albertini E, Porceddu A, Marconi G, Barcaccia G, Pallottini L and Falcinelli M (2003) Microsatellite-AFLP for genetic mapping of complex polyploids. Genome 46: 824-832

Albertini E, Marconi G, Barcaccia G, Raggi L and Falcinelli M (2004) Isolation of candidate genes for apomixis in *Poa pratensis* L. Plant Mol Biol, 56: 879-894.

Albertini E, Marconi G, Barcaccia G, Raggi L and Falcinelli M (2005) *SERK* and *APOSTART*: candidate genes for apomixis in *Poa pratensis* L. Plant Phys, 138: 2185- 2199.

Aparicio G, Gotz S, Conesa A, Segrelles D, Blanquer I, Garcia JM, Hernandez V, Robles M, Talon M (2006) Blast2GO goes grid: developing a grid-enabled prototype for functional genomics analysis. *Stud Health Technol Inform* 120: 194--204

Bajon C, Horlow C, Motamayer JC, Sauvanet A, Robert D (1999) Megasporogenesis in *Arabidopsis thaliana* L.: an ultrastuctural study. Sex Plant Reprod 12: 99-119

Barcaccia G, Mazzucato A, Albertini E, Zethof J, Gerats A, Pezzotti P, Falcinelli M (1998) Inheritance of parthenogenesis in Poa pratensis L.: auxin test and AFLP linkage analyses support monogenic control. Theor Appl Genet 97: 74-82

Barcaccia G, Albertini E, Tavoletti S, Falcinelli M and Veronesi F (1999) AFLP fingerprinting in Medicago spp.: Its development and application in linkage Mapping. Plant Breeding 118: 335-340

Barcaccia G, Varotto S, Meneghetti S, Albertini E, Porceddu A, Parrini P and Lucchin M (2001) Analysis of gene expression during flowering in apomeiotic mutants of Medicago spp.: cloning of ESTs and candidate genes for 2n eggs. Sex Plant Reprod., 14: 233-238.

Barcaccia G, Arzenton F, Sharbel T, Varotto S, Lucchin M and Parrini P (2006) Genetic diversity and reproductive biology in ecotypes of the facultative apomict *Hypericum perforatum* L. Heredity, 96: 322-334.

Barcaccia G, Bäumlein H and Sharbel TF (2007) Apomixis in St. John's Wort (*Hypericum perforatum*): An overview and glimpse towards the future. HÖRANDL E., GROSSNIKLAUS U., VAN DIJK P., SHARBEL T.F. (eds.): Apomixis: Evolution, Mechanisms and Perspectives. International Association for Plant Taxonomy, Koeltz Scientific Books pp 259-280.

Botton A, Galla G, Conesa A, Bachem C, Ramina A, Barcaccia G (2008). Large-scale Gene Ontology analysis of plant transcriptome-derived sequences retrieved by AFLP technology. BMC Genomics. 9:347

Burge C and Karlin S (1997) Prediction of complete gene structures in human genomic DNA. *J. Mol. Biol.* 268: 78-94.

Carman JG (1997) Asynchronous expressionof duplicate genes in angiosperms may cause apomixis, bispory, tetraspory, and polyembryony. *Biol. J. Linn. Soc.* 61:51-94

Carman JG (2001) The gene effect: genome collisions and apomixis. See Ref. 112a, pp. 95-110

Chandler VL, Stam M, Sidorenko LV (2002) Long-distance cis and trans interactions mediate paramutation. *Adv. Genet.* 46:215-34

Christensen C A, King EJ, Jordan JR and Drews GN (1997) Megagametogenesis in *Arabidopsis* wild type and the *Gf* mutant. Sex. Plant Reprod., 10: 49-64.

Christensen CA, Subramanian S and Drews GN (1998) Identification of gametophytic mutations affecting female gametophyte development in *Arabidopsis.* Dev. Biol., 202: 136-151.

Christensen CA, Gorsich S W, Brown RH, Jones LG, Brown J, Shaw JM and Drews GN (2002) Mitochondrial GFA2 is required for synergid cell death in Arabidopsis. The Plant Cell 14: 2215-2232

Conesa A, Götz S, Garcìa-Gòmez JM, Terol J, Talòn M and Robles M (2005) Blast2GO: a universal tool for annotation, visualization and analysis in functional genomics research. Bioinformatics 21: 3674-3676

Crooks GE, Hon G, Chandonia JM, Brenner SE (2004) WebLogo: A sequence logo generator, Genome Research, 14:1188-1190

Felsenstein J (1985) Confidence limits on phylogenies: An approach using the bootstrap. *Evolution* 39:783-791.

Galla G, Barcaccia G, Shallau A, Puente Molins M, Bäumlein H, and TF Sharbel (in press) The cytohistological basis of apospory in *Hypericum perforatum*

Groß-Hardt R, Kägi C, Baumann N, Moore JM, Baskar R, Gagliano W, Jürgens G, Grossniklaus U (2007) LACHESIS Restricts Gametic Cell Fate in the Female Gametophyte of *Arabidopsis*. PLoS Biol 5(3): e47

Grossniklaus U (2001) From sexuality to apomixis: molecular and genetic approaches. See Ref. 112a, pp. 168- 211

Gustine DL and Sherwood RT (1997) Apospory-Linked Molecular Markers in Buffelgrass. Crop Sci 37:947-951

Haig D (1990) New perspectives on the angiosperm female gametophyte. Bot. Rev., 56: 236-275

Halder G, Callaerts P, Gehring WJ (1995) Induction of ectopic eyes by targeted expression of the *eyeless* gene in *Drosophila*. *Science* 267:1788-92

Huang BQ and Russell SD (1992) Female germ unit: Organization, isolation, and function. Int. Rev. Cytol., 140: 233-292.

Huang BQ and Sheridan WF (1994) Female Gametophyte Development in Maize: Microtubular Organization and Embryo Sac Polarity The Plant Cell 6: 845-861

Jacobsen SE, Meyerowitz EM (1997) Hypermethylated *SUPERMAN* epigenetic alleles in *Arabidopsis*. *Science* 277:1100-3

Jacobsen SE, Sakai H, Finnegan EJ, Cao X, Meyerowitz EM (2000) Ectopic hypermethylation of flower-specific genes in *Arabidopsis*. *Curr. Biol.* 10:179-86

Kakutani T, Jeddeloh JA, Flowers SK, Munakata K, Richards EJ (1996) Developmental abnormalities and epimutations associated with DNA hypomethylation mutations. *Proc. Natl. Acad. Sci. USA* 93: 12406-11

Kimura M (1980) A simple method for estimating evolutionary rate of base substitutions through comparative studies of nucleotide sequences. *Journal of Molecular Evolution* 16:111-120.

Koltunow AM. (1993) Apomixis: embryo sacs and embryos formed without meiosis or fertilization in ovules. *Plant Cell,* 5:1425–37

Koltunow AM, Johnson SD and Bicknell RA (1998) Sexual and apomictic development in *Hieracium*. Sex Plant Reprod, 11: 213-230

Koltunow AM and Grossniklaus U (2003) APOMIXIS: A Developmental Perspective. Annu. Rev. Plant Biol., 54: 547-74

Liu J and Qu L-J (2008) Meiotic and mitotic cell cycle mutants involved in gametophyte development in *Arabidopsis*. Mol. Plant, 1(4): 564-574

Maheshwari P (1950) An Introduction to the Embryology of Angiosperms, McGraw-Hill, New York. pp. 453.

Mansfield SG, Briarty LG and Erni S (1991) Early embryogenesis in *Arabidopsis thaliana*. I. The mature embryo sac. *Can. J. Bot*., 69: 447-460.

Matzk F (1991) New efforts to overcome apomixis in *Poa pratensis* L. Euphytica 55: 65-72.

Matzk F, Meister A, Brutovská R and Schubert I (2001) Reconstruction of reproductive diversity in *Hypericum perforatum* L. opens novel strategies to manage apomixis. Plant J, 26: 275-282.

Mogie M (1992) The Evolution of Asexual Reproduction in Plants. London: Chapman & Hall

Moore JM, Calzada JP, Gagliano W, Grossniklaus U (1997) Genetic characterization of *hadad*, a mutant disrupting female gametogenesis in *Arabidopsis thaliana*. Cold Spring Harbor Symp. Quant. Biol. 62:35-47

Nogler GA (1971) Genetik der Aposporie bei *Ranunculus auricomus*s. l. W. Koch. I. Embryologie. *Ber. Schweiz. Bot. Ges.* 81:139-79

Okada T, Catanach AS, Johnson SD, Bicknell RA and Koltunow AM (2007) An Hieracium mutant, loss of apomeiosis 1 (loa1) is defective in the initiation of apomixis. Sex Plant Reprod 20:199-211

Ottegui M and Staehelin LA (2000) Cytokinesis in flowering plants: more than one way to divide a cell Current Opinion in Plant Biology, 3: 493-502

Ozias-Akins P, Lubbers EL, Hanna WW, and McNay JW (1993) Transmission of the apomictic mode of reproduction in *Pennisetum*: Coinheritance of the trait and molecular markers. *Theor. Appl. Genet*. 85: 632-638.

Ozias-Akins P, Roche D, and Hanna WW (1998) Tight clustering and hemizygosity of apomixis-linked molecular markers in *Pennisetum squamulatum* implies genetic control of apospory by a divergent locus which may have no allelic form in sexual genotypes. *Proc. Natl. Acad. Sci. USA* 95: 5127-5132.

Pagnussat GC, Yu HJ, Ngo QA, Rajani S, Mayalagu S, Johnson CS, Capron A, Xie LF, Ye D, Sundaresan V (2005) Genetic and molecular identification of genes required for female gametophyte development and function in *Arabidopsis*. Development, 132: 603-614.

Pagnussat GC, Yu HJ and Sundaresan V (2007) Cell Fate Switch of Synergid to Egg Cell in Arabidopsis eostre Mutant Embryo Sacs Arises from Misexpression of the BEL1-Like Homeodomain Gene BLH. The Plant Cell, 19: 3578-3592

Pessino, SC, Ortiz J, Leblanc O, do Valle C B, and Hayward MD (1997) Identification of a maize linkage group related to apomixis in *Brachiaria*. *Theor. Appl. Genet*. 94: 439-444.

Reiser L and Fischer RL (1993) The ovule and the embryo sac. Plant Cell, 5: 1291-1301

Robinson-Beers K, Pruitt RE, Gasser CS (1992) Ovule development in wild-type *Arabidopsis* and two female-sterile mutants. Plant Cell, 4: 1237-1249.

Robson NKB (2002) Studies in the genus *Hypericum* L. (Guttiferae) 4(2). Section 9. *Hypericum sensu latu* (part 2): subsection 1. *Hypericum* series 1. *Hypericum*. Bull Nat Hist Mus Lond (Bot), 32: 61-123.

Roche, D., Cong, P., Chen ZB, Hanna WW, Gustine DL, Sherwood RT, and Ozias-Akins P (1999) An apospory-specific genomic region is conserved between buffelgrass (*Cenchrus ciliaris* L.) and*Pennisetum squamulatum* Fresen. *Plant Journal* 19: 203-208.

Saitou N and Nei M (1987) The neighbor-joining method: A new method for reconstructing phylogenetic trees. *Molecular Biology and Evolution* 4:406-425.

Savidan YH (2001) Gametophytic apomixis: a successful mutation of the female gametogenesis. In *Current Trends in the Embryology of Angiosperms*, ed. SS Bhojwani, WY Soh, 419-433

Schneitz K, Hülskamp M and Pruitt RE (1995) Wild-type ovule development in *Arabidopsis thaliana*: A light microscope study of cleared whole-mount tissue. Plant J., 7: 731-749.

Schiefthaler U Balasubramanian S, Sieber P, Chevalier D, Wisman E and Schneitz K (1999) Molecular analysis of *NOZZLE*, a gene involved in pattern formation and early sporogenesis during sex organ development in *Arabidopsis thaliana.* Proc. Natl. Acad. Sci. USA, 96: 11664-11669

Schneider TD, Stephens RM. (1990). Sequence Logos: A New Way to Display Consensus Sequences. Nucleic Acids Res. *18*: 6097-6100

Scott RJ, Spielman M, Bailey J, Dickinson HG (1998) Parent-of-origin effets on seed development in *Arabidopsis thaliana.* Development 125: 3329-3341

Sheridan WF *et al.* (1999) The *mac1* mutation alters the developmental fate of the hypodermal cells and their cellular progeny in the maize anther. Genetics, 153: 933-941

Siddiqi I, Ganesh G, Grossniklaus U and Subbiah V (2000) The dyad gene is required for progression through female meiosis in *Arabidopsis*. Development, 127: 197-207.

Sieber P, Gheyselinck J, Gross-Hardt R, Laux T, Grossnikalus U and Schneitz K (2004) Pattern formation during early ovule development in Arabidopsis thaliana Devev Biol, 273: 321-334

Smyth DR, Bowman JL, Meyerowitz EM (1990) Early flower development in *Arabidopsis*. Plant Cell, 2: 755-767.

Spillane C, Steimer A, Grossniklaus U (2001) Apomixis in agriculture: the quest for clonal seeds. *Sex Plant Reprod.* 14:179-87

Stam M, Belele C, Dorweiler JE, Chandler VL (2002) Differential chromatin structure within a tandem array 100 kbupstream of the maize *b1* locus is associated with paramutation. *Genes Dev.*16:1906-18

Tamura K, Dudley J, Nei M and Kumar S (2007) MEGA4: Molecular Evolutionary Genetics Analysis (MEGA) software version 4.0. *Molecular Biology and Evolution* 24:1596-1599.

Tucker MR, Araujo ACG, Paech NA, Hecht V, Schmidt EDL, Rossell JB, de Vries SC and Koltunow AM (2003) Sexual and apomictic reproduction in Hieracium subgenus Pilosella are closely interrelated developmental pathways. Plant Cell 15: 1524-1537

Van Ooijen JW, Voorrips RE (2001) JoinMap 3.0, Software for the calculation of genetic linkage maps. Plant Research International, Wageningen, The Netherlands

Vos P, Hogers R, Bleeker M, Reijans M, van de Lee T, Hornes M, Frijters A, Pot J, Peleman J, Kuiper M.E and Zabeau M (1995) AFLP™: a new technique for DNA fingerprinting. *Nucleic Acids Res*., 23: 4407-4414.

Webb MC, Gunning BES (1994) Embryo sac development in *Arabidopsis* thaliana. II. The cytoskeleton during megagametogenesis. Sex. Plant Reprod., 7: 153-163

Willemse MTM, Went JL van (1984) The female gametophyte. In: Johri BM (ed) Embryology of angiosperms. Springer, Berlin Heidelberg New York, 159-196

Wu HM and Cheung AY (2000) Programmed cell death in plant reproduction. Plant Mol Biol 44:267-281 Yang WC and Sundaresan V (2000) Genetics of gametophyte biogenesis in *Arabidopsis*. Curr. Opin. Plant Biol., 3: 53-57

Vorrei ringraziare il Prof. Gianni Barcaccia, per l'infinita pazienza con la quale mi ha aiutato a crescere nel corso del dottorato. Vorrei anche ringraziare Franco, Silvia, Daria e "i ragazzi del piano di sopra", per avermi sopportato e aiutato nel corso degli ultimi anni.
Un ringraziamento speciale va a Luisa, a mia madre e a mio padre, per essermi stati sempre vicino ed avere sempre creduto in me.
Infine, un particolare ringraziamento va alla mia stellina, Sara, per avermi seguito, accompagnato e guidato nei migliori momenti dell'ultimo anno.